1
Bone and Cartilage – its Structure and Physical Properties

Ryszard Wojnar

1.1
Introduction

Here we describe the morphology and biology of bone, analyzing its components. The chapter is divided into two sections:

1) Macroscopic structure of bone
   a. Growth of bone
   b. Structure of body
   c. Structure of bone
2) Microscopic structure
   a. Osteons
   b. Bone innervations
   c. Bone cells
   d. OPG/RANK/RANKL signaling system
   e. Proteins and amino acids
   f. Collagen and its properties
   g. Polymer thermodynamics
   h. Architecture of biological fibers

All organs of the body are made up of four basic tissues: epithelia, connective tissue (CT), muscle tissue, and nervous tissue. Blood, cartilage, and bone are usually regarded as CTs. All tissues of an organism are subject to different stimuli, among others, to mechanical forces. These forces arise from various reasons, such as blood circulation, inertial forces created during motion, and gravity forces that act ceaselessly in normal conditions.

Bone is a specialized form of CT that serves as both a tissue and an organ within higher vertebrates. Its basic functions include mineral homeostasis, locomotion, and protection. Bone has cellular and extracellular parts. The extracellular matrix (ECM) of the bone comprises approximately 9/10 of its volume, with remaining 1/10 comprising cells and blood vessels. The ECM is composed of both organic and inorganic components.

Biomechanics of Hard Tissues: Modeling, Testing, and Materials.
Edited by Andreas Öchsner and Waqar Ahmed

ISBN: 978-3-527-32431-6

Greek philosopher and scientist Aristotle of Stageira maintained that ''Nature, like a good householder, is not in the habit of throwing away anything from which it is possible to make anything useful. Now in a household the best part of the food that comes in is set apart for the free men, the inferior and the residue of the best for the slaves, and the worst is given to the animals that live with them. Just as the intellect acts thus in the outside world with a view to the growth of the persons concerned, so in the case of the embryo itself does Nature form from the purest material the flesh and the body of the other sense-organs, and from the residues thereof bones, sinews, hair, and also nails and hoofs and the like; hence these are last to assume their form, for they have to wait till the time when Nature has some residue to spare'' [1].

About two-thirds of the weight of a bone, or half of its volume, comes from an inorganic material known as the *bone salt* that conforms, so to say, the bone to a nonliving world. It is an example of biomineralization: the process by which living organisms produce minerals. Owing to the inorganic architecture of the bone its biological properties may often be assumed as time independent, and the bone may be described by the methods of mathematics and mechanics developed for inanimate materials. However, by treating the bone as a live tissue, we observe that its biological activity is essentially directed toward keeping the whole organism in a state of well-being. The functionality of a bone is closely related to that of a cartilage tissue. In embryogenesis, a skeletal system is derived from a mesoderm, and chondrification (or chondrogenesis) is a process by which the cartilage is formed from a condensed mesenchymal tissue, which differentiates into chondrocytes and begins secreting the molecules that form an ECM. Cartilage is a dense CT and, along with collagen type 1, can be mineralized in the bone.

The high stiffness and toughness of biomineralized tissues of a bone are explained by the material deformation mechanisms at different levels of organization, from trabeculae and osteons at the micrometer level to the mineralized collagen fibrils at the nanometer length scale. Thus, inorganic crystals and organic molecules are intertwined in the complex composite of the bone material [2].

Bone, like every living tissue, cannot be described completely in terms of a nonanimate matter description. It breaks as a lifeless stick if overloaded, but if set up it recovers after some time. Under some loads, microcracks can appear; these are *ad hoc* healed, and the bone undergoes reinforcement. These properties of a bone are due to a complicated but coordinated structure, as it is seen during remodeling. Living bone could be treated as a solid-state fluid composite with circulating blood and living cells, while a bone skeleton has hierarchical structure and variable biomechanical properties. In addition, the blood flows through bones according to the rhythm of the heart beat.

Following Erwin Schrödinger, one sees that most physical laws on a large scale are due to stochasticity on a small scale (''order-from-disorder'' principle). For example, the diffusion, in macroscopic description, is an ordered process, but in microscopic view it is caused by random movement of particles. If the number of atoms in the particle increases, the behavior of the system becomes less and

less random. The life greatly depends on order and the master code of a living organism has to consist of a large number of atoms. The living organism seems to be a macroscopic system, the behavior of which approaches the purely mechanical (as contrasted with thermodynamical) conduct to which all systems tend, as the temperature approaches absolute zero and the molecular disorder is removed. The life is based on ''order-from-order'' principle. Schrödinger indicates that a periodic crystal is the material carrier of life, in contrast to periodic crystal of classical (inanimate) physics [3].

The asymmetry of living bodies was emphasized first by Louis Pasteur, who widely used examples with spiral structures. Upon examination of the minuscule crystals of sodium ammonium tartrate, Pasteur noticed that the crystals came in two asymmetric forms that were mirror images of one another (1849): solutions of one form rotated polarized light clockwise, while the other form rotated light counterclockwise. As a result, he devoted himself to the study of what he called *dissymmetry*, pointing out that inorganic substances are not dissymmetrical in their crystallization, while all the products of vegetable and animal life are dissymmetric. He concluded that there was some great biological principle underlying this: ''All artificial products of the laboratory and all mineral species are superposable on their images. On the other hand, most natural organic products (I might even say all, if I were to name only those which play an essential part in the phenomena of vegetable and animal life), the essential products of life, are asymmetric and possess such asymmetry that they are not superposable on their images'' [4, 5]. Geometry itself makes distinction between living and inanimate bodies, and this difference protects the autonomy of life. In the bone, both seemingly opposite substances, living and unliving, meet together and cooperate toward creating bone tissue.

This is the problem of three-dimensional growth through spiral forms, discussed in 1884 by Lord Kelvin [6], who earlier proposed (1873) the term *chirality*, cf. [7] and [8]. The repetition of such a way of development is observed from molecular level until macroscopic forms. In nature, helical structures arise when identical structural subunits combine sequentially, the orientational and translational relation between each unit and its predecessor remaining constant. A helical structure is thus generated by the repeated action of a screw transformation acting on a subunit. A plane hexagonal lattice wrapped around a cylinder provides a useful starting point for describing the helical conformations of protein molecules, investigating at the same time the geometrical properties of carbon nanotubes, and certain types of dense packings of equal spheres.

Essential for life proteins are organic compounds made of amino acids that are arranged in a linear chain and joined together by peptide bonds between the carboxyl and amino groups of adjacent amino-acid residues. The sequence of amino acids in a protein is defined by the sequence of genes that is encoded in the genetic code, which specifies 20 standard amino acids. The collagen is the main protein of CT in animals and the most abundant protein in mammals.

Among the substances, some are ungenerated and imperishable, while others partake in generation and perishing. Linus Pauling in 1970 indicated several

attributes that distinguish a living organism from an inanimate object [9]. One is the ability to reproduce – the power of having progeny belonging to the same species, being sufficiently similar to the parental organism. Another attribute is the ability to ingest certain materials and subject them to own metabolism. Also a capacity to respond to environment, possibility of healing, as well as the memory, and the capacity to learn are typical for living organisms. The complicacy of chemical processes and the constancy of biological systems that we recognize so easily in the heredity phenomenon appear to contradict our intuitions.

The cell theory states that all living beings are composed of cells, which can be regarded as the basic units of life, and that cells come from other cells [10]. Botanist Matthias Jakob Schleiden (1804–1881) was a cofounder of the cell theory, along with Theodor Schwann and Rudolf Virchow. The growth of an organism is effected by consecutive cell divisions (such a cell division is called *mitosis*). In biology, another division process, namely, meiosis is dealt with. Meiosis is a process of reductional division in which the number of chromosomes per cell is halved. In animals, meiosis always results in the formation of gametes, while in other organisms it can give rise to spores.

Many important substances in cells and tissues occur as thin, of the order of 20 Å, and highly elongate particles. (1 angström $\equiv$ 1 Å = 0.1 nm = 10^{-10} m.) Proteins (such as myosin, collagen, and nerve-axon protein), nucleic acids (DNA and RNA), and polysaccharides (cellulose and hyaluronic acid) are examples. Many of these substances are themselves polymers (as the protein macromolecules are polymers of many amino-acid residues) but, as monomers, these elongated macromolecules polymerize end-to-end and laterally to form fibrous structures. Schmitt *et al.* [12] suggested that tropocollagen (TC), the macromolecule of collagen, has dimensions of about 14 × 2800 Å [11–15].

The nucleic acids can be longer. DNA polymers contain millions of repeating units called *nucleotides*. One nucleotide unit is 3.3 Å (0.33 nm) long. Two nucleotides on opposite complementary DNA (or RNA) strands that are connected *via* hydrogen bonds are called a *base pair* (bp). In DNA, adenine forms a base pair with thymine, as does guanine with cytosine, and the DNA chain is 22–26 Å wide. The largest human chromosome, chromosome number 1, is approximately 220 million bp long. This gives a length of $0.33 \times 10^{-9} \times 220 \times 10^{6} = 72.6$ mm [16–18].

In Figures 1.1 and 1.2, one sees results of interactive computer animation – simulation of the famous Bragg–Nye bubble raft experiment. Two-dimensional crystallization is realized by equalizing distribution of atoms on torus, not only globally as enforced by Descartes–Euler Law, but also locally. Consecutive iterations repel atoms and shift them to centroids of Voronoi polygons. In consequence, the fraction of pentagon–heptagon pairs of defects (disclinations, curvatures, vortices, ...) among prevailing crystalline hexagons is gradually diminishing. A progressive coalescence and coarsening of crystal grains are occurring during rotations and growth of circular inclusions while five to seven edge dislocations align into migrating and rearranging grain boundaries [19]. In such systems, a local order cannot propagate throughout space. Contradiction

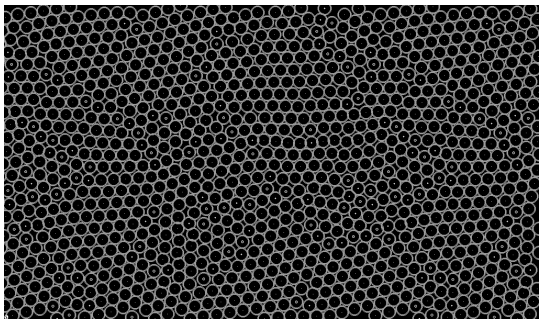

Figure 1.1 Frustrated matter – a prototype of biological medium: numerical simulation of Bragg–Nye bubble raft experiment [21], with Centroidal Voronoi network. Experiment produced image of a bubble raft showing vacancies and five to seven edge dislocations. Disclination 5 (with five neighbors) is denoted by white point, while disclination 7 (with seven neighbors) is denoted by white circle. Courtesy of Andrzej Lissowski.

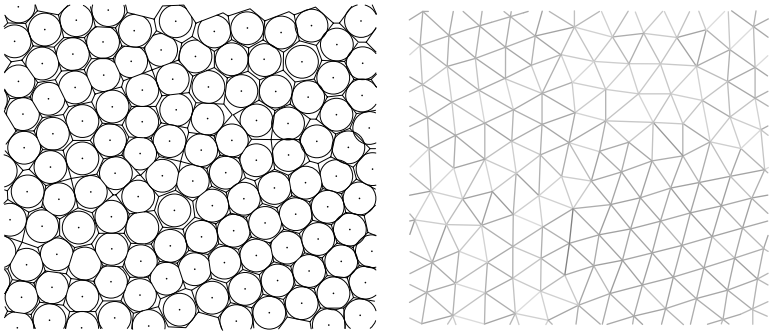

Figure 1.2 Pentagon–heptagon dipoles of dislocations in hexagonal lattice. (a) Numerical simulation of Bragg–Nye bubble raft experiment with Centroidal Voronoi network. (b) The same experiment in dual (triangular) representation. Courtesy of Andrzej Lissowski.

between local and global configurations is known as *geometrical frustration* [20].

From microorganisms to man, from the smallest cell organelle to the human brain, life presents us with examples of highly ordered cellular matter, precisely organized and shaped to perform coordinated functions [22].

A topological distribution of approximately hexagonal lattice of osteocytes in osteon and osteons in a compact bone is observed (cf. Figure 1.16). Creation of one new osteon leads to disturbance of the lattice and is equivalent to the lattice defects – two pentagon–heptagon (5–7) dislocations – analogous to those observed in crystal lattice, cf. Figure 1.1.

The problem of cell, in particular bone cell, communication is important. Paracrine signaling is a form of cell signaling in which the target cell is near

("para" = near) the signal-releasing cell. Two neurons would be an example of a paracrine signal. Only neighbor–neighbor interactions of osteocytes would permit them to create an image of the bone state. This would be in the spirit of the research by David G. Kendall, who in the 1970s discussed recovery of a structure from fragmentary information [23, 24]. Such a behavior was observed in a colony of bacteria or in another collective response to external disturbances by Howard Bloom in 2007, cf. [25]. The bone marrow, distributed in many parts, acts and reacts as one organ [26].

A quantitative experimentation is still needed for understanding the behavior of regulatory actions that manifest themselves in many biological systems, explaining principles of cellular information processing, and to advance predictive modeling of cellular regulation.

The body is made up of cells that communicate with each other and with external cues *via* receptors at their surfaces. To generate cellular responses, signaling pathways are activated, which initiate movement of proteins to specific locations inside the cells, notably the nucleus, where DNA is situated.

Enzymes called *kinases* are widely used to transmit signals and control processes in cells. One particular pathway is the extracellular signal-regulated kinase (ERK) pathway. ERKs act as messenger molecules by relaying signals that are received from outside the cell to the administrative core, the nucleus. To do so, ERK must move from the intracellular fluid to the nucleus of the cell and turn on several genes while turning off others, which in turn finally makes the cell to divide or differentiate. ERK's entry in the nucleus is unconventional, because the protein lacks the ability to bind to the known nuclear import proteins. Recently, Lidke and her colleagues showed that protein pairing – known as *dimer formation* – is not necessary for ERK to move into the nucleus after all. Instead, the process was found to be dependent solely on the rate at which stimuli activate the ERK. A delay in activation triggers a delay in nuclear entry of ERK, indicating that ERK entry in the nucleus is a direct consequence of activation [27].

Shekhter has applied the systems approach to the analysis of mechanisms whereby CT is integrated into one functional system. The primary CT functions in health and in disease (biomechanical, trophic, protective, reparative, and morphogenetic) are carried out by means of cell–cell, cell–matrix, and intertissue interactions based on feedback between these components. Both CT as a whole and its cellular and extracellular components exhibit structural and functional heterogeneity, which increases the capacity of CT for adaptation. Shekhter's study supports the concept of internal network regulation of the CT composition, functions, and growth through intercellular interactions at different levels of structure [28].

There is another analogy in which a bone structure resembles the mechanical structure of a tree trunk. In plants, the carbohydrate cellulose is the most important constituent of the wall cells, while in bones the hard skeleton in the exterior of bone cells is created by osteocytes. The resulting mechanical effect – a strong sponge-like structure – is similar. In biology, convergence of analogous (but without apparent common origin) structures is known as *homoplasy*.

1.1.1 The Structure of Living Organisms

The structure of the organism is realized by tissues. Malpighi (1628–1694), physician and biologist, studied subdivisions of the bone, liver, brain, spleen, kidneys, and skin layers, concluding that even the largest organs are composed of minute glands [29]. In 1835, before the final cell theory (which regards cells as the basic unit of life) was developed, Jan Evangelista Purkyně observed small ''granules'' while looking at the plant tissue through a microscope [30, 31].

As remarked by Pauling, chemical investigation of the plant viruses has shown that they consist of the materials called *proteins and nucleic acids*. Molecular weight of the enzyme urease is 483 000. The viruses (looked at sometimes as giant molecules) with a molecular weight of the order of magnitude of 10 000 000 may be described as aggregates of smaller molecules [9]. Viruses vary from simple helical and icosahedral shapes to more complex structures. Most viruses are about 100 times smaller than an average bacterium. Tobacco mosaic virus (TMV) is a rod-shaped virus of length 3000 Å, diameter 150 Å, and molecular weight 50 million. Franklin has shown that the TMV protein is in the form of structural subunits of molecular weight about 29 000 that are arranged on a helix of pitch 23 Å and the axial repeat period 69 Å [32, 33].

Many microorganisms, such as molds, bacteria, protozoa, consist of single cells, cf. Figure 1.3. These cells may just be big enough to be seen with an ordinary microscope, having diameter around 10 000 Å (=1000 nm = 1 μm = 1×10^{-6} m), or they may be much bigger – as large as a millimeter or more in diameter. For comparison, atomic diameters range between 1 and 2 Å. The cells have a structure, consisting of a cell wall, a few hundred angströms in thickness, within which is enclosed a semifluid material called *cytoplasm*, and other components. Other plants and animals consist largely of tissues – aggregates of cells, which may be of many different kinds in one organism. The muscles, blood vessels and lymph vessel walls, tendons, CTs, nerves, skin, and other parts of the body of a man consist of cells attached to each other to constitute a well-defined structure. There are also cells that are not attached to this structure, but float around in the body fluids. Most numerous among these cells are the red corpuscles of the blood. The red corpuscles in man are flattened disks, about 7500 nm in diameter and 2000 nm thick. There are about 5 million red cells per cubic millimeter of blood, and a man contains about 5 l of blood. Some cells are smaller, like the red cells, and some larger – single nerve cell may be about 1 μm in diameter and 100 cm long – extending from the toe to the spinal cord. A typical cell size is 10 μm, and a typical cell mass is 1 ng. The total number of cells in the adult human body is about 5×10^{14} [9]. Groups of cells combine and form tissue, which combines to form organs, which work together to form organ systems. The study of tissues is known as *histology*.

Some foreign cells, often nocive, also can dwell in bone. Osteomyelitis (osteo- from the Greek word osteon, meaning bone, myelo- meaning marrow, and its meaning is inflammation) means an infection of the bone or bone marrow. The infection is often caused by bacteria called *Staphylococcus aureus*, a member of the

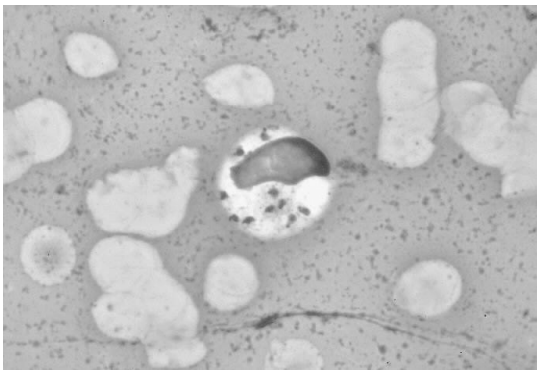

Figure 1.3 A protozoan *Leishmania donovani* in a bone marrow cell. Leishmania is a genus of parasites that are the etiologic agents of diseases of humans, such as leishmaniasis. After [34].

normal flora found on the skin and mucous membranes. In children, osteomyelitis usually affects the long bones of the arms and legs. Osteomyelitis often requires prolonged antibiotic therapy, and may require surgical debridement. Severe cases may lead to the loss of a limb [35, 36].

Leishmania is a genus of trypanosome protozoa and is the parasite responsible for the disease leishmaniasis, Figure 1.3. It is spread through sandflies. *Leishmania* commonly infects vertebrates: hyraxes, canids, rodents, and humans [34].

The body also contains the body fluids such as blood and lymph, as well as fluids that are secreted by other organs [9]. The bones are laid down as excretions of bone-making cells, called *osteocytes*. The quantitative proportion of cells in the mass of cartilage and bone is very low, while the major part is taken by extracellular substances. In the hollow interior of bones, bone marrow tissue is found. In adults, marrow in large bones produces new blood cells. It constitutes 4% of total body weight. The bone marrow is composed of stroma and parenchyma parts. Hematopoiesis is performed by parenchymal cells, while the stroma provides hematopoietic microenvironment.

Interaction of huge biomolecules with precision and infallibility is the essence of the living state. Looking at cell metabolism in relation to the intricate structure of a cell Peters (1930) stated that in the cell ''extreme order has to be reconciled with a fluid anatomy (. . .). The cell must be considered as a reflex entity, structurally organized so far as even its chemistry is concerned, with chains of chemical substances acting as it were as reflex arcs (. . .). It is perfectly possible to appreciate how a coordinated structure may be maintained in a medium which is apparently liquid. This theory is all, that is, needed to enable us to understand how substances can reach a special site in the cell. Between the chains of molecules, fixed by their radiating webs, there will exist paths from the external to the internal surface, the capillaries of the cell'' [37].

Wheatley observes that "as many as 4000 reactions may be occurring simultaneously in a cell (. . .) and every one has to be harmoniously controlled. There is no factory on earth that comes anywhere near this complexity and, at the same time, gives the fidelity or replicative performances while remaining flexible and adaptable to its environment" [38].

1.1.2 Growth of Living Organisms

It is supposed from the works of Braun, Schimper, brothers Bravais, Schwendener, Wulff, and Lewis that the crystallization and growth of a living tissue are similar [39–46]. The dislocations' gliding and climbing is the basis for such similarity. In two-dimensional packing, it is realized by the motion of pentagons and heptagons (five to seven) among crystalline hexagons.

One of the most striking aspects of symmetry in plants is in phyllotaxis – the arrangement of leaves on a stem or of flowers in the inflorescences. It is an interdisciplinary study involving mathematics, botany, and crystallography among others. The phyllotaxis should be properly studied at the shoot apical meristem (SAM). It is at the meristemic apex that the organs of shoot such as primordia of leaves, buds, or flowers originate, cf. also [47]. A *primordium*, in embryology, is defined as an organ or tissue in its earliest recognizable stage of development.

Biological systems are the best prototypes of genuine smart structures. A unique example is provided by considering the important and mysterious phenomenon of spiral phyllotaxis – leaf primordia packing with Fibonacci differences between nearest neighbors, Figure 1.4. For the Fibonacci spiral, in polar coordinates r and ϕ, the nth primordium has the position

$$r_n = A\sqrt{n}, \quad \varphi_n = C$$

where A is a constant, $C = 360^\circ \cdot u \approx 222.5^\circ$, and $u = (\sqrt{5} - 1)/2$, or, what is equivalent for structural form $C = 360^\circ/(2 + u) \approx 137.5^\circ$. The golden symmetry ratio u is typical for quasicrystals, and for the icosahedron dimensions.

As they grow, older primordia are displaced radially away from the center of the circular meristem. The newest primordium initiates in the least crowded space at the edge of the meristem. The growth process is accomplished in an exceptional order. Phyllotaxis compromises local interactions giving rise to long range order and assures the best way of optimal close packing.

Meristems are classified according to their location in the plant as apical (located at the root and shoot tips), lateral (in the vascular and cork cambia), and intercalary (at internodes, or stem regions between the places at which leaves attach, and leaf bases). Lateral meristems, found in all woody plants and in some herbaceous ones, consist of the vascular cambium and the cork cambium. They produce secondary tissues from a ring of vascular cambium in stems and roots. The lateral meristems surround the stem of a plant and cause it to grow laterally, cf. Figure 1.5. Nature uses the same pattern to place seeds on a seedhead, to arrange petals around the edge of a flower, and to place leaves around a stem.

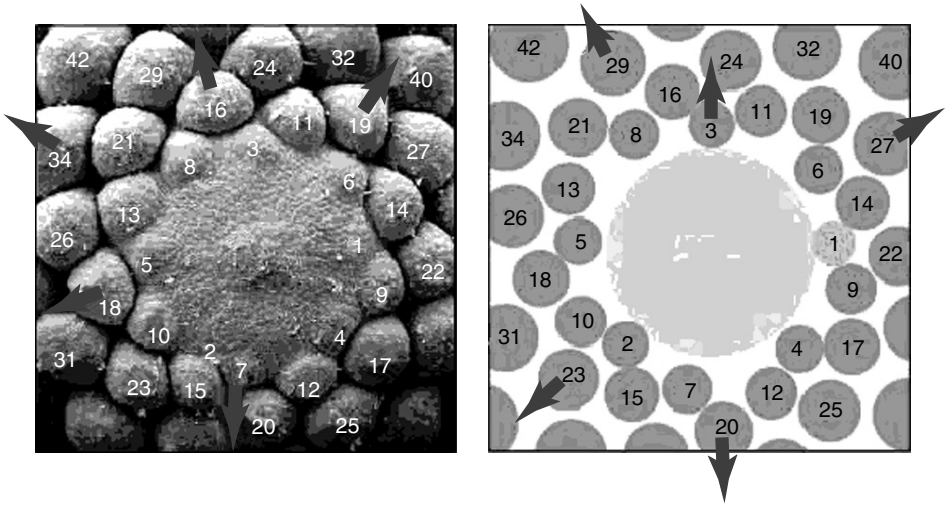

Figure 1.4 Norway Spruce (*Picea abies*): spiral phyllotaxis of needle primordia emerging from central SAM. The primordial numbers are in reverse order of their appearance. The newest primordium initiates at the periphery of the meristem where there is the largest free space. As they grow, older primordia are displaced radially away from the center of the circular meristem. Then, the older the primordium, the farther it is from the center. For example, the contact on the parastichy spiral with difference 5 (between 8 and 13 spirals) changes after 5–7 flip to the contact on the spiral with difference 21. After [48]. With kind permission of the author Pau Atela.

1.1.2.1 **Ring-Shaped Grain Boundary**

D'Arcy Thompson emphasized the deep correlation between mathematical statements, physical laws, and fundamental phenomena of organic growth of biological structures. At the end of "On Growth and Form" we read: " . . . something of the use and beauty of mathematics I think I am able to understand. I know that in the study of material things number, order, and position are the threefold clue to exact knowledge" [49].

Occurrence of defects begins a process of destruction of a crystal. Destruction is therefore necessary for the crystal growth, as shown by Rivier and Lissowski [50]. In a similar manner, appearance of one new osteon leads osteon lattice defects to arise – a pair of pentagon–heptagon (five to seven) dislocations. Hence, the bone turnover is realized by the defects of osteonic structure, cf. Figures 1.15 and 1.16 of compact bone structure.

In 1868, from his microscopic study of plant meristems, botanist Hofmeister [51] proposed that a new primordium always forms in the least crowded spot along the meristem ring, at the periphery of SAM.

In a manner analogous to the propagation of defects during crystallization, the growth of a tissue stress leads to buckling and undulation down to the order of the cell diameter. Structural control in tissue development is accomplished by wavelike 5–7 dislocation rearrangement. The oriented cell divisions as 5–7 climbing can

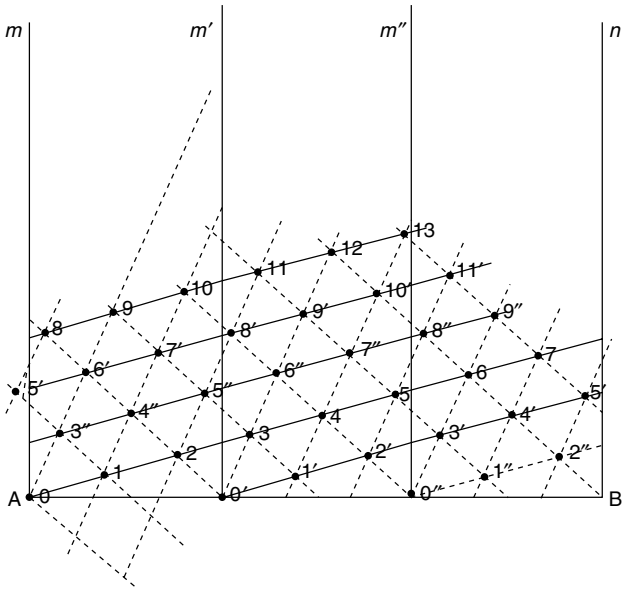

Figure 1.5 Spiral distribution of primordia around the cylindrical stem, after development on a plane, as observed by Bravais in 1837. The neighboring primordia differ by Fibonacci numbers: 1 along the solid lines, 3 along the dashed lines. After [42].

be explained in a similar manner. A vortex interpretation of the 5–7 pair in SAM growth was given in [52].

In a trial to explain the phyllotaxis pattern, Newell, Shipman, and Sun assume that the auxin-produced growth is proportional, in a first approximation, to how much average tensile stress the local elemental volume (which will contain many cells) feels. This is best measured by the trace of the stress tensor at that location. Fluctuations in auxin concentration influence the mechanical forces in the tunica by creating uneven growth and are manifested by an additional strain contribution in the stress–strain relationships. On the other hand, inhomogeneities in the stress distribution are assumed to lead to changes in auxin concentration. The exact way in which stresses influence biological tissue growth (weight-bearing bones and fruit stems become stronger) is still an open challenge to biologists [53].

Gebhardt in 1911 found a similarity between bone formation and the chemistry of colloids [54, 55]. He found that collagen fibrils are organized into distinct lamellae, the molecular orientations being parallel in each lamella. Much later, in 1988, it was pointed out by Giraud-Guille that together with normal (i.e., Gebhardt's) plywood architecture, a twisted plywood distribution of collagen fibrils in human compact bone osteons is observed, comparable with a liquid crystalline self-assembly [56]. Geometrical resemblance of long fibrils and long molecules leads to a similar arrangement of these objects.

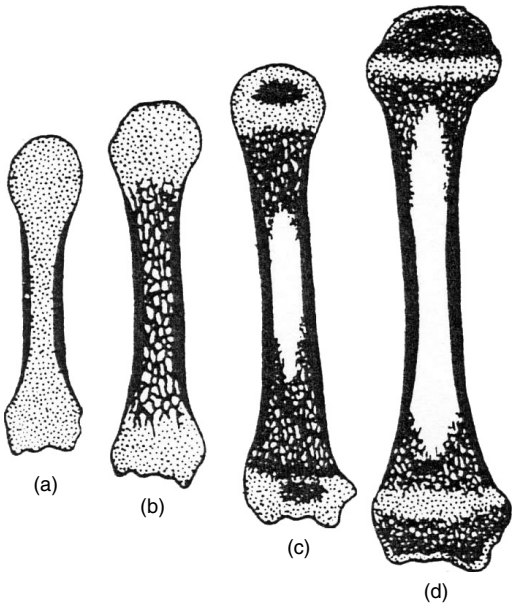

Figure 1.6 Ossification of a long bone: (a) hyaline cartilage model with surface ossification only; (b) development of trabecular bone network; (c) development of medullary cavity; (d) after achievement of bone maturity, only articular cartilage and epiphyseal plate are left from the cartilage tissue, while the medullary cavity is enlarged. Cartilage part is denoted by dots and the bone part is denoted by black color. After [66].

Remarkable symmetry characterizes crystals and organic forms, because both are subdued primarily to the topological laws of close packing by the Descartes–Euler theorem.

1.1.3 Planarity of Biological Structures

The development of living world is accomplished in two-dimensional structures. Such structures are easily accessible to environment and external influence. But it seems that the fundamental reason is geometrical topology. The Descartes–Euler theorem on polyhedra in three-dimensional space assures that, for a polyhedron, the following relation among the number of vertices N_V, number of edges N_E, and number of faces N_F is satisfied $N_V - N_E + N_F = 2$.

In two dimensions, this relation becomes more sharp, as only two independent numbers are left. Therefore, all processes with phase transformation are accomplished more easily in two dimensions. The Descartes–Euler Law forces the compensation of positive and negative curvatures in planar tissue: $3 \times p3 + 2 \times p4 + p5 = p7 + 2 \times p8 + 3 \times p9 +$ sum of $(N - 6) \times pN$ for $N > 9$ where pN are percentages of N-sided cells and each cell gives 6-N units of curvature.

The predominantly hexagonal cell pattern of simple epithelia was noted in the earliest microscopic analyses of animal tissues: a topology commonly thought to reflect cell sorting into optimally packed honeycomb arrays. The development of specific packing geometries is tightly controlled. For example, in the *Drosophila* wing epithelium, cells convert from an irregular to a hexagonal array shortly before hair formation. Packing geometry is determined by developmental mechanisms that likely control the biophysical properties of cells and their interactions, cf. [57–60].

1.2 Macroscopic Structure of the Bone

Bone tissue (or osseous tissue) is the main structural and supportive tissue of the body. The basic elements of the bone tissue are cells (osteocytes, osteoblasts, osteoclasts) and extracellular substance (ECM). The bone matrix consists of an organic part (collagen of type I and other proteins) and a nonorganic one (mainly hydroxyapatite).

CT consists of cells and extracellular materials secreted by some of those cells. Thus, the cells in CT may be separated from one another within the ECM. The ECM consists of ground substance and fibers. In many types of CTs, the matrix-secreting cells are called *fibroblasts*. Frequently, other cell types (e.g., macrophages, mast cells, and lymphoid cells) may also be present. Ground substance is a term for the noncellular components of ECM containing the fibers. This substance is gel like, amorphous, and is primarily composed of glycosaminoglycans (mostly hyaluronan), proteoglycans, and glycoproteins. CT is the most diverse of the four tissue types and fulfills different functions. Its consistency ranges from the gel-like softness of areolar CT to the hardness of bone.

Cells are surrounded by ECM in tissues, which acts as a support for the cells. Ground substance does not include collagen but does include all the other proteinaceous components, such as proteoglycans, matrix proteins, and, most prevalent, water. The noncollagenous components of ECM vary depending on the tissue, cf. monographs by Ross *et al.* [61, 62] and Gray's anatomy [63, 64].

1.2.1 Growth of the Bone

The development of all large complex animals and human beings is accomplished in a two-dimensional, layered way. The mesoderm germ layer is formed in the embryos of triploblastic animals. During gastrulation, some of the cells migrating inward contribute to the mesoderm (middle layer), an additional layer between the endoderm and the ectoderm. From the mesoderm, skeletal muscle, the skeleton, the dermis of skin, CT, the urogenital system, the heart, blood (lymph cells), and the spleen are formed [63].

There are two different methods of the ossification process: intramembranous ossification is bone formation from an organic matrix membrane, whereas endochondral ossification occurs within a cartilaginous model. However, there is only one mechanism of bone formation: the laying down of the osteoid matrix by osteoblasts, followed by the deposition of crystalline apatite [65].

In embryogenesis, the skeletal system is derived from the mesoderm germ layer. Chondrification (or chondrogenesis) is the process by which cartilage is formed from the condensed mesenchymal tissue, which differentiates into chondrocytes and begins secreting the molecules that form the ECM. Early in the fetal development, the greater part of the skeleton is cartilaginous. It is the *temporary* cartilage that is gradually replaced by the bone (endochondral ossification), a process that ends at puberty. The cartilage in the joints is *permanent* – it remains unossified during the whole of life.

During the fetal stage of development the bone can be formed by two processes: intramembranous or endochondral ossification. Intramembranous ossification mainly occurs during the formation of the flat bones of the skull; the bone is then formed from the mesenchymal tissue.

Endochondral (intracartilaginous) ossification occurs in long bones. In this process, the bone is formed from cartilage, which is gradually replaced by the bone as the embryo grows. The steps of endochondral ossification are visible in Figure 1.6.

Adult hyaline articular cartilage is progressively mineralized at the junction between cartilage and bone. It is termed *articular calcified cartilage*. A mineralization front advances through the base of the hyaline articular cartilage at a rate dependent on cartilage load and shear stress. Adult articular calcified cartilage is penetrated by vascular buds, and the new bone produced in the vascular space in a process similar to endochondral ossification at the physis. A cement line separates the articular calcified cartilage from the subchondral bone.

Both the bone and the cartilage are classified as supportive CT.

- Bone (osseous tissue) makes up the skeleton in adult vertebrates.
- Cartilage makes up the skeleton in chondrichthyes (known also as *cartilaginous fishes*). In most other adult vertebrates, the cartilage is primarily found in joints, where it provides bearing and cushioning.

Bone-forming cells called *osteoblasts* deposit a matrix of collagen, but they also release calcium, magnesium, and phosphate ions, which chemically combine and harden within the matrix into the mineral hydroxyapatite. The combination of hard mineral and flexible collagen makes the bone harder than cartilage without being brittle.

Bone marrow can be found in almost any bone that holds cancellous tissue. In newborns, all such bones are filled with red marrow only, but as the child ages it is mostly replaced by yellow, or fatty, marrow. In adults, red marrow is mostly found in the flat bones of the skull, the ribs, the vertebrae, and pelvic bones, cf. [67–73].

Figure 1.7 Cross section of the young rat tibia in development. The trabecular bone network with medullary cavity in the center is exposed. To the left, a smaller cross section of fibula is seen. Courtesy of Litwin and Gajda.

Endochondral ossification begins with points in the cartilage called *"primary ossification centers."* They mostly appear during fetal development, though a few short bones begin their primary ossification after birth. They are responsible for the formation of the diaphyses of long bones, short bones, and certain parts of irregular bones. Secondary ossification occurs after birth, and forms the epiphyses of long bones and the extremities of irregular and flat bones. The diaphysis and both epiphyses of a long bone are separated by a growing zone of cartilage (the epiphyseal plate), cf. Figures 1.6 and 1.7.

Epiphyseal plates (growth plates) are located in the metaphysis and are responsible for growth in the length of the bone, cf. Figure 1.10. Because of their rich blood supply, metaphysis of long bones are prone to hematogenous spread of *Osteomyelitis* in children.

When the child reaches skeletal maturity, all of the cartilage is replaced by the bone, fusing the diaphysis and both epiphyses together (epiphyseal closure).

Exterior shape of the bone is characteristic of every species and is revealed by different roughnesses, spikes, spicules, openings, and holes; it is an effect of modulating influence from the side of the soft components of the organism. This *paradoxal* observation is explained by the fact that bones develop relatively late when soft parts are formed, and the growing bone has to match its form to the shape of soft components.

1.2.2
Structure of the Body

The bones of vertebrates compose the internal skeleton of these organisms. Bones are divisible into four classes: long, short, flat, and irregular. The number of bones in the organism is variable and depends on the age.

There are 206 bones in the adult human body and about 270 in an infant. A human adult skeleton consists of the following distinct bones: skull (22): cranium (8), face (14); spine and vertebral column (26), hyoid bone, sternum and ribs (26), upper extremities (64), lower extremities (62), and auditory ossicles (6). The patellae are included in this enumeration, but the smaller sesamoid bones are not taken into account, cf. [66, 71–73, 77].

In particular, the metatarsal bones are a group of five long bones in the foot that are located between the tarsal bones of the hind- and mid-foot and the phalanges of the toes, see Figure 1.8. The metatarsal bones are numbered from the medial side (side of the big toe): the first, second, third, fourth, and fifth metatarsal. The metatarsals are analogous to the metacarpal bones of the hand. In human anatomy, the metacarpus is the intermediate part of the hand skeleton that is located between the phalanges (bones of the fingers) distally and the carpus, which forms the connection to the forearm.

The bone fulfills three essential roles in the organism:

- Mechanical (constructional) – being a scaffold of the body and being responsible together with skeletal muscles for the movement and locomotion of the organism;
- protective – shielding internal organs against external hurts;
- metabolic – hematopoietic processes of blood production by red and yellow marrow, within the medullary cavity of long bones and interstices of cancellous bone, storage of fat as yellow bone marrow, storage of minerals such as calcium and phosphorus, assuring acid–base balance by absorbing or releasing alkaline salts, necessary for holding the ionic homeostasis in the organism.

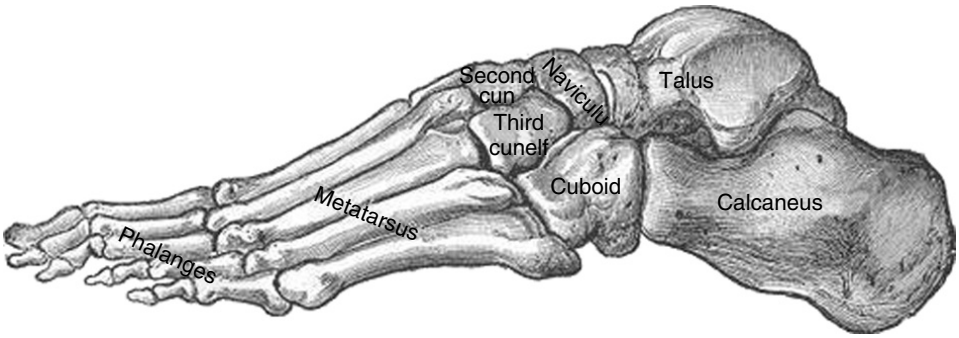

Figure 1.8 Skeleton of human foot with metatarsus, in lateral aspect. After [63].

The skeleton supports soft parts of the body, enables the movements of body and its members, and protects its internal organs (e.g., the skull protects the brain and the ribs protect the heart and lungs). Bones together with tendons, ligaments, joints, and skeletal muscles, steered by the nervous system, create forces and motion of the entire body or its parts only. Another mechanical function of the bone is linked to sound transduction in the ear and hearing. These mechanical functions are the subject of study in biomechanics.

The bone owes its hardness to the osseous tissue, which can be regarded as a composite material (mineralized organic matrix) formed of a mineral – hydroxyapatite and a protein – collagen. The living cells are embedded in the osseous tissue.

Bones are organs made up of bone tissue as well as marrow, blood vessels, epithelium, and nerves, while the term *bone tissue* specifically refers to the mineral matrix that forms the rigid sections of the organ.

1.2.3 Macroscopic Structure of Skeleton

The bones of the skeleton are joined to one another at different parts of their surfaces, and such connections are termed *joints* or *articulations*. It happens that the joints are *immovable*, as in the articulations between practically all the bones of the skull; the adjacent margins of the bones are almost in contact, being separated merely by a thin layer of fibrous membrane (sutural ligament). In certain regions at the base of the skull, this fibrous membrane is replaced by a layer of cartilage. In the *freely movable* joints, the surfaces are completely separated; the bones forming the articulation are expanded for greater convenience of mutual connection, covered by cartilage and enveloped by capsules of fibrous tissue. The cells lining the interior of the fibrous capsule form an imperfect membrane – the synovial membrane – which secretes a lubricating fluid. The joints are strengthened by strong fibrous bands called *ligaments*, which extend between the bones forming the joint.

Bones constitute the main elements of all the joints. In the long bones, the extremities are the parts that form the articulations; they are built of spongy cancellous tissues with a thin coating of compact substance. The layer of compact bone that forms the joint surface, and to which the articular cartilage is attached, is called the *articular lamella*. It differs from ordinary bone tissue in that it contains no Haversian canals, and its lacunae are larger and have no canaliculi. The vessels of the cancellous tissue, as they approach the articular lamella, turn back in loops, and do not perforate it; this layer is consequently denser and firmer than ordinary bone, and forms an unyielding support for the articular cartilage.

Cartilage is a nonvascular structure found in various parts of the body: in adult life, chiefly in the joints, in the parietes of the thorax, and in various tubes, such as the trachea, bronchi, nose, and ears, which require to be kept permanently open [63–73, 77].

1.2.4
Apatite in the Bone

The bone tissue is a mineralized CT. The bones consist of inorganic constituents, calcium hydroxyphosphate, $Ca_5(PO_4)_3OH$, also known as the *mineral apatite* (or hydroxyapatite, abbreviated sometimes as HA or HAP), and calcium carbonate $CaCO_3$, and an organic constituent, collagen, which is a protein. Nature has evolved sophisticated strategies for developing hard tissues through the interaction of cells and, ultimately, proteins with inorganic mineral phases.

Hydroxyapatite (or hydroxylapatite – according to the nomenclature accepted by the International Mineralogical Association) is a naturally occurring form of calcium apatite with the formula $Ca_{10}(PO_4)_6(OH)_2$ (it is written in this form to denote that the crystal unit cell comprises two entities). We have $Ca_{10}(PO_4)_6(OH)_2 \leftrightarrow 10Ca^{2+} + 6PO_4^{3-} + 2OH^-$. It has relatively high compressive strength but low tensile strength of the order of 100 MPa. It has a specific gravity of 3.08 and is 5 on Mohs hardness scale. It crystallizes in the hexagonal system.

Pure hydroxylapatite powder is white. Naturally occurring apatites can, however, also have brown, yellow, or green colorations, comparable to the discolorations of dental fluorosis. It is estimated that a modified form of the inorganic mineral hydroxylapatite (known as *bone mineral*) accounts for about 50% of the dry weight of bone.

A calcium phosphate mineral found in the bone is similar in composition and structure to minerals within the apatite group. It belongs to biominerals – minerals produced by living organisms. Apatites are widely distributed as accessory minerals in different rocks and are important for the study of geological thermal history [78–81].

Apatites have the general formula $Ca_{10}(PO_4)_6\ X_2$ where X denotes F (fluorapatite, abbreviated as FAp), OH (hydroxyapatite, abbreviated OHAp), or Cl (chlorapatite, ClAp). The apatite lattice is tolerant of substitutions, vacancies, and solid solutions; for example, X can be replaced by $1/2CO_3$ or 1/2O; Ca by Sr, Ba, Pb, Na, or vacancies; and PO_4 by HPO_4, AsO_4, VO_4, SiO_4, or CO_3.

The mineral of bones and teeth is an impure form of OHAp, the major departures in composition being a variable Ca/P mol ratio (1.6–1.7, OHAp is 1.66), and a few percent CO_3 and water. The mineral is microcrystalline. The crystals are approximately 15 nm wide by 40 nm long in bone and dentine, and 40 nm wide by 100 nm to 5 μm or more long in dental enamel. They are much thinner compared to their width. The mineral in the bone comprises crystals that are smaller than those in dental enamel, so that many of the constituent ions occupy surface, or near-surface, positions. The result is that there are greater uncertainties about the crystal structure of bone mineral, compared with that of dental enamel. Apatite OHAp is also used as a biomaterial, for bone replacement, and for coating metal prostheses to improve their biocompatibility. The osseous tissue without collagen would be hard and brittle, and its fairly large elasticity is contributed by collagen. Biological apatites present in the natural bone, dentin, and enamel

contain different amounts of carbonate: 7.4, 5.6, and 3.5 wt % (weight percent), respectively [78–80].

In 1945, Beevers and McIntyre, as a result of X-ray crystal analysis, discovered the (nano)porous structure of hydroxyapatite, recognized then as an essential mineral constituent of bone and of the enamel and dentin of teeth [81]. They have shown that the unit cell of the apatite structure has two equal edges inclined at 120° to one another. These edges are of length 9.37 Å in the case of fluorapatite and 9.41 Å in the case of hydroxyapatite. The third edge is at right angles to these and has a length of 6.88 Å in both fluor- and hydroxyapatites. They also indicated the three important properties of apatite structure: (i) apatites have a tunnel structure with walls composed of corner-connected CaO_6 and PO_4 polyhedra as relatively invariant units; (ii) filling of these tunnels by Ca and anions (OH, F) leads to adjustments that best satisfy bond-length requirements; and (iii) even slight changes in the ionic radii of the tunnel atoms lead to expansion or contraction of the tunnel. It was proposed that the ''very critical fit'' of the fluorine and hydroxyl ions was responsible for the greater stability of fluorapatite, consistent with the fact that bone could take up fluorine selectively even from dilute solutions.

The size of the hexagonal channels is mainly determined by the calcium and phosphate arrangement. Another feature is the planar arrangement of three Ca atoms around each F in fluorapatite or OH in hydroxyapatite. From these two features, it results that the structure is selective in its choice of ions to occupy the position of the F ions in fluorapatite.

The only ions known to occupy these positions are the ions F^- and OH^-, and these two are nearly of the same size. Each has two K and eight L electrons, but F^- has one nucleus with charge +9, while OH^- possesses two nuclear charges +8 and +1, respectively. This makes OH^- just a little larger than F^-. The hydroxyapatite structure is a little expanded as compared with the fluorapatite one.

The critical fit of the F or OH ion is responsible for the difference in the stability of the two apatites. The fluorapatite is more stable. It is shown by the well-known facts that the fossil bone becomes gradually transformed from hydroxyapatite to fluorapatite, and that bone will take up fluorine selectively even from media very dilute in fluorine. The sensitivity of the macroscopic structure of teeth to fluorine and the relation between the incidence of dental caries and fluorine content are the other observations that have practical implications.

As is seen in Figure 1.9, there are four different types of crystallographic positions in the apatitic unit cell: (i) tetrahedral sites for six P^{5+} ions, each in fourfold coordination with oxygen, (ii) Ca [1] sites for four of the Ca^{2+} ions, (iii) Ca [2] sites for the six other Ca^{2+} ions (arranged in such a way that they form a channel along the *c*-axis, the so-called anion-channel), and (iv) the channel site, which is typically occupied by two monovalent anions (most commonly OH^-, F^-, and Cl^-) per unit cell. Among these anions, the one that best fits into the channel site is F^-. Its ionic radius is small enough to permit F^- in the most symmetric position in the channel (i.e., on mirror planes perpendicular to the *c*-axis), and thus fluorapatite is the apatite with the highest symmetry. Because the OH^- ion is not spherical, the two mirror planes normal to the *c*-axis channel cannot be

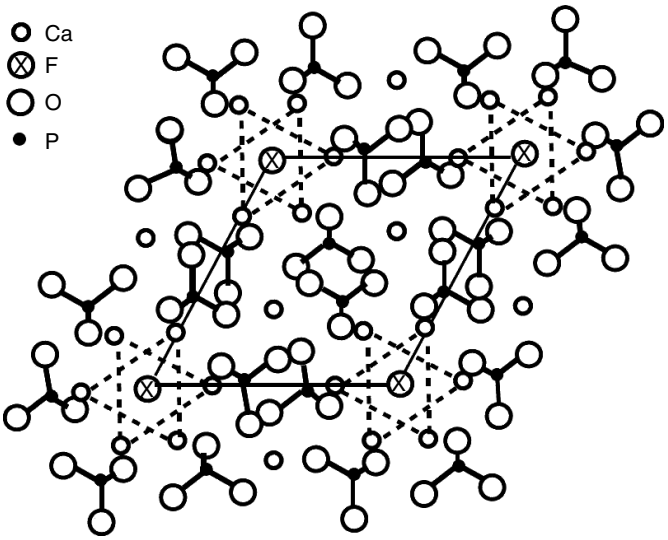

Figure 1.9 Three-dimensional structure of fluorapatite. View down the *c*-axis showing PO_4 tetrahedral ionic groups, Ca-ions, and channel ions. The parallelogram indicates the outline of the unit cell. The unit cell consists of two triangular prismatic subcells forming a rhombic prism. Six of the Ca^{2+} atoms form a sixfold site (indicated by dashed lines) in which the channel ions reside (F^- in the case of fluorapatite). These channels are oriented perpendicular to the page. Every crystallographic site (including the channel site) has a certain size, and thus not every atom or ionic group will fit into each site (the sizes of atoms are not drawn to scale). After [82].

preserved in hydroxylapatite. Thus, it has a lower symmetry than fluorapatite. Such differences in symmetry impact the growth morphology of the crystals, important to the mechanical properties of a composite material like bone.

Wopenka and Pasteris commented in 2005 that in the contemporary biomedical, orthopedic, and biomaterials literature, the mineral component of bone is still usually referred to as *hydroxy(l)apatite* or *carbonated hydroxy(l)apatite*, as if biological apatite were a well defined and well understood material. Whereas the Raman spectra of apatite in enamel, just like those of both geologic OHAp and synthetic OHAp, show the O–H modes for hydroxyl within the apatite structure, the spectra for apatite in bone do not. This is the property of all cortical bones of different mammals that were analyzed in [82].

The crystallographic structure of bone apatite is similar to that of OHAp, but there are important differences. The Raman spectra of synthetic OHAp, geologic OHAp, human enamel apatite, and cortical mouse bone apatite provide several differences between OHAp and biological apatites.

The bone apatite does not have a high concentration of OH groups, which is the feature of the mineral hydroxylapatite. Some bone apatites may not contain any OH groups at all. There is growing evidence for the lack of OH in bone apatite based not only on the results obtained *via* Raman spectroscopy but also on

results of infrared spectroscopy, inelastic neutron scattering, and nuclear magnetic resonance spectroscopy, cf. [82–86].

1.2.5 Structure of the Bone

The structure of bone is nonhomogeneous. The bone tissue contains two main types of tissues: dense cortical bone and porous trabecular bone, cf. Figure 1.10. The tissues have similar biological activity; the difference is in geometry – in the arrangement of the microstructure. The outer layer of bone tissue is hard and is called the *compact bone* (known also as *cortical* or *dense bone*). This part of the tissue gives bones their smooth, white, and solid appearance, and accounts for 80% of the total bone mass of an adult skeleton. Compact bone tissue is called so because of its very small gaps and spaces in comparison with the inner trabecular bone.

Trabecular (cancellous or spongy) bone accounts for approximately 15% of the total bone mass. The vertebrae and pelvic bones contain relatively high amounts of trabecular tissue and are common sites of osteoporotic fractures, whereas the long bones (e.g., femoral neck) contain a relatively high amount of cortical bone.

The metaphysis is the wider portion of a long bone adjacent to the epiphyseal plate, cf. Figure 1.10b. It is this part of the bone that grows during childhood; as

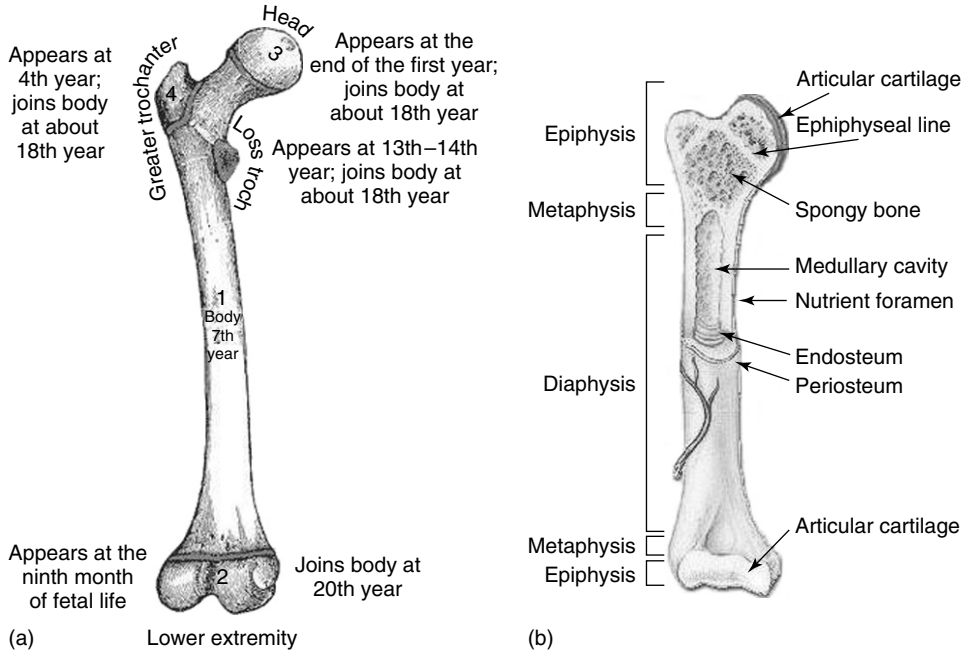

Figure 1.10 Human femur. (a) Development and (b) anatomical structure. It is noted that the metaphysis is essential for the growth of long bone. After [63, 74–76].

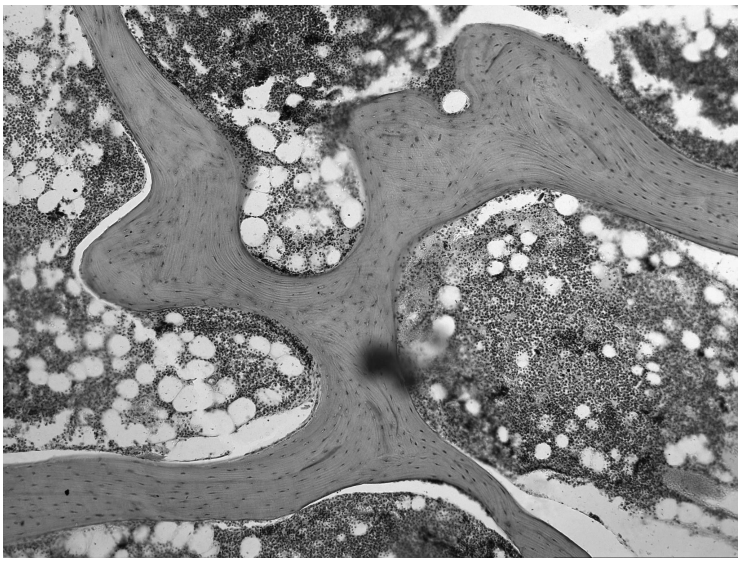

Figure 1.11 The spongy bone in histological section. The trabecules are surrounded by the marrow, and white spheres of fat in the marrow are seen. Courtesy of Litwin and Gajda.

it grows, it ossifies near the diaphysis and the epiphyses. At about 18–25 years of age, the metaphysis stops growing and completely ossifies into a solid bone.

The interior of the bone is known as the *spongy bone* (or cancellous or trabecular bone), cf. Figures 1.10b and 1.11. Spongy tissue has porous appearance and is composed of a network of trabecules, and rod- and plate-like elements that make the tissue lighter and allow space for blood vessels and marrow. Spongy bone accounts for 20% of the total bone mass, but (from macroscopic point of view) has nearly 10 times the surface area of compact bone.

1.3 Microscopic Structure of the Bone

1.3.1 General

Bone is composed of three major components: (i) small plate-shaped crystals of carbonate apatite, (ii) water, and (iii) macromolecules, of which type I collagen is the major constituent. The manner in which the crystals and the collagen fibrils are organized in a bone has not been resolved yet. In mineralized collagen fibrils of turkey tendon, the crystals are arranged in parallel layers across the fibrils, with the crystal *c* axes aligned with the fibril lengths, and in rat bones the plate-shaped crystals are also arranged in parallel layers within individual lamellae [76].

There are two methods of preparing sections for microscopy. One method provides the dry bone section. A piece of dead bone is broken or sawed from the main bone. Next, it is ground and polished to be very thin (about 15–45 μm thick). That polished piece is placed on a microscope slide and viewed directly. The bone cells are missing from the dead, polished bone specimen, and in a humorous sense one is looking at a skeleton of the skeleton. A second method for obtaining bone for histology is to soak a piece of bone in an acid solution for some time. The acid treatment dissolves the bone salts from the tissue in a process called *demineralization*. With this method, the cells stay behind and can be stained before observation under the microscope, cf. [87].

It is seen in Figure 1.12 that the bone is porous at two scales: containing macropores measuring 100 μm or more (Haversian and Volkmann's canals, lacunae), and micropores measuring up to 0.02 μm (= 20 nm) in diameter (canaliculi). The double porosity and interconnectedness of pores enable the bone to fulfill two vital

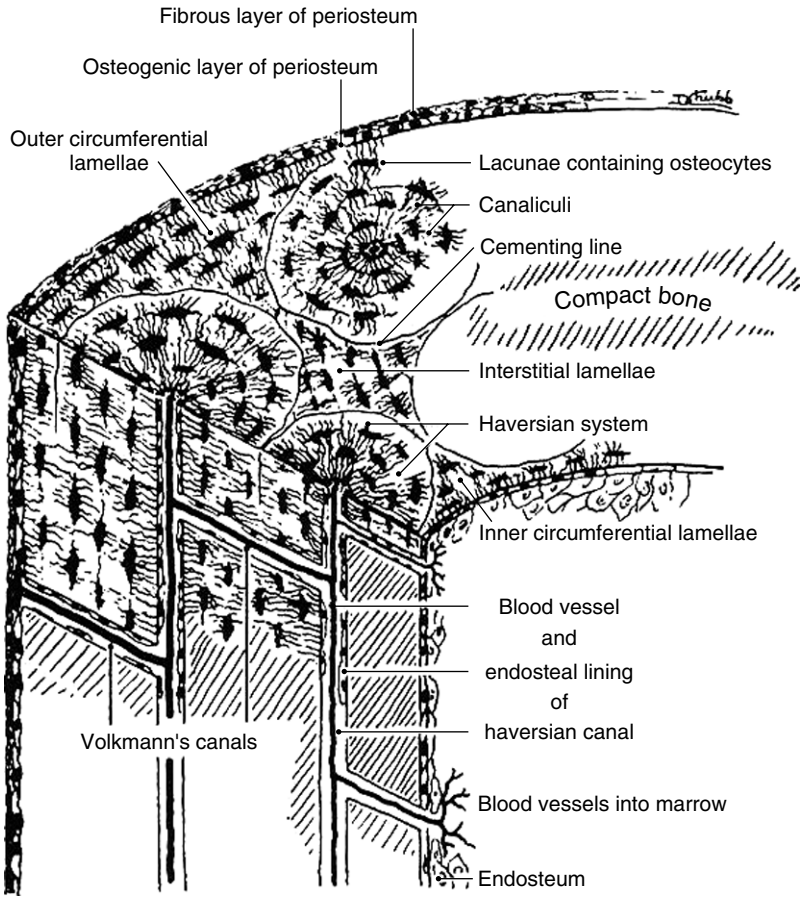

Figure 1.12 Design of the microstructure of cortical bone. After Piekarski and Munro [88].

functions. The macropores give space to permit bone cells to grow and allow blood to circulate, and the micropores facilitate the cell adhesion and crystallization of bone structure.

1.3.2 Osteon

The principal organizing unit of the compact bone is the osteon. A synonym for osteon is Haversian system. The osteon can be approximated as a long narrow cylinder that is 0.2 mm (200 μm) wide and 10 mm long. Osteons are found in the bones of mammals, birds, reptiles, and amphibians, running in a meandering way but generally parallel to the long axis of bones. Morphology of the osteon, obtained by electron microscopic techniques, for the study of compact bone is given in [89].

When the compact bone osteons are being formed, collagen fibers are laid down first. The collagen patterns are reflected in the structure known as a *lamella*. Osteons have between 4 and 20 lamellae with each measuring between 3 and 7 μm in width.

Leeuwenhoek, the father of microbiology, had reported his observations of the canal system in bones to the Royal Society of London in 1678. He called the canals *pipes*, and pointed out that they run both longitudinally and transversely in bones [90–92]. Thirteen years later, Havers did provide a more extensive description of the canal system in bones, linking it with his ideas of the lamellar nature of the bone tissue [93]; see also [94–96].

The group of cells functioning as an organized unit was called *basic multicellular unit* or bone multicellular unit (BMU) by Frost [97–100]. Remodeling process occurs with a specific sequence of events in the BMU.

The microscopic structure of a mammalian compact bone consists of repeating units called *osteons* or *Haversian systems*. Each system has concentric layers of mineralized matrix, called *concentric lamellae*, which are deposited around a central canal, also known as the *Haversian canal*, containing blood vessels and nerves that service the bone. By the longitudinal axis of the osteon runs a central canal, called the *Haversian canal* (synonyms: *Canalis nutricius*, *Canalis nutriens*, Haversian space, nutrient canal of bone) [101–103]. The elements of the osteon are shown in Figure 1.13.

The central canal is surrounded by concentric layers of matrix called *lamellae*. The lamellae are laid down one after the other over time, each successive one inside

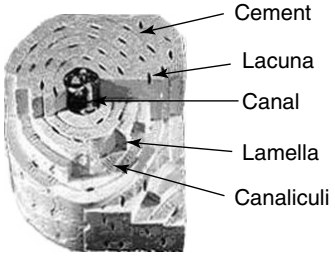

Figure 1.13 Elements of an osteon. After [87]. With permission of the author Blystone.

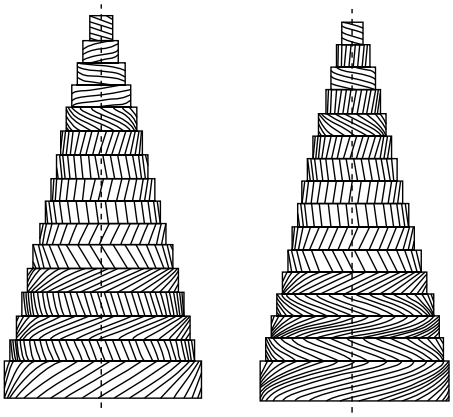

Figure 1.14 Examples of the osteon structure according to Gebhardt, with different collagen fiber orientations in the osteon lamellae. Helical course of fibers are noted at the successive lamellae. After [104].

the preceding one. Collagen fibers in a lamellae run parallel to each other but the orientation of collagen fibers across separate lamellae is oblique, cf. Figure 1.14. The fiber density is also lower at the border between adjacent lamellae, which accounts for the distinctive appearance of an osteon. In addition to blood vessels, Haversian canals contain nerve fibers and bone cells called *bone lining cells*. Bone lining cells are actually osteoblasts that have taken on a different shape following the period in which they have formed bone.

In 1905, Gebhardt [104, 105] performed research on bone structure, in particular on osteon architecture, using optical polarized microscope. Observations under polarized light indicate preferable directions of fibers in the lamellae of osteon. As a result, Gebhardt found that osteons are composed of a number of lamellae in which collagen fibers lay in different directions, cf. Figure 1.14.

These observations were repeated half a century later by Ascenzi and Bonucci [106–108]. They suggested that osteons that appear bright under polarized light are composed of lamellae in which collagen fibers lay (in prevailing number) parallel to the plane and perpendicular to the Haversian canal. The dark osteons under polarized light in their model consist of lamellae in which collagen fibers are oriented parallel to the long axis of the bone. In intermediate (alternating) osteons, collagen fibers should in this classification alternate orientation from one lamella to the other, having some lamella in which collagen fibers are orientated parallel (dark bands) and some orientated perpendicular (bright bands) to the long axis of the bone.

Ascenzi and Bonucci examined the mechanical properties of these three classes of osteons. Dark osteons were found to be the strongest under tensile loading. Bright osteons were stronger under compression. Intermediate osteons possess intermediate properties between bright and dark osteons, cf. [106–112] (also [113]).

The structure used by Gebhardt (as well as by Ascenzi and Benucci) is known as the *orthogonal plywood model*: only two fibril directions exist, making an angle 90°. Next, in 1988, Giraud-Guille presented the twisted plywood model of collagen fibril orientation within cortical bone lamellae. The twisted plywood model allows for parallel collagen fibrils, which continuously rotate from one plane to another in a helical structure [56].

Lying between or within the lamellae are special holes known as *lacunae*. Each lacuna has an oblong ellipsoidal form and provides enough space for an individual bone cell (osteocyte) to reside. In a microscopic section, viewed by transmitted light, lacunae appear as fusiform opaque spots. Lacunae are connected to one another by small canals called *canaliculi*. The osteocyte inside the lacuna is responsible for secreting the bone salts surrounding it. Osteocytes are found between concentric lamellae, within their cavelike lacunae, and connected to each other and the central canal by cytoplasmic processes through the canals called *canaliculi*. Osteocytes communicate with each other, and their network permits the exchange of nutrients and metabolic waste. The human osteocyte under normal conditions lives for about 25 years. Thus, in the lifetime of a person there would be about four generations of osteocytes.

Osteons are separated from each other by cement lines. Collagen fibers and canaliculi do not cross cement lines. The space between separate osteons is occupied by interstitial lamellae, which were formed by preexisting osteons that have since been reabsorbed. Osteons are connected to each other and the periosteum by oblique channels called *Volkmann's canals*.

Figures 1.15 and 1.16 are images of a sectioned bone. Cross section of a real osteon is not perfectly circular and the lamellae are not perfectly concentric.

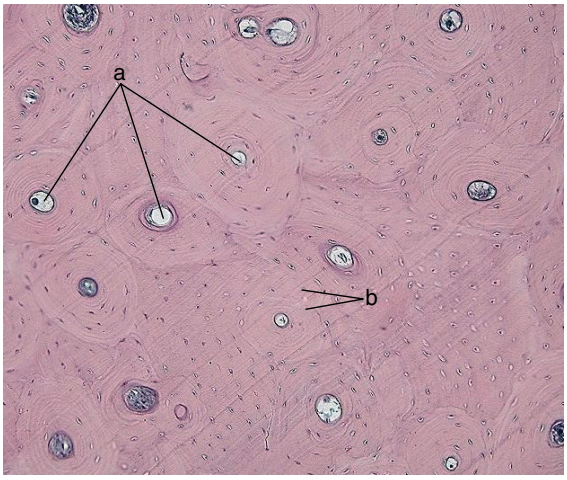

Figure 1.15 Compact bone – decalcified cross section. Osteonic structure is seen in the magnification: a – Haversian canals; b – lacunar spaces. Courtesy of Litwin and Gajda.

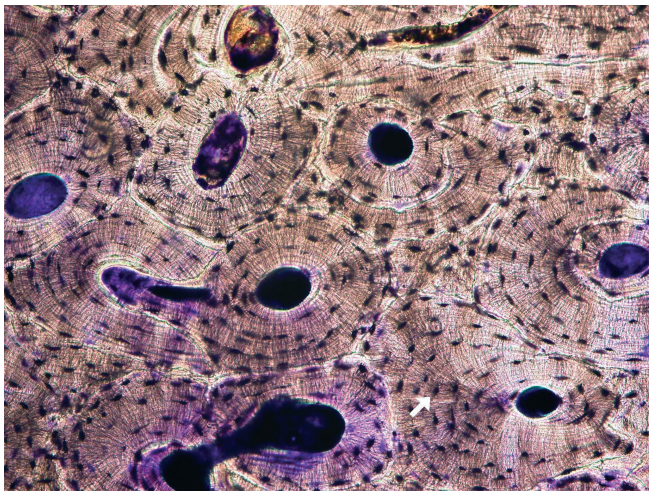

Figure 1.16 Compact bone – ground cross section. System of osteons that is visible in transverse histological section of the cortical bone. Haversian canals (large dark circular holes) are surrounded by the rings of lamellae. The Haversian canal in the center of the osteon has a diameter ranging between 50 and 90 μm. The smaller dark circles or ellipses (one is indicated by white arrow) are lacunar spaces within the osteon. In lacunae, the bone cells – osteocytes – are sheltered. Volkmann's canals, linking Haversian ones, are also seen in the lower part of the figure. Courtesy of Litwin and Gajda.

Impressive microphotographs, being the images of osteon in large magnification, obtained by means of scanning electron microscopy (SEM), were provided by Frasca *et al.* [114]. The arrangements of collagen fibers in lamellae are shown here, for example, decalcified osteon sample with exposed lamellar interfaces (×200), coexisting longitudinal and transverse fibers in one lamella (×1000), and complex fiber arrangement in one lamella, with partial stripping of two sequential lamellae.

The manner in which the crystals and the collagen fibrils are organized in the osteon has still not been resolved, even though it is known that they are intimately related.

Weiner, Arad, and Traub observed in 1991 that the plate-shaped crystals of rat bone are arranged in parallel layers that form coherent structures up to the level of individual lamellae. The crystal layers of the thin lamellae are parallel to the lamellar boundary, whereas those of the thicker lamellae are oblique to the boundary. The basic structure of rat bone can be described as *rotated plywood* [115].

Enlow in his microscopic study of the bone at the tissue level considered that a bone section is always a slice at the time of ontogeny. The actual tissue types express the succession of events that took place at that very level during bone development [116].

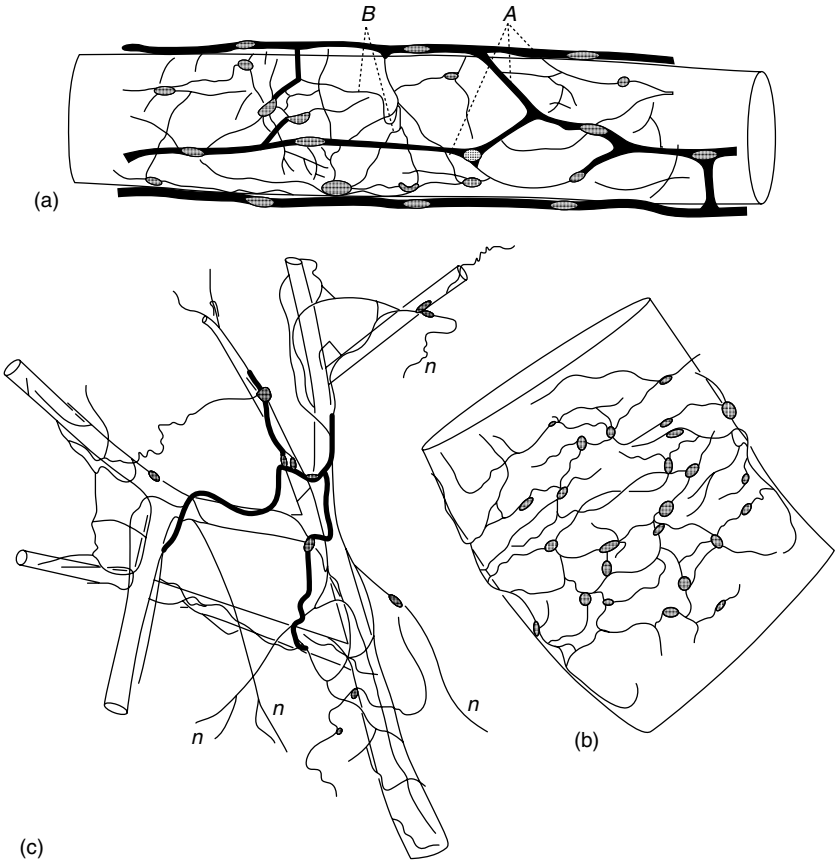

Figure 1.17 Innervation of bone marrow. (a) Plexus of nerve fibers around a vein in the marrow of rabbit tibia. (b) Portion of nerve plexus around an artery in the marrow of rabbit tibia. (c) Plexus of nerve fibers touching arteriola in the marrow of chicken tibia. The thinnest nerve fibers, denoted by *n*, penetrate in the pulp of marrow. After [118].

1.3.3 Bone Innervation

Bone is not only richly supplied with blood but is also abundantly innervated. The study of bone innervation dates back to the first half of the nineteenth century when Gros described the distribution of nerves in the femur of a horse [117]. Even early morphological studies applying classic histological methods, such as methylene blue staining and silver impregnation, revealed an intense innervation pattern of the bone in mature animals and humans, cf. also [118–120]. That the bone marrow is innervated is known since 1901 when Ottolenghi discussed the presence of nerves surrounding marrow arteries with fibers passing into the parenchyma,

cf. Figure 1.17. According to Ottolenghi, the nerve fibers within the marrow cavity fall into three main groups: (i) those that penetrate the walls of arterioles and form delicate plexiform networks between the adventitia and the media, (ii) those that surround the capillaries, and (iii) those that terminate between the cells of parenchyma.

Fliedner *et al.* [26] studied the question concerning the mechanisms that allow the bone marrow hemopoiesis to act as one cell renewal system although the bone marrow units are distributed throughout more than 100 bone marrow areas or units in the skeleton. The effect that ''the bone marrow'' acts and reacts as ''one organ'' is due to the regulatory mechanisms: the humeral factors (such as erythropoietins, granulopoietins, thrombopoietins, etc.), the nerval factors (central nervous regulation), and the cellular factors (continuous migration of stem cells through the blood to assure a sufficient stem cell pool size in each bone marrow ''subunit'').

The nervous system is differentiated into efferent nerves and afferent nerves. Efferent nerves – otherwise known as *autonomic or motor or effector neurons* – carry nerve impulses *away* from the central nervous system to effectors such as muscles or glands. The opposite activity of direction or flow is afferent (sensory) [121].

The majority of the skeletal innervation system is composed of sensory fibers originating from primary afferent neurons located in the dorsal root and some cranial nerve ganglia, whereas the other nerve fiber populations are adrenergic and cholinergic in nature and originate from paravertebral sympathetic ganglia. The

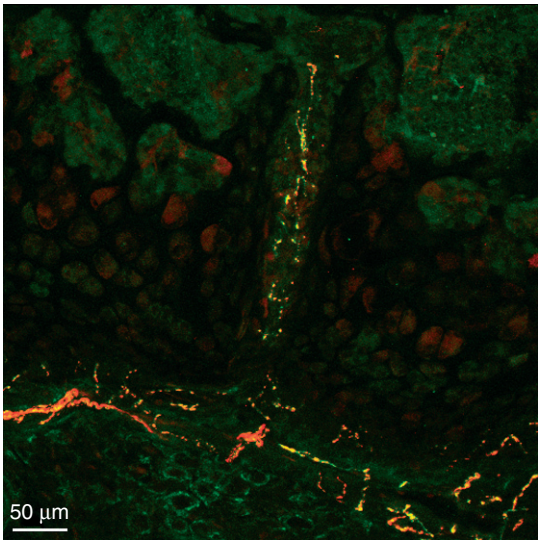

Figure 1.18 Nerve fibers in the canal between periosteum and proximal mataphysis of four-week rat tibia. Growth-associated protein (GAP-43) and protein gene product (PGP) 9.5 are visible. Courtesy of Litwin and Gajda.

sensory fibers were detected in the periosteum, bone marrow cavity, and vascular canals in long bones of mature and developing animals.

The blood vessels in the bone marrow are abundantly innervated, through both sympathetic and afferent nerve fibers. Afferent nerve fibers are also connected with receptors imbedded in the parenchyma of marrow [121]. In Figure 1.18, an example of the innervations is given.

Growth-associated protein (GAP-43) is expressed in conditions of embryonic growth, during axonal regeneration, and even at maturity in certain areas of the brain known to exhibit synaptic plasticity. Protein gene product (PGP) 9.5 is a cytoplasmic protein specific for neurites, neurons, and cells of the diffuse neuroendocrine system. GAP-43 and PGP 9.5 are often used as neuronal markers, cf. [122].

In the field of neuroscience, tachykinin peptides are one of the largest families of neuropeptides, found from amphibians to mammals. They are named so because of their ability to rapidly induce contraction of gut tissue. Tachykinins are widely distributed in the body and function as neurotransmitters and neuromodulators. Five tachykinin subtypes: substance P (SP), neurokinin A, neurokinin B, neuropeptide K, and neuropeptide Y; and three receptor subtypes: neurokinin-1, -2, and -3 receptors, have been identified. SP was the first peptide of the tachykinin family to be identified. It is considered to be an important neuropeptide, and to function in the nervous system and intestine. However, recent studies in the analysis of SP receptors, particularly neurokinin-1 receptors (NK_1-Rs) that have high affinity for SP, have demonstrated that NK_1-Rs are distributed not only in neurons and immune cells but also in other peripheral cells, including bone cells [123]. The distribution of tachykinin-immunoreactive axons and neurokinin receptors suggests that tachykinins may directly modulate bone metabolism through neurokinin receptors, cf. survey paper on the bone innervations by Goto [124], and also [125].

SP is an undecapeptide with multiple effects on the cardiovascular, gastrointestinal, and urinary systems as well as complex central nervous system functions such as learning and memory. SP is released from the terminals of specific sensory nerves; it is found in the brain and spinal cord, and is associated with inflammatory processes and pain [126, 127].

1.3.3.1 Anatomy of Bone Innervation

An extensive plexus of nerve fibers investing the periosteum and joints gives bone the lowest pain threshold of any of the deep tissues. A-delta (small myelinated) fibers and C (small unmyelinated) fibers contain deep somatic nociceptors with free nerve endings. Deep somatic pain is usually described more as aching than sharp, and is less well localized than cutaneous somatic pain. In the human femur, all cortical Volkmann's and Haversian canals contain unmyelinated fibers, and some contain both myelinated and unmyelinated fibers. SP, which mediates pain sensation, is attached to these fibers.

In rat and dog models, nerves in bone marrow have been found to be associated with venous sinuses. These are single fiber nerves, independent of the blood

vessels in the marrow, that enter the Haversian canals from both periosteum and the marrow.

Gajda *et al.* [128] investigated the development of sensory innervation in long bones, see Figure 1.18. Their model was rat tibia in fetuses and in juvenile individuals on postnatal days. A double immunostaining method was applied to study the co-localization of the neuronal growth marker GAP-43 and the pan-neuronal marker PGP 9.5 (9.5) as well as that of two sensory fiber-associated neuropeptides, calcitonin gene-related peptide (CGRP) and SP. The earliest, not yet chemically coded, nerve fibers were observed in the perichondrium of the proximal epiphysis. Further development of the innervation was characterized by the successive appearance of nerve fibers in the perichondrium/periosteum of the shaft, the bone marrow cavity and intercondylar eminence, the metaphyses, the cartilage canals penetrating into the epiphyses, and finally in the secondary ossification centers and epiphyseal bone marrow. Maturation of the fibers, manifested by their immunoreactivity for CGRP and SP, was investigated in these cases also.

1.3.4 Bone Cells

1.3.4.1 Cells

The living cells are divided into two types: prokaryotic and eukaryotic. The prokaryotes are organisms that lack a cell nucleus (karyon). Prokaryotes are divided into the bacteria and archea. Animals, plants, fungi, and protists are eukaryotes – organisms whose cells are organized into complex structures enclosed within membranes. The defining membrane-bound structure that differentiates eukaryotic cells from prokaryotic cells is the nucleus. The cells of protozoa, higher plants, and animals are highly structured. These cells tend to be larger than the cells of bacteria, and have developed special packaging and transport mechanisms that are appropriate to their larger size. There are many different cell types: approximately 210 distinct cell types in the adult human body.

In Figures 1.19 and 1.20, the animal and plant cells may be compared. It is seen that a cell wall – a thick, rigid membrane – surrounds a plant cell. This layer of cellulose fiber gives the cell most of its support and structure. The cell wall also bonds with other cell walls to form the structure of the plant.

Existence of wall in the plant cell provides the main difference between plant and animal body from a mechanical point of view. The wall in plant cell gives the plant support and structure. The animal body whose cells have no walls should be supported by special tissues – the bones in the case of vertebrates.

The cytoskeleton (a cellular skeleton or cell scaffolding) is present in all cells, being contained within the cytoplasm. It is a dynamic structure made out of protein molecules that protects the cell, maintains the cell shape, enables cellular motion (using structures such as flagella, cilia, and lamellipodia), and plays important roles in both intracellular transport (such as the movement of vesicles and organelles) and cellular division. Microfilaments (or actin filaments) are the thinnest filaments of the cytoskeleton found in the cytoplasm of all eukaryotic cells [130–135].

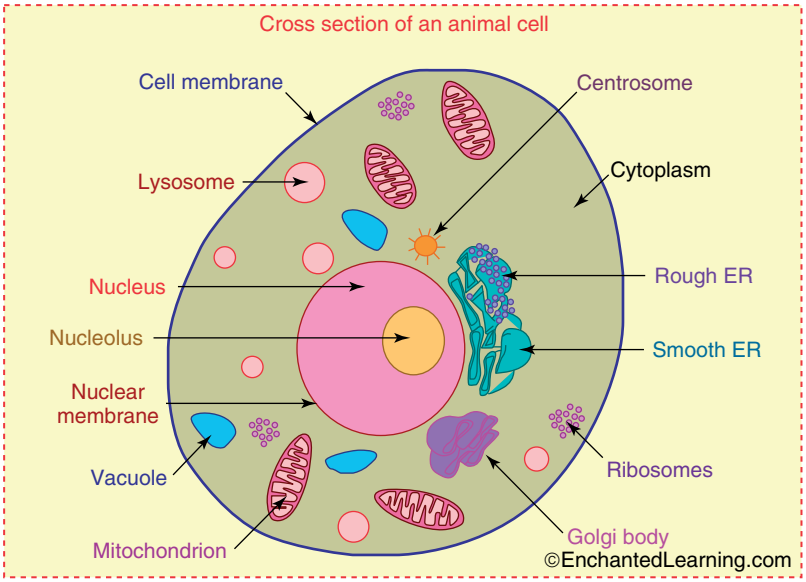

Figure 1.19 An animal cell. Peptide chains, alpha-1 and alpha-2 chains, known as pre-procollagen, are formed during translation on ribosomes along the rough endoplasmic reticulum (Rough ER, RER) inside the cell. Triple helical structure is formed inside the endoplasmic reticulum from each two alpha-1 chains and one alpha-2 chain. Procollagen is shipped to the Golgi apparatus, where it is packaged and secreted by exocytosis. After [129].

Leeuwenhoek [91] pointed out an analogy between the structures of bone and wood. This analogy is almost apparent and shows how different methods are developed by the nature to reach the same goal, in our case: resistance and moderate stiffness. Similar opinion was expressed by Monceau (1700–1782), a botanist and agronomist.

The bones have to support the body of vertebrates and the tree trunk with branches has to support the weight of a plant, cf. [136]. These similar mechanical requirements lead at first sight to similar solutions, known as *homoplasy*. The stem of a plant is built from large cells. Every cell of the plant has a rigid cover – the cellulose wall, in distinction from animal cell. Therefore, the skeleton of a plant itself is composed of cells. The internal geometry of the bone resembles the geometry of the trunk. It is built from a rigid material and it is partitioned into (cellular in general meaning) structures, but this hydroxyapatite structure does not belong to the bone cells (osteocytes). Moreover, while all parts of the bone are active, in the stem of a vascular plant, only the phloem with cambium situated under the bark is the living tissue.

1.3.4.2 **Cell Membrane**

Amphiphile (Gr. *αμφις*, amphis: both and *φιλία*, philia: love, friendship) is a term describing a chemical compound possessing both hydrophilic (*water-loving)*

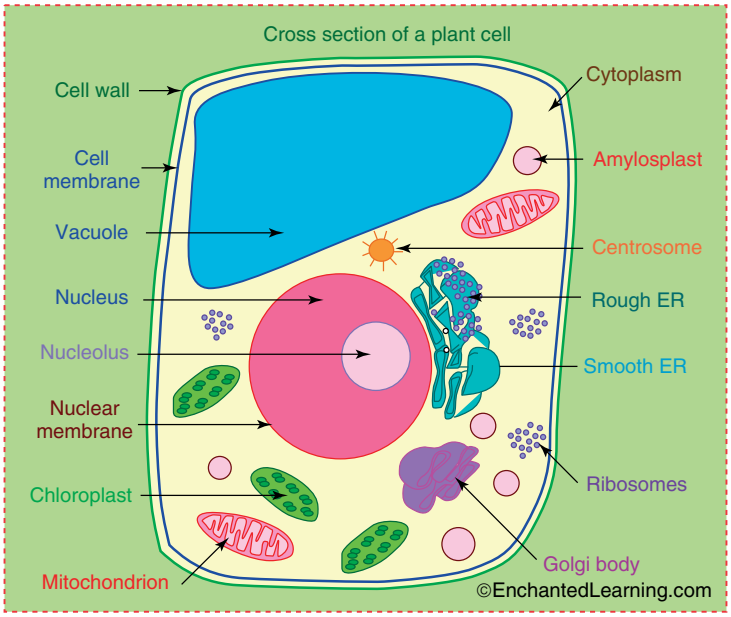

Figure 1.20 A plant cell. In vascular plants cellulose is synthesized at the cell membrane (also called the plasma membrane) by rosette terminal complexes. After [129].

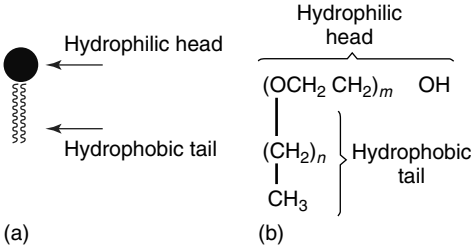

Figure 1.21 An example of an amphiphilic molecule: (a) symbolic representation and (b) chemical structure (alkyl polyoxyethylene).

and lipophilic (*fat-liking*) properties. Such a compound is called *amphiphilic* or *amphipathic*. Common amphiphilic substances are soaps and detergents.

An amphiphilic molecule is composed of two different parts: hydrophobic tail and hydrophilic head. The tail is composed of one or more hydrocarbon chains, and the head is composed of chemical groups with high affinity to water, Figure 1.21.

Phospholipids, a class of amphiphilic molecules, are the main components of biological membranes. When the phospholipids are immersed in an aqueous solution, they arrange themselves into bilayers, by positioning their polar groups toward the surrounding aqueous medium, and their lipophilic chains toward the inside of the bilayer, defining a nonpolar region between the two polar ones.

There are three different major classes of lipid molecules – phospholipids, cholesterol, and glycolipids. Different membranes have different ratios of the three lipids. However, what makes the membrane truly special is the presence of different proteins on the surface that fulfill various functions such as cell surface receptors, enzymes, surface antigens, and transporters [137–141].

1.3.4.3 **Membrane Transport**

The cell membrane primarily consists of a thin layer of amphipathic phospholipids that spontaneously arrange so that the hydrophobic *tail* regions are shielded from the surrounding polar fluid, causing the more hydrophilic *head* regions to associate with the cytosolic and extracellular faces of the resulting bilayer. This forms a continuous lipid bilayer.

The arrangement of hydrophilic heads and hydrophobic tails of the lipid bilayer prevents polar solutes (e.g., amino acids, nucleic acids, carbohydrates, proteins, and ions) from diffusing across the membrane, but generally allows for the passive diffusion of hydrophobic molecules. This affords the cell the ability to control the movement of these substances *via* transmembrane protein complexes such as pores and gates.

Thus, the cell is surrounded by a semipermeable membrane that separates the cell interior from exterior and controls the movement of substances in and out of the cell. Efflux pumps are proteinaceous transporters localized in the cell membranes. They are called *active transporters*, and they require a source of chemical energy to perform their function, cf. [142]. In eukaryotic cells, the existence of efflux pumps has been known since the discovery of p-glycoprotein in 1976 by Juliano and Ling [143]. They remarked that the relative amount of surface-labeled p-glycoprotein correlates with the degree of drug resistance in a number of independent mutant and revertant clones. A similar high-molecular-weight glycoprotein is also present in drug-resistant mutants from another cell line. Observations on pleiotropic drug resistance are interpreted in terms of a model wherein certain surface glycoproteins control drug permeation by modulating the properties of hydrophobic membrane regions. (Pleiotropy means the influence of a single gene on multiple phenotypic traits.)

Enzymes are proteins that catalyze (i.e., increase the rates of) chemical reactions. Almost all processes in a biological cell need enzymes to occur at proper rates. In enzymatic reactions, the molecules at the beginning of the process are called *substrates*, and the enzyme converts them into different molecules, called the *products*. Enzyme kinetics is the investigation of how enzymes bind substrates and turn them into products.

Diastase catalyzes the hydrolysis (breakdown) of carbohydrates [144] and a protease (or proteinase) catalyzes the hydrolysis of proteins. Sucrase is the name given to a number of enzymes that catalyze the hydrolysis of sucrose to fructose and glucose. Invertase is a sucrase enzyme. It breaks down sucrose (table sugar) to fructose and glucose, usually in the form of inverted sugar syrup.

In 1902, Henri investigated the action of diastases and proposed a quantitative theory of enzyme kinetics [145, 146]. In 1913, Michaelis and his postdoc Menten

performed experiments on kinetics of invertase activity [147] and confirmed Henri's equation, which is referred now to as *Henri–Michaelis–Menten kinetics* (sometimes as Michaelis–Menten kinetics only). The important contribution of Henri was to consider enzyme reactions in two stages. In the first, the substrate binds reversibly to the enzyme, forming the enzyme–substrate complex. The enzyme then catalyzes the chemical step in the reaction and releases the product.

A membrane transport protein is a protein involved in the movement of ions, small molecules, or macromolecules, such as another protein across a biological membrane [148]. Transport proteins are integral membrane proteins; that is, they exist within and span the membrane across which they transport substances. The proteins may assist in the movement of substances by facilitated diffusion or active transport. The permeases are membrane transport proteins, a class of multipass transmembrane proteins that facilitate the diffusion of a specific molecule in or out of the cell. Many membrane transporters behave as permeases and have several characteristics in common with enzymes. For example, both have binding sites on their surfaces that bind substrate (enzymes) and solute (transporters), both lower the activation energy, both exhibit saturation with increases in substrate or solute concentration, and both exhibit kinetic constants, K_M and v_{max}. The Michaelis–Menten enzyme kinetics is the principal analytical method used to characterize the kinetic properties of enzymes and also that of membrane transport proteins [149, 150]. The Michaelis–Menten equation relates the initial reaction rate v_0 to the substrate concentration S

$$v_0 = \frac{v_{max} S}{K_M + S}$$

The corresponding graph is a hyperbolic function; the maximum rate is described as v_{max}. Constant K_M is the substrate concentration at which the reaction rate v_0 is one-half of v_{max}. The limitation for the Henri–Michaelis–Menten equation is that it relies upon the law of mass action, which is derived from the assumptions of Fickian diffusion. However, many biochemical or cellular processes deviate significantly from such conditions. Voituriez *et al.* have shown that the state attained by reversible diffusion-limited reactions at time $t = \infty$ is generally *not a true thermodynamic equilibrium*, but rather a nonequilibrium steady state, and that the law of mass action is invalid [151, 152], see also [153–156].

1.3.4.4 **Bone Cell Types**

The living substance of the bone, the bone cells (or bone corpuscles, German: Knochenkörperchen), account for only 1–5% of the bone volume in the adult skeleton. There are five types of bone cells:

- Osteoprogenitors – immature cells which differentiate to form osteoblasts. Only at this stage, bone cells may divide. Mesenchymal stem cells (MSCs) residing in bone marrow are the progenitors for osteoblasts and for several other cell types, [157]. Osteoprogenitors are induced to differentiate under the influence of growth factors, in particular, the bone morphogenetic proteins (BMPs).

- Osteoblasts are the bone-forming cells. They secrete osteoid, which forms the bone matrix. They also begin mineralization. Osteoblasts arise from osteoprogenitor cells located in the periosteum and the bone marrow. Osteoblasts, when entombed within the osteoid, become osteocytes, with cytoplasmic processes that communicate with each other.
- Osteocytes are the mature osteoblasts that no longer secrete matrix, but being surrounded by it maintain metabolism, and participate in nutrient/waste exchange *via* blood. Osteoblasts and osteocytes develop in the mesenchyme. (Mesenchyme is the meshwork of embryonic CT in the mesoderm from which the CTs of the body and the blood and lymphatic vessels are formed.)
- Osteoclasts function in the resorption and degradation of the existing bone; in this role, they are the opposite of osteoblasts. Monocytes (white blood cells) fuse together to create these huge cells, which are concentrated in the endosteum. Osteoclasts play a key role in bone remodeling: they destroy bone cells and reabsorb calcium.
- Bone lining cells are essentially inactive osteoblasts; they cover all of the available bone surface and function as a barrier for certain ions [157, 158].

Bone is a dynamic tissue. It is constantly being reshaped by osteoblasts, which build bone, and osteoclasts, which resorb bone. An osteoblast (Gr. bone and germ) is a mononucleate cell, responsible for bone formation. Osteoblasts produce osteoid, which is composed mainly of Type I collagen, and osteoblasts are responsible for mineralization of the osteoid matrix. Osteoblast cells tend to decrease as individuals become older, thus decreasing the natural renovation of the bone tissue, cf. [158, 159].

Osteocytes are networked to each other *via* long cytoplasmic extensions that occupy tiny canals called *canaliculi*, which are used for exchange of nutrients and waste. Hence, osteocytes *in vivo* possess a distinctive morphology – that of dendricity – connecting osteocyte to osteocyte creating the osteocyte syncytium and also connecting osteocytes with cells on the bone surface. It is thought that bone fluid surrounding the dendrite within the canaliculi is responsible for the transmission of mechanical strain through fluid flow shear stress. Dendrites may be essential for osteocyte function, viability, and response to load [160–162]. Osteocytes, dendritic or star-shaped cells, are the most abundant cells found in a compact bone, cf. Figures 1.22 and 1.23. There are about 10 000 cells per cubic millimeter and 50 processes per cell.

Cell contains a nucleus and a thin ring of cytoplasm. When osteoblasts get trapped in the matrix they secrete, they become osteocytes. The space that an osteocyte occupies is called a *lacuna*. Although osteocytes have reduced synthetic activity and, like osteoblasts, are not capable of mitotic division, they are actively involved in the routine turnover of bony matrix, through various sensory mechanisms. They destroy the bone through a rapid, transient (relative to osteoclasts) mechanism called *osteocytic osteolysis*. Hydroxyapatite, calcium carbonate, and calcium phosphate are deposited around the cell.

Interesting images of osteocyte lacuno-canalicular network have been obtained. For example, in [160] one can see morphology of osteocytes, osteoblasts, and

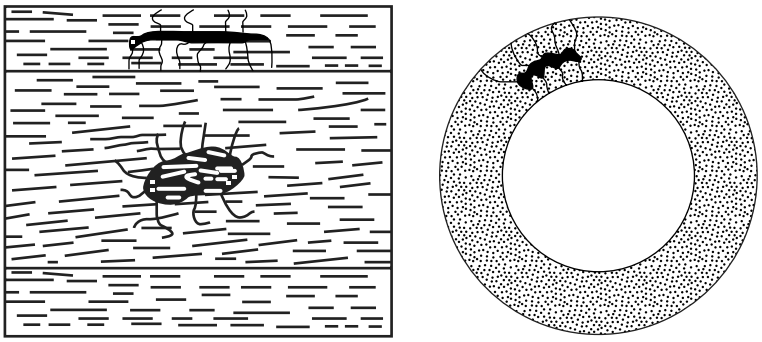

Figure 1.22 Osteocytes under a polarized light microscope (parallel polaroids, i.e., white background), in the cross sections parallel (a) and perpendicular (b) to the axis of osteon. After [104].

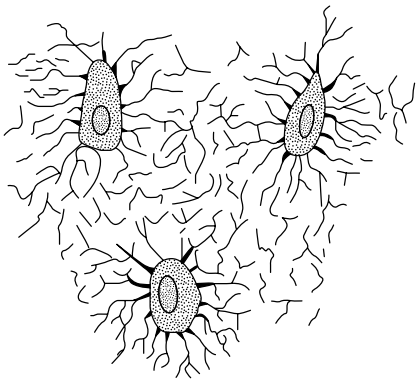

Figure 1.23 Osteocytes (bone cells) and their processes (long extensions), contained in the bone lacunae and their canaliculi, respectively, from a section through the vertebra of an adult mouse. After [63].

periosteal fibroblasts isolated from embryonic chicken calvariae and observed by fluorescence or phase contrast microscopy after 2×24 h of culture.

The osteocytes function to keep the bone alive. Since osteon is lamellar, the lacunae are located between adjacent lamellae; hence, they are arranged in rows, which coincide with the division between one lamella of the osteon and the next. Osteocytes have long extensions (processes): the processes of adjacent osteocytes remain in contact by passing through the minute canaliculi. The canaliculi radiate outward from each lacuna, each one filled by an osteocyte process which contacts that of another osteocyte. At the points of contact, gap junctions allow for a cell-to-cell pathway for nutrients and waste products through the otherwise impermeable hard substance of the bone [161].

Each canaliculus carries a fine osteocyte process; at the points of contact of these processes, gap junctions between the adjacent plasma membranes are the sites of interchange of materials and information between the cells. This system is essential to the survival of compact osteonal bone. Canaliculi are not extensively developed in the flat plates of cancellous (spongy) bone, because the plates are thin and diffusion transfer of products can occur between the osteocyte and the nearby marrow space, cf. Figure 1.11. Osteocytes are thought to function as a network of sensor cells in bones, which can mediate the effects of mechanical loading through their extensive communication network of Kendall's type, cf. [23, 24], also [26, 27].

It was found by Tanaka *et al.* that osteocytes from chick embryonic calvariae stimulated the osteoclast formation and function while maintaining osteocytic features *in vitro*. Isolated chick osteocytes stimulate formation and bone-resorbing activity of osteoclast-like cells. These results suggested that osteocytes may play a role in osteoclast recruitment [163].

The problem was also studied by Rubinacci *et al.*, who have proposed a model system for integrated osseous responses to mechanical, pharmacological, and endocrine signals [164].

The distribution of the osteocyte processes through the bulk of bone differs from their distribution on the bone surface. In [161] and [165], Bonewald presented observations made under a magnification of 3000× in scanning electron: micrographs of resin-embedded acid-etched mouse bone samples. It is visible as to how osteocyte cell processes pass through the bone in thin canals (canaliculi), connecting osteocytes with each other and with cells on the bone surface. In [165], Bonewald gives an analysis indicating that the osteocytes (not only osteoclasts) have both matrix forming and matrix destroying activities and that the osteocytes can remodel bone's local environment including lacunae and canaliculi, cf. also [101].

1.3.4.5 **Osteoclasts**

Osteoclasts are specialized cells responsible for bone resorption. They are derived from the monocyte/macrophage hematopoietic lineage. They develop and adhere to bone matrix and then secrete acid and lytic enzymes that degrade the bone matrix in a specialized, extracellular compartment.

Osteoclasts are large multinucleated cells (Figure 1.24). The nuclei resemble the nuclei of the osteoblasts and osteocytes. The cytoplasm has often a foamy appearance due to a high concentration of vesicles and vacuoles. An osteoclast cell frequently has branching processes.

Osteoclasts may arise from stromal cells of the bone marrow, being related to monocyte/macrophage cells, derived from granulocyte/macrophage-forming colony units (CFU-GM). They may represent fused osteoblasts or may include fused osteocytes liberated from resorbing bone. Osteoclasts lie in shallow cavities (depressions, pits, or irregular grooves) called *Howship's lacunae* (or resorption lacuna), formed in the bone that is being resorbed by osteoclasts [166–169].

At the site of active bone resorption, the osteoclast forms a specialized cell membrane, *the ruffled border*, that touches the surface of the bone tissue. The ruffled border increases the surface area interface for bone resorption, facilitates

removal of the bone matrix, and is a morphologic characteristic of an osteoclast that actively resorbs the bone. The mineral portion of the matrix (hydroxyapatite) includes calcium and phosphate ions. These ions are absorbed into small vesicles, which move across the cell and eventually are released into the extracellular fluid, thus increasing the levels of the ions in the blood.

Osteoclasts possess an efficient pathway for dissolving crystalline hydroxyapatite and degrading organic bone matrix rich in collagen fibers. When initiating bone resorption, osteoclasts become polarized, and three distinct membrane domains appear: a ruffled border, a sealing zone, and a functional secretory domain. Simultaneously, the cytoskeleton undergoes extensive reorganization. During this process, the actin cytoskeleton forms an attachment ring at the sealing zone, the membrane domain that anchors the resorbing cell to the bone matrix.

The ruffled border appears inside the sealing zone, and has several characteristics of late endosomal membrane. Extensive vesicle transport to the ruffled border delivers hydrochloric acid and proteases to an area between the ruffled border and the bone surface called the *resorption lacuna*. In this extracellular compartment, crystalline hydroxyapatite is dissolved by acid, and a mixture of proteases degrades the organic matrix. The degradation products of collagen and other matrix components are endocytosed, transported through the cell, and exocytosed through a secretory domain. This transcytotic route allows osteoclasts to remove large amounts of matrix-degradation products without losing their attachment to the underlying bone. It also facilitates further processing of the degradation products intracellularly during the passage through the cell.

1.3.5
Cellular Image – OPG/RANK/RANKL Signaling System

Recently, it has become clear that osteoclasts are not simply trench digging cells, but that they have important regulatory functions as immunomodulators in pathologic states and that they may also regulate osteoblast function. Proper growth and functioning of osteoclasts is controlled by a pathway in which three factors, osteoprotegerin (OPG), receptor activator of nuclear factor-kappaB (RANK), and receptor activator for nuclear factor-kappa B ligand (RANKL), play the main role. RANK and its ligand (RANKL) are important members of the tumor necrosis factor receptor (TNFR) and tumor necrosis factor (TNF) superfamilies, respectively.

OPG is secreted by osteoblasts and osteogenic stromal stem cells and protects the skeleton from excessive bone resorption by binding to RANKL and preventing it from interacting with RANK. The RANKL/OPG ratio in bone marrow is an important determinant of bone mass in normal and disease states. RANKL/RANK signaling also regulates the lymph node formation and mammary gland lactational hyperplasia in mice, and OPG protects large arteries from medial calcification. OPG and RANKL proteins are mainly located in Golgi areas.

RANK, also known as tumor necrosis factor-related activation-induced cytokine (TRANCE) receptor, is a type I membrane protein, which is expressed on the surface of osteoclasts and is involved in their activation upon ligand binding. RANK is also

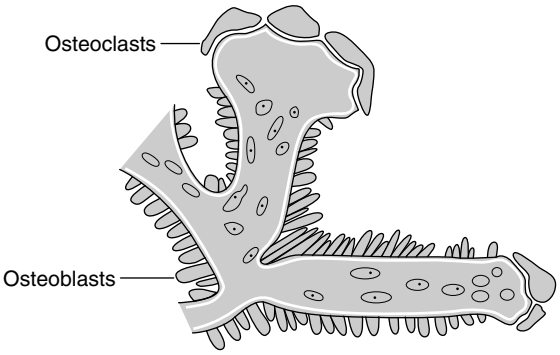

Figure 1.24 Osteoblasts and osteoclasts on trabecula of lower jaw of calf embryo. After [63].

expressed on dendritic cells and facilitates immune signaling. RANKL is found on the surface of stromal cells, osteoblasts, and T cells. RANK is expressed on osteoclasts, T lymphocytes, and dendritic cells, and its ligation with RANKL leads to cellular activation. However, another member of the TNFR family, OPG, acts as a decoy receptor, binding to RANKL and preventing its interaction with RANK.

RANKL is a member of the TNF, and is essential in osteoclastogenesis. RANKL, also known as *tumor necrosis factor-related activation-induced cytokine*, osteoprotegerin ligand (OPGL), and osteoclast differentiation factor (ODF), is a molecule participating in bone metabolism. This surface-bound molecule activates osteoclasts, cells involved in bone resorption.

RANKL knockout mice exhibit a phenotype of osteopetrosis and defects of tooth eruption, along with an absence or deficiency of osteoclasts. RANKL activates NF-$\kappa\beta$ (nuclear factor-kappa B) and NFATc1 (nuclear factor of activated T-cells, cytoplasmic, calcineurin-dependent 1) through RANK. NF-$\kappa\beta$ activation is stimulated almost immediately after the occurrence of RANKL–RANK interaction, and is not upregulated. Overproduction of RANKL is implicated in a variety of degenerative bone diseases, such as rheumatoid arthritis and psoriatic arthritis.

1.3.5.1 **Osteoprotegerin**

Cytokines (Greek *cyto*: cell; and *kinos*: movement) are substances (proteins, peptides, or glycoproteins) that are secreted by specific cells of the immune system, which carry signals between cells, and thus have an effect on other cells. Thus, they belong to a category of signaling molecules that are used in cellular communication. The term *cytokine* encompasses a large family of polypeptide regulators that are widely produced throughout the body by cells of diverse embryological origin.

Researchers in the field of bone biology have, for a long time, sought to understand the mechanisms responsible for the cross-talk between osteoblasts and osteoclasts. A major step toward answering this question was provided by the discovery of OPG. OPG was identified in 1997 by three different groups working in different areas [170–173].

It was isolated as a secreted glycoprotein that blocked osteoclast differentiation from precursor cells, prevented osteoporosis (decreased bone mass) when administered to ovariectomized rats, and resulted in osteopetrosis (increased bone mass) when overexpressed in transgenic mice. It was shown that OPG inhibits the differentiation of osteoclast precursors into osteoclasts and also regulates the resorption of osteoclasts *in vitro* and *in vivo*.

Studies in mutant mice have validated the idea that OPG is identical to the osteoblast-derived osteoclast inhibitory factor. Transgenic mice overexpressing OPG exhibit increased bone density and increased mineralization due to a decrease in osteoclasts terminal differentiation.

OPG is a member of the TNF receptor superfamily. OPG is a protein that plays a central role in regulating bone mass: it is a cytokine, which can inhibit the production of osteoclasts. OPG is also known as osteoclastogenesis inhibitory factor (OCIF). It is a basic glycoprotein comprising 401 amino-acid residues arranged into seven structural domains, cf. Figure 1.25. It is found as either a 60 kDa monomer or a 120 kDa dimer linked by disulfide bonds.

Studies have shown that OPG inhibits osteoclastogenesis by binding ODF (RANKL/OPGL/TRANCE) and blocking its interaction with its receptor, RANK, on osteoclasts (TRANCE receptor or TRANCE-R).

OPG contains a cysteine-rich amino-terminal domain, a putative death domain, and a COOH-terminal heparin-binding domain, but unlike other members of the TNF receptor family, it does not contain a transmembrane domain (Figure 1.25). Therefore, it is thought to act as a soluble receptor. OPG has been detected in the bone, heart, lung, liver, stomach, placenta, calvaria, dendritic cells, and blood vessels [175].

In addition, a role for OPG in the development of germinal centers in secondary lymphoid tissues has been postulated. OPG has also been implicated as a cell survival factor: OPG protects endothelial cells from apoptosis induced by serum withdrawal and NF-κB inactivation.

1.3.5.2 **RANK/RANKL**

RANKL is produced by a variety of cell types and its expression is regulated by many physiologic and pathologic factors. Preclinical studies in mice and studies of human tissues have revealed the functions of RANKL/RANK signaling in normal

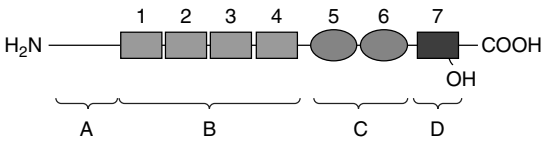

Figure 1.25 Schematic structure of osteoprotegerin OPG polypeptide: A, signaling peptide; B, cysteine-rich amino-terminal domains; C, putative death domains; and D, COOH-terminal heparin-binding domain. After [174].

and pathologic states. The role of the RANKL/RANK system is important not only in bone but also in other tissues.

OPG is a RANK homolog, and works by binding to RANKL on the osteoblast/stromal cells, thus blocking the RANKL–RANK ligand interaction between osteoblast/stromal cells and osteoclast precursors. This has the effect of inhibiting the differentiation of the osteoclast precursor into a mature osteoclast. Recombinant human OPG acts on the bone, increasing bone mineral density and bone volume [176–181]. OPG can bind to RANKL and prevent its interaction with RANK to inhibit osteoclast formation, but its effects on other cellular functions of RANKL have yet to be determined.

Discovery of the RANK signaling pathway in the osteoclast has provided insight into the mechanisms of osteoclastogenesis and activation of bone resorption, and how hormonal signals impact bone structure and mass. Further study of this pathway has provided the molecular basis for developing therapeutics to treat osteoporosis and other diseases of bone loss [180].

Osteoclast formation requires the presence of RANK osteoblasts (RANK) and macrophage colony-stimulating factor (M-CSF). These membrane-bound proteins are produced by neighboring stromal cells and osteoblasts. Thus, a direct contact between these cells and osteoclast precursors is required [168, 169, 178–183].

1.3.5.3 **TACE**

Tumor necrosis factor-alpha converting enzyme (TACE) is a kind of metalloprotease disintegrins, also known as *ADAM17*. It is a modular transmembrane protein with a zinc-dependent catalytic domain. TACE can cleave or shed the ectodomain of several membrane-bound proteins. In particular, TACE can shed several cytokines from the cell membrane, including RANKL [184, 185].

1.3.5.4 **Bone Modeling and Remodeling**

Bone modeling develops during the organism's youth and deals with the bone growth in length and width. In this process, a new bone is added (a subprocess called *ossification* or *bone formation*) to a side of the periosteal surface, and the old bone is removed from the skeleton (a subprocess called *bone resorption*) on the side of the endosteal surface. The modeling differs from remodeling in that processes of bone formation and bone resorption are realized at different surfaces of the bone Figure 1.26.

A bone is constantly renewed. The old bone is removed and the new bone is laid down. This process is called *bone remodeling*. Thus, bone remodeling is a lifelong process, where an old bone is removed from the skeleton and a new bone is added. These processes control not only the reshaping or replacement of bone during growth and following injuries like fractures but also microdamage, which occurs during normal activity. Remodeling responds also to functional demands of the mechanical loading. As a result bone is added where needed and removed where it is not required.

In the first year of life, almost 100% of the skeleton is replaced. In adult compact bone, remodeling proceeds at about 10% per year, and in spongy bone, it proceeds

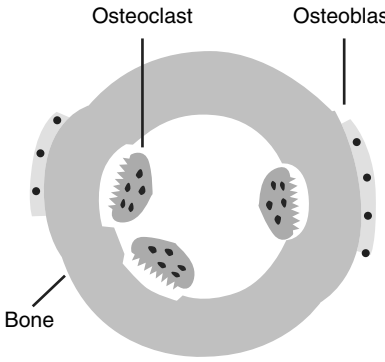

Figure 1.26 Bone modeling. Osteoclasts remove the bone from the endosteal surface. The new bone is added as a result of the osteoblast action from the side of periosteal surface. After [174].

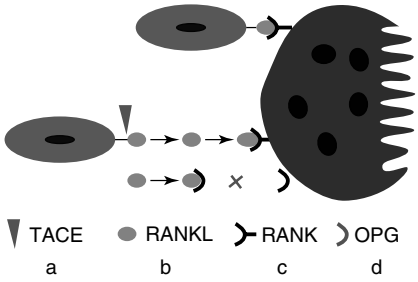

Figure 1.27 The ways of communication between an osteoblast and a maturing osteoclast. Inhibiting action of OPG; TACE (tumor necrosis factor-α converting enzyme): a, ectodomain RANKL after cleavage by the enzyme TACE; b, ectodomain RANKL; c, RANK – membrane receptor of RANKL; and d OPG – solvable receptor-inhibitor of RANKL. After [174].

at about 15–30%. It is so efficient that it is able to exchange constituents of the entire skeleton every 3–10 years [186].

RANKL/RANK/OPG system regulates the differentiation of precursors into multinucleated osteoclasts as well as osteoclast activation and survival, both normally and in most pathologic conditions associated with increased bone resorption (Figure 1.27). Osteoclast differentiation is inhibited by OPG, which binds to RANKL, thereby preventing interaction with RANK, cf. Figure 1.28.

Bisphosphonates exhibit high affinity for hydroxyapatite mineral in the bone and are used to prevent osteoclast-mediated bone loss. The nitrogen-containing bisphosphonate, zoledronic acid (ZOL), influences RANKL expression in human osteoblast-like cells by activating TACE. Bisphosphonates are used to prevent osteoclast-mediated bone loss. ZOL indirectly inhibits osteoclast maturation by increasing OPG protein secretion and decreasing transmembrane RANKL expression in human osteoblasts. The decreased transmembrane RANKL expression seems

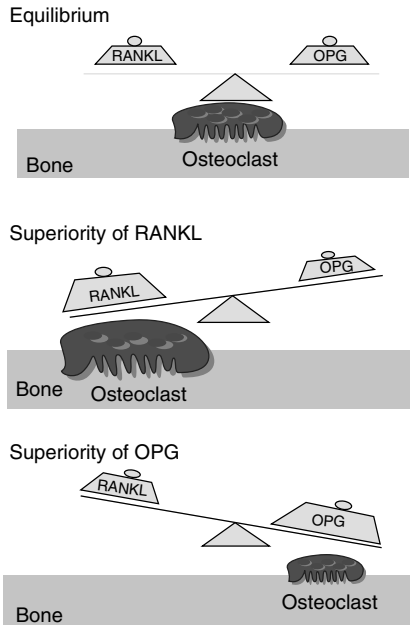

Figure 1.28 Resorption activity of the osteoclast depends on the ratio RANKL/OPG. OPG, osteoprotegerin; RANKL, receptor activator of nuclear factor-κB ligand. After [174].

to be related to the upregulation of the RANKL sheddase, TACE. The reduction in transmembrane RANKL expression was preceded by a marked increase in the expression of the metalloprotease disintegrin, TACE. Studies undertaken by Pan *et al*. indicate that ZOL, in addition to its direct effects on mature osteoclasts, may inhibit the recruitment and differentiation of osteoclasts by cleavage of the transmembrane RANKL in osteoblast-like cells by upregulating the sheddase, TACE [165, 187].

Wedemeyer *et al*. investigated the effect of a single subcutaneous dose of ZOL on particle-induced osteolysis and observed excessive regional new bone formation. They utilized the murine calvarial osteolysis model and polyethylene particles in C57BL/J6 mice. Bone thickness was measured as an indicator of bone growth. Net bone growth was significantly increased in animals with ZOL treatment [166, 188].

Proresorptive molecules that trigger bone loss (hormones and cytokines) induce RANKL expression on osteoblasts. In the inflammatory conditions, activated T-cells also produce RANKL. RANKL binding to RANK on mature osteoclasts and their precursors activates a signal transduction cascade that leads to osteoclast formation and activation. OPG protects bones because of binding to RANKL and inhibiting osteoclastogenesis and osteoclast activation Figure 1.29.

Khosla remarks in his minireview that the identification of the OPG/RANKL/RANK system as the dominant mediator of osteoclastogenesis represents a major advance in bone biology. It ended a long-standing search for the specific factor

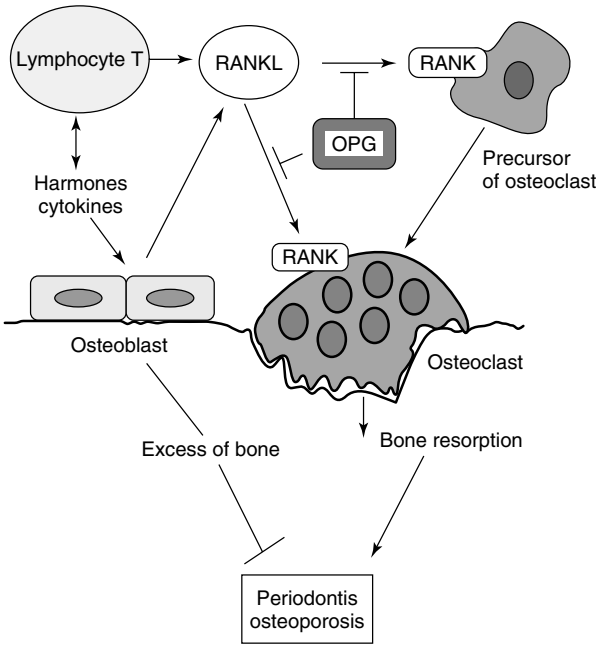

Figure 1.29 The balance of RANKL and osteoprotegerin (OPG) controls osteoclast activity. Most (perhaps all) known inducers of bone resorption and hypercalcemia act indirectly through the production of RANKL; hence OPG can be used in pharmacy to control osteoclast activity, independent of the inducing cytokine. After Stawińska [189].

produced by preosteoblastic/stromal cells that was both necessary and sufficient for osteoclast development. The decisive role played by these factors in regulating bone metabolism was demonstrated by the findings of extremes of skeletal phenotypes (osteoporosis vs osteopetrosis) in mice [168, 169, 190, 191].

When the rate of bone resorption exceeds that of bone formation, destruction of bone tissue occurs, resulting in a fragile skeleton. The clinical consequences, namely, osteoporosis and fragility fractures, are common and costly problems. Treatments that normalize the balance of bone turnover by inhibiting bone resorption preserve bone mass and reduce the risk of fracture. The discovery of RANKL as a pivotal regulator of osteoclast activity provides a new therapeutic target [171, 192].

Thus, the TNF-family molecule OPGL (also known as *TRANCE*, *RANKL*, and *ODF*) has been identified as a potential ODF and regulator of interactions between T cells and dendritic cells *in vitro*. OPGL is a key regulator not only of osteoclastogenesis but also of lymphocyte development and lymph-node organogenesis [172–174, 193–195].

Mice belong to a commonly used animal research model with hundreds of established inbred, outbred, and transgenic strains. Line MC3T3 is a strain of

tissue culture cells derived from *Mus musculus* (house mouse). Various derivatives of this strain have been widely used as model systems in bone biology. The subline MC3T3-E1 is one of the most convenient and physiologically relevant systems for the study of transcriptional control in calvarial osteoplasts.

Kim *et al*. tried to understand the biochemical reaction of RANKL in response to mechanical loading. The MC3T3-E1 cells were biequiaxially stretched. A murine RANKL cDNA with double epitopes, pEF6 HARANKL-V5His, was transfected into MC3T3-E1 cells, which were then stretched. They found that endogenous RANKL protein expression increased in response to mechanical loading. Membrane-bound RANKL (HA-RANKL-V5His) increased in cell lysates while soluble RANKL (RANKL-V5His) decreased in the conditioned media after mechanical loading. This may have resulted from the decreased activity of TACE after mechanical loading. Increased membrane-bound RANKL may be one of the mechanisms through which osteoblasts adapt to mechanical loading by regulating osteoclastogenic activity, [196].

1.3.6 Proteins and Amino Acids

An amino acid is a molecule containing both amine and carboxyl functional groups. There are about 200 amino acids in nature. Protein amino acids or alpha amino acids are the building blocks of proteins. In these amino acids, the amine and carboxyl functional groups are linked to the same atom of carbon, cf. [197–199].

Proteinogenic amino acids are those 22 amino acids that are found in proteins and that are coded for in the standard genetic code. Proteinogenic literally means *protein building*. Proteinogenic amino acids are assembled into a polypeptide (the subunit of a protein) through a process known as *translation* (the second stage of protein biosynthesis, part of the overall process of gene expression).

Peptides (Greek: $\pi\varepsilon\pi\tau\acute{\iota}\delta\iota\alpha$, small digestibles) are short polymers formed from the linking, in a defined order, of α-amino acids. The link between one amino-acid residue and the next is called an *amide bond* or a *peptide bond*. Proteins are polypeptide molecules or consist of multiple polypeptide subunits. The distinction is that peptides are short and proteins (polypeptides) are long. Proteins are defined by their sequence of amino-acid residues; this sequence is the primary structure of the protein. It is the genetic code that specifies 20 standard amino acids.

Since the works of Hofmeister (1850–1922) and Fischer (1852–1919), it has been regarded that the proteins are in some fundamental fashion chainlike, that they are constructed from polypeptides of the general formula, given in Figure 1.30, in which $-R'$, $-R''$, $-R'''$, and so on, stand for various univalent groups – 22 different kinds are known – which act as side chains to a common main chain (backbone). Two of these can be specified by the genetic code, but are rare in proteins.

The α-amino acids from which the proteins are formed, and into which they are resolved again on digestion, have the general formula $H_2NCHRCOOH$, where R is an organic substituent, cf. Figure 1.31. In the α-amino acids, the amino and

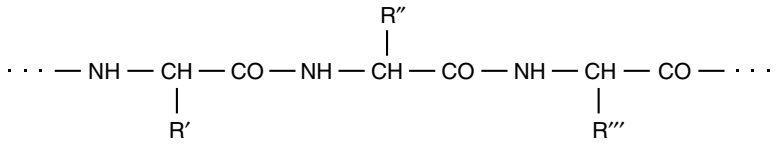

Figure 1.30 "Amino acids in chains are the cause, so the X-ray explains, of the stretching of wool and its strength when you pull, and show why it shrinks when it rains" (A. L. Patterson). After Astbury [200].

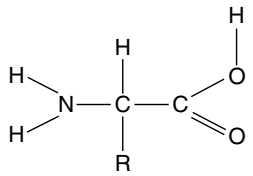

Figure 1.31 An α-amino acid molecule, with the amino group on the left and the carboxyl group on the right. After Pauling Chemistry [9].

carboxyl groups are attached to the same carbon, which is called the *α-carbon*. The various α-amino acids differ in the side chain (R group) that is attached to their α-carbon.

Twenty standard amino acids are used by cells in protein biosynthesis, and these are specified by the general genetic code. These 20 amino acids are biosynthesized from other molecules. Organisms differ in the types of amino acids synthesized by them and the ones that are obtained from food. The amino acids that cannot be synthesized by an organism are called *essential amino acids*. Of the 20 standard amino acids, 8 are essential amino acids.

Glycine and proline, used in building the collagen chain, belong to nonessential amino acids. Hydroxyproline, also appearing in the collagen, is a modification of proline: hydroxyproline differs from proline by the presence of additional hydroxyl (OH) group.

Glycine (abbreviated as *Gly* or G) is the organic compound with the formula NH_2CH_2COOH and is considered a glucogenic amino acid; it is the smallest of the 20 amino acids. Most proteins contain only small quantities of glycine. An exception is collagen, which contains almost one-third of glycine. Glycine is a colorless, sweet-tasting crystalline solid. It is unique among the proteinogenic amino acids in that it is not chiral. It can fit into both hydrophilic and hydrophobic environments, because of its single hydrogen atom side chain. Glycine was discovered in 1820 by Braconnot, who obtained a *gelatin sugar*, named later as glycocolle. It is now called glycine [201].

Proline (abbreviated as *Pro* or P) is an α-amino acid, one of the 20 DNA-encoded amino acids. Its molecular formula is $C_5H_9NO_2$. The distinctive cyclic structure of the proline side chain gives proline an exceptional conformational rigidity as compared to other amino acids. Hydroxyproline (abbreviated as *Hyp*) is an uncommon amino acid and differs from proline by the presence of a hydroxyl (OH) group attached to the C atom.

Because glycine is the smallest amino acid with no side chain, it plays a unique role in fibrous structural proteins. In collagen, *Gly* is required at every third position, because the assembly of the triple helix puts this residue at the interior (axis) of the helix, where there is no space for a larger side group than glycine's single hydrogen atom. For the same reason, the rings of *Pro* and *Hyp* must point outward. These two amino acids, *Pro* and *Hyp*, help stabilize the triple helix. A lower concentration of them is required in animals such as fish, whose body temperatures are lower than those of warm-blooded animals. Proline or hydroxyproline constitute about one-sixth of the total sequence. With glycine accounting for one-third of the sequence, this means that approximately half of the collagen sequence is not glycine, proline, or hydroxyproline.

The element phosphorus is not present in any of the 20 amino acids from which proteins are made (but is present in DNA, cf. the Hershey–Chase experiments [202]).

1.3.7
Collagen and its Properties

Collagen belongs to the long fibrous structural proteins. These are main components of the ECM that supports most tissues and assures cells structure from the outside. Collagen is the main protein of CT in animals and the most abundant protein in mammals, making up about 25% of the total protein content. Thus, collagen is found in large quantities in tendon, bone, skin, cornea, and cartilage. Collagen is also found inside certain cells, cf. [127, 128].

The TC or ''collagen macromolecule'' is a subunit of larger collagen aggregates such as fibrils. It is approximately 300 nm long and 1.5 nm in diameter, made up of three polypeptide strands (called *α-chains*), each possessing the conformation of a left-handed helix. These three left-handed helices are twisted together into a right-handed triple helix or ''super helix'' [11]. The triple helix is composed of three polypeptide chains, each with the repeating triplet Gly-X-Y, where X and Y are frequently proline and hydroxyproline, respectively.

The TC macromolecules are synthesized within fibroblast cells, pass into the intercellular tissue spaces, and in particular, aggregate at the appropriate places and time to form fibers. Possibly in all fibrillar collagens if not in all collagens, each TC triple helix associates into a right-handed super-super-coil, which is referred to as the *collagen microfibril*.

The molecular conformation of collagen has been determined primarily from an interpretation of its high-angle X-ray diffraction pattern. Following the pioneering work [203] of Herzog and Jancke, a number of investigators have attempted to find the structure of collagen (and of gelatin, which gives similar X-ray photographs). Astbury showed that there were drastic changes in the diffraction of moist wool or hair fibers as they were stretched significantly (100%). The data suggested that the unstretched fibers had a coiled molecular structure with a characteristic repeat of 5.1 Å (= 0.51 nm). Astbury proposed that (i) the unstretched protein molecules formed a helix (which he called the *α-form*) and (ii) the stretching caused the helix to

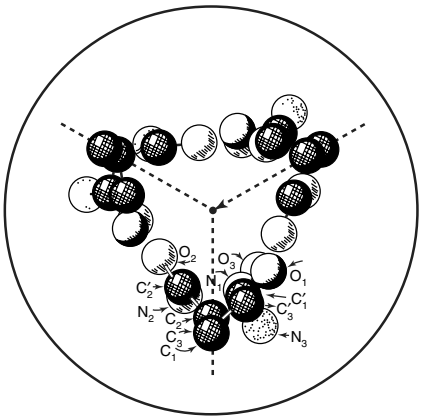

Figure 1.32 The three-chain configuration proposed for collagen and gelatin by Pauling and Corey in 1951 [204].

uncoil, forming an extended state (which he called the *β-form*) [200]. The α-helix has now been recognized as a feature of the majority of protein structures. Astbury's models were correct in essence and correspond to modern elements of secondary structure, the α-helix and the β-strand (Astbury's nomenclature was used), which were developed later by Pauling and Corey. These authors have attempted to account for the positions and intensities of the X-ray diffraction maxima, and pointed out that the equatorial reflections correspond to a hexagonal packing of circular cylinders [204]. They proposed a structure (now withdrawn) having three chains helically intertwined, see Figure 1.32.

The X-ray pattern of an unstretched collagen fiber is rather diffuse and poor in detail. Its principal features are a strong meridional axe at about 2.9 Å and weaker arcs at 4.0 and 9.5 Å. There are also strong equatorial reflections with spacings corresponding to approximately 6 and 12 Å (which depend on the humidity), and a diffuse distribution of intensity around 4.5 Å, mainly near the equator. This pattern is improved in orientation and detail if the fiber is kept stretched during the X-ray exposure [205].

A structural model was built based on various stereochemical properties of the polypeptide chains, and the intensity distribution expected of it was calculated using the helix diffraction theory proposed in 1952 by Cochran *et al.* [206]. Next, the calculated intensity distribution was compared with the observed one [207–211]. The effect of introducing the various side chain atoms on the calculated intensity distribution has been studied in detail by the Madras group of Ramachandran [207].

An interpretation of the X-ray pattern led Rich and Crick in 1955 to the conclusion that the collagen helix has a unit height of approximately 3 Å, the number of units per turn being close to 10/3, which corresponds to a unit twist of 108° [208, 209].

However, the determination of the molecular structure of collagen from X-ray diffraction data has proven extremely difficult, despite the progresses of fiber

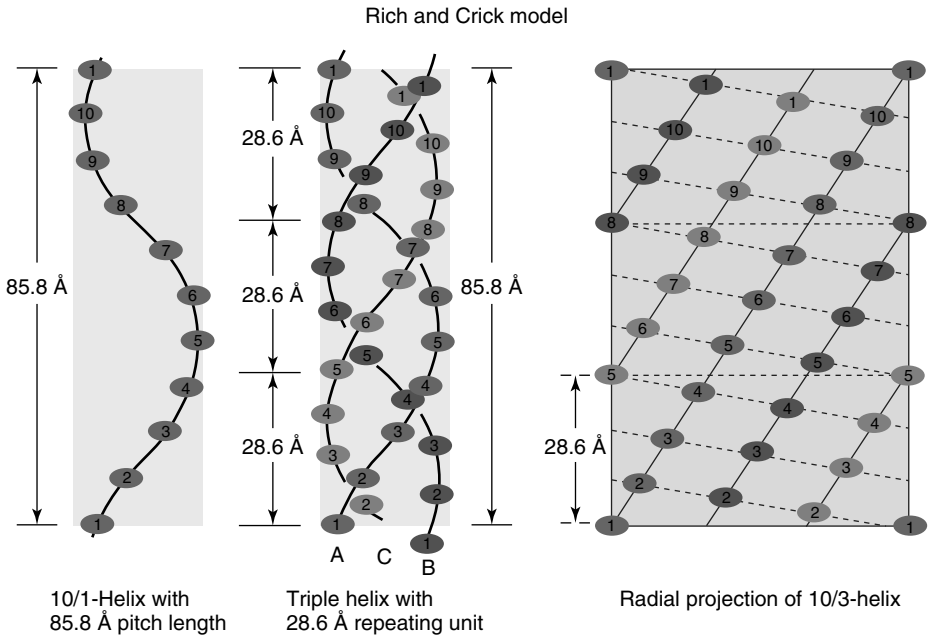

Figure 1.33 The three-chain configuration proposed for collagen by Rich and Crick [208, 209]. For comparison, see Figure 1.5, in which phyllotaxis disposition is given, as depicted by Bravais brothers in 1837. The analogy indicates the screw type development appearing at different levels of living structures and growth of molecules and organs. Courtesy of Kenji Okuyama.

diffraction techniques over the last eight decades. Because of a deficiency of diffraction spots on the layer lines in the wide-angle region (about 1–30 Å resolution), it could not even be determined whether the average helical symmetry of the collagen superhelix was 7/2 (seven tripeptide units for every two turns) or 10/3, [212]. In an article published in 2006, *Microfibrillar structure of type I collagen in situ*, Orgel *et al*. reported the three-dimensional molecular and packing structure of type I collagen determined by X-ray fiber diffraction analysis, which was based on 414 reflections with a completeness of 5% in the range of 5–113 Å resolution. The collagen molecule is made of three chains of more than 1000 residues each.

However, as remarked by Okuyama, it is difficult to determine the three-dimensional molecular conformation based on such a small number of reflections at low resolution [213]. In particular, there are significant differences between the triple helical parameters from the Rich and Crick model. These differences, which led to a 7/2 (with fiber period ~20 Å) as opposed to 10/3 (with fiber period ~29 Å) triple helical symmetry, initiated a debate regarding the actual symmetry of the natural collagen.

In Figures 1.33 and 1.34, two models of the molecular structure of collagen are compared: the first one proposed by Rich and Crick [208, 209] and the second one proposed by Okuyama *et al*. [212–216].

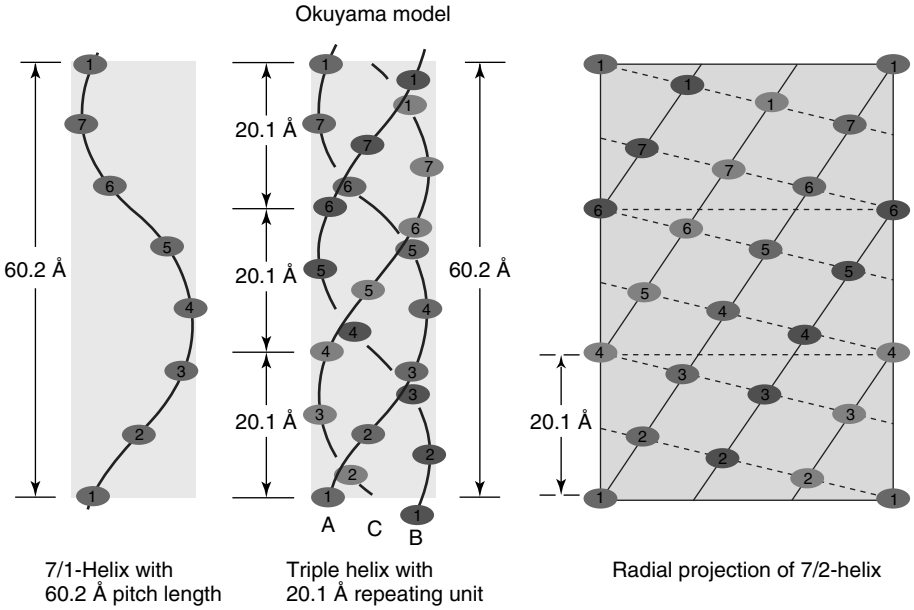

Figure 1.34 The three-chain configuration proposed for collagen by Okuyama [216]. Courtesy of Kenji Okuyama.

The triple-helix motif has now been identified in proteins other than collagens, and it has been established as being important in many specific biological interactions as well as being a structural element. Triple-helix binding domains consist of linear sequences along the helix, making them amenable to description by simple model peptides. Advances, principally through the study of peptide models, have led to an enhanced understanding of the structure and function of the collagen triple helix. In particular, the first crystal structure has clearly shown the highly ordered hydration network that is critical for stabilizing both the molecular conformation and the interactions between triple helices.

Collagen is almost unique among proteins in its use of triple helical secondary structure. Collagen is also unique among animal proteins in its high content of hydroxyproline, which is formed as a post-translational modification of prolines, which are incorporated in the Y position of *Gly*-X-Y triplets. The analysis of collagen structure emphasizes the dominance of enthalpy and hydrogen bonding in the stabilization of the triple helix [217–230].

1.3.7.1 **Molecular Structure**

There are 29 types of collagens known. Over 90% of the collagens in the body, however, are of types I, II, III, and IV.

- **Collagen I** – skin, tendon, vascular, ligature, organs, bone (main component of bone);
- **Collagen II** – cartilage (main component of cartilage);

- **Collagen III** – reticulate (main component of reticular fibers), commonly found alongside type I;
- **Collagen IV** – forms bases of cell basement membrane.

Type I collagen is the most abundant protein in human body, and it helps to maintain the integrity of many tissues *via* its interactions with cell surfaces, other ECM molecules, and growth and differentiation factors. Nearly 50 molecules have been found to interact with type I collagen, and for about half of them, binding sites on this collagen have been elucidated. In addition, over 300 mutations in type I collagen, associated with human CT disorders, have been described.

The type I collagen is the main component of the bone; it is present in the scar tissue, the end product when the tissue heals by repair. It is found in tendons, skin, artery walls, the endomysium of myofibrils, fibrocartilage, and the organic part of bones and teeth.

The type II collagen is the basis for articular cartilage and hyaline cartilage. It makes up 50% of all proteins in the cartilage and 85–90% of collagen of articular cartilage. The fibrillar network of collagen II allows cartilage to entrap the proteoglycan aggregate as well as provide tensile strength to the tissue. Type II is present in small amounts, with salts, sugars, and vitrosin, in vitreous humor of the eye [222–225].

1.3.8 Geometry of Triple Helix

The triple helix is a unique secondary structural motif that is primarily found within the collagens, and a distinctive feature of collagen is the regular arrangement of amino acids in each of the three chains of collagen subunits.

Coxeter [231, 232] suggested an extension of the concept of a regular polygon. A regular polygon as usually defined is a cycle of vertices ... 1, 2, 3, ... and edges ... 12, 23, ... which is obtained from a single point by repeated action of a rotation. Coxeter's extension replaces ''rotation'' by the more general ''isometry'' (distance-preserving transformation). A screw transformation generates a helical polygon (or polygonal helix), an infinite sequence of vertices $\ldots -1, 0, 1, 2, \ldots$, and edges joining consecutive vertices. A Coxeter helix is a polygonal helix such that every set of four consecutive vertices forms a regular tetrahedron. This produces a twisted rod of tetrahedra, the Boerdijk–Coxeter (B–C) helix (Figures 1.35 and 1.36).

Helices and dense packing of spherical objects are two closely related problems. By stacking regular tetrahedral along one direction, one obtains a configuration called the *Bernal* or *B–C helix*. Also, the name tetrahelix given to the chain of tetrahedra by Fuller is used, cf. also [20, 236, 237].

The construction of helix is as follows: to one face of the tetrahedron, the next tetrahedron is glued, and this process of gluing new tetrahedron is continued, with the condition that at one vertex six triangular faces meet (Figure 1.36). The chain of tetrahedra built in such a manner is not periodic because of incommensurability between the distances separating the centers of neighboring tetrahedra and the pitch of the three helices.

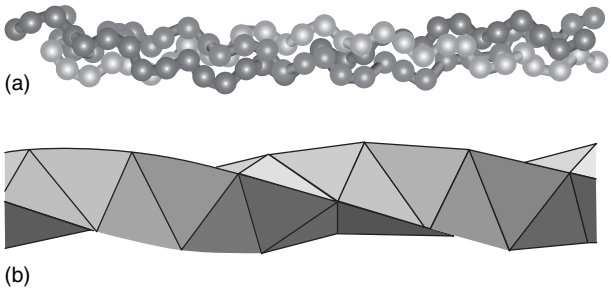

Figure 1.35 Tropocollagen triple helix (a) and the Boerdijk–Coxeter helix (b).

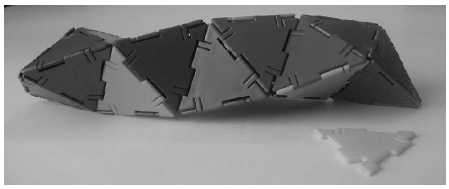

Figure 1.36 The B–C helix as a deltahedron (polyhedron whose faces are all equilateral triangles). Helical structure is generated by the repeated action of a screw transformation acting on a subunit (regular tetrahedron). The tetrahedral helix is called the *Bernal spiral* in association with discussions of liquid structure [233, 234]. Fuller [235] named this helical structure *the tetrahelix* [233].

An infinite strip of a tiling of the Euclidean plane by equilateral triangles, bounded by two parallel lines, can be wrapped around a circular cylinder so that the two strip edges meet. The resulting structure is referred to as a *cylindrical hexagonal lattice*. Alternatively, instead of rolling the strip around a cylinder, corresponding points on the edges may be brought into coincidence by folding along the fundamental lattice lines, keeping the triangular facets flat. The resulting structure is referred to as a *triangulated helical polyhedron* (THP). A THP is an ''almost regular'' polyhedron, in that its symmetry group, a rod group, acts transitively on the vertices and faces, although not on the edges. The rodlike sphere packings investigated by Boerdijk are derived from the Coxeter helix, which is the simplest THP. In a nanotube, the atomic positions correspond to a subset of the vertices of a THP.

The geometrical properties of the THPs are of relevance in structural chemistry for several reasons. As Sadoc and Rivier [238, 239] have shown, the helical structures commonly occurring in proteins are metrically quite close to polygonal helices consisting of edges of THPs. Sadoc and Rivier proposed a B–C helix with the collagen sequence *Gly*-X-Y.

The value of angle ψ is found from the symmetry: the edges AB, BC, and CD of a tetrahedron projected on the cross section of the circumscribed cylinder are all equal to a certain value c.

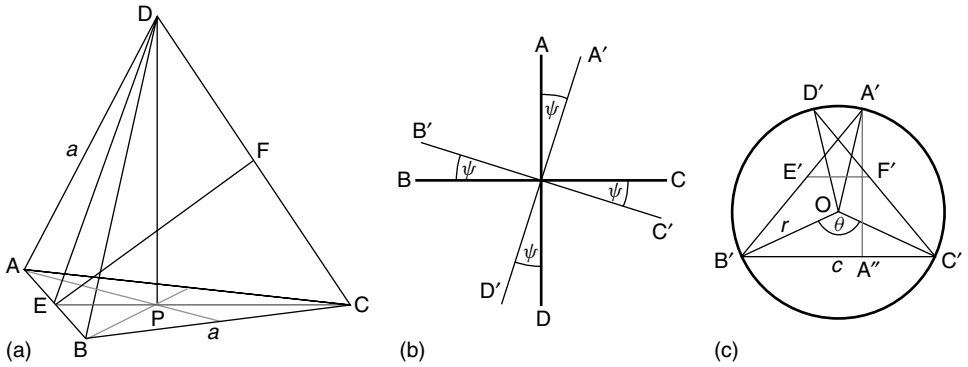

Figure 1.37 (a) A tetrahedron has four faces, four vertices, and six edges. A regular tetrahedron is composed of four equilateral triangular faces. All edges are equal: $AB = BC = AC = AD = BD = CD = a$. The height of the triangular face, for example, $EC = \sqrt{3}\,a/2$, the height of tetrahedron: $PD = \sqrt{2/3}\,a$, the distance between perpendicular edges, for example, AB and CD is equal to $EF = a/\sqrt{2}$. (b) Top view of two perpendicular tetrahedron edges: AD and BC. In order to inscribe the tetrahedron in a cylinder of radius r, the edges should be turned with respect to the axis of the cylinder through an angle of ψ. The distance $a/\sqrt{2}$ between the perpendicular edges AD and BC remains unchanged. (c) Projection of tetrahedron edges on the cross section of the cylinder circumscribed on the tetrahedron. The segment $A'A'' = a/\sqrt{2}$ (the distance between perpendicular edges AD and BC). The length scale between figures (a), (b), and (c) is not preserved.

According to Figure 1.37, we have projections $A'D' = a\sin\psi$ and $B'C' = a\cos\psi$. Hence, $B'A'' = (a/2)(\sin\psi + \cos\psi)$. Further $(A'A'')^2 + (B'A'')^2 = (A'B')^2$. Subsequently, $\cos\psi = 3/\sqrt{10}$ and $A'B' = B'C' = C'D' = c = 3a/\sqrt{10} \cong 0.9486\,a$. Moreover, $A'D' = a/\sqrt{10}$. Because $A'D' = 2r\sin((3\theta - 2\pi)/2)$ and $B'C' = 2r\sin(\theta/2)$, we get the angle θ and radius r of the cylinder. We get $\sin(\theta/2) = \sqrt{5/6}$, $\cos\theta = -2/3$. Thus $\angle A'OB' = \angle B'OC' = \angle C'OD' = \theta$ and $r = 3\sqrt{3}a/10 = \sqrt{3/10}c$.

The spiral moves along the tetrahelix by an angle $\theta = \arccos(-2/3) \approx 131.81^\circ$. The angle θ is an irrational number, and the tetrahelix has no period. It belongs to aperiodic crystals (according to Schrödinger [3]) or quasicrystals (according to the contemporary notion).

Let the edge of the tetrahedron be equal to 1. The whole structure of a B–C helix is generated by a screw transformation $\mathbf{x} \to R\mathbf{x} + \mathbf{a}$ where

$$R = \frac{1}{3}\begin{bmatrix} 221 \\ 2-1-2 \\ -12-2 \end{bmatrix}, \quad a = \begin{bmatrix} 1/3\sqrt{2} \\ 1/3\sqrt{2} \\ 1/3\sqrt{2} \end{bmatrix}$$

Sadoc and Charvolin have indicated that the idea of three-sphere fibrations may be a tool for analyzing twisted materials in condensed matter. They indicated that chiral molecules, when densely packed in soft condensed matter or biological materials, build organizations that are most often spontaneously twisted. The formation of these organizations is driven by the fact that compactness, which tends to align the

molecules, enters into conflict with torsion, which tends to disrupt this alignment. This conflict of topological nature, or frustration, arises because of the flatness of the Euclidean space, but does not exist in the curved space of the three-sphere where particular lines, its fibers, can be drawn which are parallel and nevertheless twisted. As these fibrations conciliate compactness and torsion, they can be used as geometrical templates for the analysis of organizations in the Euclidean space [240].

1.3.9 Polymer Thermodynamics

The first experiments suggested that TC molecules are rigid, rod-shaped structures. However, on the basis of hydrodynamic methods and transmission electron microscopy (TEM), it was found that TC molecules demonstrate some flexibility, which can be measured by the persistence length [241].

1.3.9.1 Thermodynamics

From the first law of thermodynamics, the increase in internal energy $\mathrm{d}U$ during any change in a system is equal to the sum of the elementary amount of heat $\overline{\mathrm{d}}Q$ added to it and the elementary amount of work $\overline{\mathrm{d}}L$ performed on it.

$$\mathrm{d}U = \overline{\mathrm{d}}Q + \overline{\mathrm{d}}L$$

The second law states that the increase in heat $\overline{\mathrm{d}}Q$ is expressed in any reversible process by the relation

$$\overline{\mathrm{d}}Q = T\,\mathrm{d}S$$

where $\mathrm{d}S$ denotes the entropy differential and T denotes the (absolute) temperature. Hence, for a reversible process

$$\mathrm{d}U = T\,\mathrm{d}S + \overline{\mathrm{d}}L$$

The Helmholtz free energy is defined by

$$A = U - TS$$

Its change at constant temperature is given by

$$\mathrm{d}A = T\,\mathrm{d}U + T\,\mathrm{d}S$$

which means that

$$\mathrm{d}A = \overline{\mathrm{d}}L$$

The work done on the system by a tensile force F in a displacement $\mathrm{d}x$ is

$$\overline{\mathrm{d}}L = F\,\mathrm{d}x$$

Then,

$$F = \left(\frac{\partial A}{\partial x}\right)_{\tau}$$

This means that the force of tension is equal to the change in Helmholtz free energy per unit extension. In the normal unstressed state, the free energy has a minimum $(\partial A/\partial x)_T = 0$ at certain $x = x_0$, and for small strains we get

$$F = \left(\frac{\partial^2 A}{\partial x^2}\right)_T (x - x_0)$$

where x denotes the length of the system under the force F. In this approximation, the force is a linear function of the deformation $(x - x_0)$. The tension force, like free energy, may be expressed as the sum of two terms

$$F = \left(\frac{\partial A}{\partial x}\right)_\tau = \left(\frac{\partial U}{\partial x}\right)_\tau - T\left(\frac{\partial S}{\partial x}\right)_\tau$$

In general, the force results in both the internal energy and entropy changes.

1.3.9.2 **Ideal Chain**

Ideal chain model (Gaussian chain) or the freely joined chain assumes that there are no interactions between chain monomers. The ideal chain is the simplest model of a polymer. In this model, fixed length polymer segments are linearly connected, and all bond and torsion angles are equiprobable: the polymer can be described by the random walk statistics [242–244].

Monomers are regarded as rigid rods (segments) of a fixed length l, and their orientation is independent of the orientations and positions of neighboring monomers. This means that no interactions between monomers are considered, the energy of the polymer is taken to be independent of its shape, and all of its configurations are equally probable. If N monomers form the polymer chain, its total length is $L = Nl$.

Let $\mathbf{b}_0, \ldots, \mathbf{b}_{N-1}$ be the vectors corresponding to individual monomers, and let $\boldsymbol{r}$ denote the end-to-end vector of a chain, that is, the distance between the ends of the chain, Figure 1.38. The monomer vectors have randomly distributed components in the three directions of space. With the assumption that the number of monomers N is large, and the central limit theorem applies, the length r is described by the following Gaussian probability density function:

$$p(r) = \left(\frac{3}{2\pi Nl^2}\right)^{3/2} \mathrm{e}^{-\frac{3r^2}{2\pi Nl^2}}$$

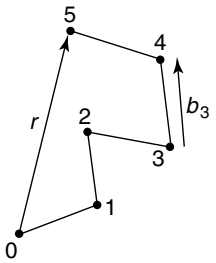

Figure 1.38 Chain of rigid, randomly oriented rods. In this example, we have five rods only, with directions described by vectors $\boldsymbol{b}_0, \ldots, \boldsymbol{b}_4$, and with end-to-end vector $\boldsymbol{r}$.

The entropy of the ideal chain is given by

$$S(r) = k_B \ln p(r) + C$$

where k_B is Boltzmann's constant and C is a constant. As ideal chain has no internal energy, the force appearing as a result of stretching the ideal chain is given by

$$F_{IC} = -T\left(\frac{\partial S}{\partial x}\right)_T$$

This force has purely entropic origin. If the stretching of polymer ideal chain is made in direction of the end-to-end vector $\boldsymbol{r}$, the force exerted on the chain is given by

$$F_{IC} = -T\frac{dS}{dr} = k_B T\frac{3r}{2Nl^2}$$

The above result gives the equation of state of the ideal chain: the force is linearly proportional to the temperature. Since the result was derived using the central limit theorem, it is exact for polymers containing a large number of monomers (known as the *thermodynamic limit*).

1.3.9.3 Wormlike Chain

The ideal chain model provides a starting point for the investigation of more complex systems.

An important model for polymers in solution is the Kratky–Porod model, sometimes referred to as the wormlike chain (WLC). The WLC model is used to describe the behavior of semiflexible polymers. The model replaces a polymer macromolecule by an isotropic rod that is continuously flexible, in contrast to the freely joined chain model that is flexible only between discrete segments [245–247].

For a polymer chain of length L, parametrize the path along the polymer chain with variable s, $0 \le s \le L$. Consider $\boldsymbol{t}(s)$ being the unit tangent vector to the chain at s. It can be shown that the orientation correlation function for a WLC follows an exponential decay law

$$\langle \boldsymbol{t}(s)\boldsymbol{t}(0)\rangle \equiv \langle \cos\theta(s)\rangle = e^{-s/\xi}$$

In this expression, the quantity ξ is a characteristic constant for a given polymer, known as *persistence length*, regarded as a mechanical property describing the stiffness of a macromolecule.

The stretching force F_{WLC} acting on a WLC with contour length L and persistence length ξ is described by the following interpolation formula:

$$F_{WLC}(r) = \frac{k_B T}{\xi}\left(\frac{1}{4\left(1-\frac{r}{L}\right)^2} - \frac{1}{4} + \frac{r}{L}\right)$$

For small values of fraction r/L, one obtains

$$F_{WLC}(r) \approx \frac{k_B T}{\xi}\left[\frac{1}{4}\left(1+\frac{2r}{L}\right) - \frac{1}{4} + \frac{r}{L}\right] = k_B T\frac{3r}{2\xi L}$$

The force F_{WLC} becomes divergent for the straightened chain, when $r \to L$ [245–247].

Stretching individual biomolecules are now achieved by a variety of techniques including flow stress, microneedles, optical tweezers, and magnetic tweezers that allow measurement of forces from 10 fN to hundreds of piconewtons.

Different biological molecules have now been analyzed and the accuracy of these techniques has sufficiently improved so that the theoretical models used to analyze force-extension curves must be refined. In particular, Bustamante *et al*. have shown that the force-extension diagram of a DNA molecule is well described by a WLC model [248, 249], and DNA has persistence length $\xi \approx 50$ nm.

The TC molecules have lengths of $L \approx 300$ nm, and are roughly 1.5 nm in diameter. Hydrodynamic methods and TEM permitted us to show that TC molecules exhibit some flexibility. Hydrodynamic methods suggested a persistence length of 130–180 nm; and TEM-based methods estimated the range between 40 and 60 nm. Experiments using optical tweezers suggested a much lower persistence length, between 11 and 15 nm.

Buehler and Wong reported molecular modeling of stretching single molecule of TC, the building block of collagen fibrils and fibers that provide mechanical support in CTs. For small deformation, they observed a dominance of entropic elasticity. At larger deformation, they have found a transition to energetic elasticity, which is characterized by first stretching and breaking of hydrogen bonds, followed by deformation of covalent bonds in the protein backbone, eventually leading to molecular fracture. Their force–displacement curves obtained at small forces show excellent quantitative agreement with optical tweezer experiments. Their model predicts a persistence length $\xi \approx 16$ nm, confirming experimental results suggesting the flexible elastic nature of TC molecules [241].

1.3.9.4 **Architecture of Biological Fibers**

Most biological tissues are built with polymeric fibers. Two of the most important and abundant fibers found in nature are cellulose and collagen. Cellulose is the structural component of the cell walls of green plants, many forms of algae, and the oomycetes. Some species of bacteria secrete it to form biofilms. As a constituent of the plant cell wall, it is responsible for the rigidity of the plant stems. One of the questions deals with the relation between the arrangement of cellulose fibrils inside the cell wall and its mechanical properties, and the way in which the cellulose architecture is assembled and controlled by the cell.

Similar problems arise with the structure of collagen fibrils. The TC molecules are arranged in microfibrils, which are seen under an electron microscope. Microfibrils are arranged into fibrils visible under a light microscope, and fibrils built connective tissues (CTs). The TC molecules and microfibrils are also cross-linked. Examples of fibrous system that achieves high tensile strength by a lateral bonding of macromolecular polymers are the materials such as skin, tendon, and other forms of CTs containing the protein collagen. The tensile strength is about 700 MPa; it is of the order of greatness observed for silk and stainless steel. The tensile strength of a bone is about 100 MPa [17, 250].

1.3.9.5 **Architecture of Collagen Fibers in Human Osteon**

Gross [15] proposed that collagen develops in seven steps:

1) the starting materials are free amino acids;
2) hydroxyproline is produced from proline after molecular chain has been formed;
3) the chain twists itself into a left-handed helix;
4) three chains intertwine to form a right-handed superhelix, the TC molecule;
5) many molecules line up in a staggered fashion;
6) the molecules overlap by one-quarter of their length to form a fibril;
7) fibrils in CTs are often stacked in layers with fibrils aligned at right angles.

Collagen is synthesized within fibroblast cells as a precursor, procollagen, which also consists of three chains. Molecular mass of procollagen molecules is ≈140 000. The polypeptides synthesized on the ribosomes do not contain hydroxyproline or hydroxylysine, which are generated as post-translational modifications before the procollagen is extruded. The TC chains that pass into the intercellular space spontaneously form microfibrils. Then, a variety of cross-links are formed that contribute to the strength of collagen.

This monomeric and microfibrillar structure of the collagen fibers that was discovered by Fraser, Miller, Wess (amongst others) was closest to the observed structure, although their description was oversimplified in topological progression of neighboring collagen molecules and hence did not predict the correct conformation of the discontinuous *D*-periodic pentameric arrangement [251–254].

The properties of collagen and associated polymers are important to understand the structure and functional mechanisms of biocomposites such as bone and cartilage on the microscopic level. The TC subunits spontaneously self-assemble, with regularly staggered ends, into even larger arrays in the extracellular spaces of tissues. In the fibrillar collagens, the TC molecules are staggered from each other by about 67 nm (a distance that is referred to as "*D*" and changes depending upon the hydration state of the aggregate). Each *D*-period (or *D*-spacing) contains approximately 4.4 of TC molecules. This is because 300 nm divided by 67 nm does not give an integer (the length of the collagen molecule divided by the stagger distance *D*). Therefore, in each *D*-period repeat of the microfibril, there is a part containing five molecules in cross section – called the *overlap* and a part containing only four molecules, Figure 1.39.

Studies are carried out on the assembly properties of concentrated solutions of type I collagen molecules. They are, for example, compared before and after sonication, breaking the 300 nm triple helices into short segments of about 20 nm, with a strong polydispersity. Whereas the nonsonicated solutions remain isotropic, the sonicated solutions transform after a few hours into a twisted liquid crystalline phase, well recognizable in polarizing microscopy. The evidence of a twisted assembly of collagen triple helices *in vitro* is relevant in a biological context since it was reported in various collagen matrices.

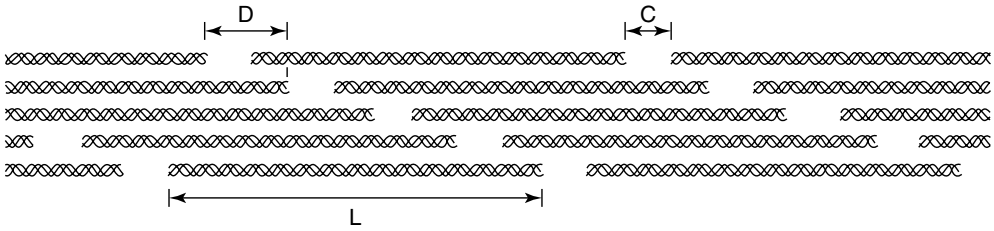

Figure 1.39 Scheme of the structure of collagen microfibril. Microfibrils have a characteristic striation with a repeated distance of $D = 668$ Å because of the end-to-end alignment of the TC molecule. The *D*-period distance corresponds to one hole zone and one region of short overlap: *C* – an overlap region; *L* – length of the tropocollagen molecule, the length of TC molecule $L = 4.4 \times D$; *C* – a hole zone.

The triple helices are also arranged in a hexagonal or quasi-hexagonal array in cross section, in both the gap and overlap regions.

Owing to the noninteger relationship between molecular length and the *D*-period, the projection of the axial structure repeat for a type I collagen fibril consists of a gap region and an overlap region in the ratio of 0.54 : 0.46 *D*, respectively. The ends of the triple helical region are defined by telopeptides, which do not conform to the repeating *Gly*-X-Y pattern of the helical region. The telopeptide region is known to be responsible for the formation of intermolecular cross-links.

Progress has been made in describing the relation between structure and deformation mechanisms of collagen-rich tissues. The principles for the self-assembly of collagen fibrils into larger scale structures still remain a mystery [250].

Cameron, Cairns, and Wess observed the Bragg peaks of diffracted rat tail tendon with sample-to-detector distances of 2000 mm, and obtained an X-ray diffraction image of the meridional region from fibrillar type I collagen. The meridional Bragg peaks were formed from the interactions of the X-rays with the regular repeating structure of the axial packing scheme of the collagen molecules. Next, they investigated the modeling of the nonuniform axial translation of amino acids in the collagen helix through the utilization of a genetic algorithm, and tried to evolve a sequence-based structure that obtains the best fit to the observed meridional X-ray diffraction data. Three structural elements of the model were investigated – the telopeptide inter-residue spacing, folding of the telopeptide, and the helical inter-residue spacing. They found that the variability in amino acid axial rise *per* residue of the collagen helix is an important parameter in structural models of fibrillar collagen [255].

1.3.9.6 **Collagen Elasticity**

Collagen has great tensile strength, and is the main component of fascia, cartilage, ligaments, tendons, bone, and skin. It strengthens blood vessels and plays a role in tissue development. It is present in the cornea and lens of the eye in crystalline form.

Collagen has well-defined mechanical properties (strength, reversible extensibility through only a small range) that make it suited to the special goals for which it is present in the different parts of animal body. Collagen characteristics, in particular, the specific shape of stress–strain curve, are important while considering the properties of a number of tissues, like bones, tendons, or arteries. The experimental trials to determine the mechanical properties of collagen molecule were performed by several groups of researchers, using the X-ray diffraction technique and Brillouin light scattering, beginning from Cowan *et al.* in 1955 [256, 257]. Despite its importance to the biological function of collagen, there is still a lack of understanding of the correlation between the specific shape of the stress–strain curve and the deformations of collagen at the molecular level.

Contemporary efforts to determine the shape of the stress–strain curve of collagen widely exploit synchrotron X-ray diffraction. Synchrotron radiation studies of fibril behavior in tissues have been critical to the investigation of structural details and changes, since they allow transient structural features to be monitored in realistic timescale.

Three experiments using this radiation, by Misof *et al.*, Puxkandl *et al.*, and Gupta *et al.*, should be mentioned here [258–261].

Misof *et al.* have performed *in situ* synchrotron X-ray scattering experiments, which show that the amount of lateral molecular order increases upon stretching of collagen fibers. In strain cycling experiments, the relation between strain and diffuse equatorial scattering was found to be linear in the ''heel'' region of the stress–strain curve [258].

The stress–strain curve of collagen is characterized by a region of relatively low elastic modulus at small strains (''toe region'') followed by an upward bend of the curve (''heel region'') and, finally, a linear region with high elastic modulus at large strains. The toe region of the stress–strain curve had been linked to a macroscopic crimp with a period of about 100 μm, found in unstretched collagen fibers by polarized light microscopy, cf. [262, 263].

In tendons, this crimp disappears upon stretching at extensions of the order of 4% – a value that may depend on the age of the animal. At larger strains, X-ray diffraction measurements of the axial molecular packing were interpreted as a side-by-side gliding of the molecules, accompanied by a stretching of the cross-linked telopeptide terminals and a stretching of the triple helices themselves, as was shown by Mosler *et al.* [264].

Although the axial packing of collagen fibrils is regular, as was shown in 1963 by Hodge and Petruska [265], there is a disorder in the structure, in the lateral packing of the molecules.

The following form of the stress–strain relation ($\sigma = \sigma(\varepsilon)$) was proposed in [258] by Misof *et al.*

$$\sigma = \frac{K\varepsilon}{1 - \varepsilon/\varepsilon_0}$$

with

$$K = k_B T \rho \frac{\nu}{\varepsilon_0^2 D} \quad \text{and} \quad \varepsilon_0 = \nu l \frac{\delta_0}{D}$$

Here $k_B = 1.38 \times 10^{-23}$ J K^{-1} is the Boltzmann constant, T is the absolute temperature, ρ is the number of molecules per unit surface in the equatorial plane, D is the length of the axial collagen period after the removal of all kinks, and ν is the total number of kinks of a molecule *per D*-period. Moreover, δ_0 denotes the average value $<\delta>$, obtained in the absence of external stress. Thus, the entropic regime may account for the initial regime of stress–strain behavior for fibril strains up to 8%, as is shown in figure 6 in the Misof *et al.* paper, cf. also [244].

Hence, when ε is small compared to ε_0, the prediction is a linear elastic behavior with the elastic modulus K. When ε approaches ε_0 (that is, when almost all of the kinks are removed), the tension σ required to get a further extension by the removal of the remaining kinks tends to infinity, which means that other mechanisms must become dominant for the sample behavior. The stress–strain curve corresponding to the Misof relation is bent upward. When tension σ becomes too large, other mechanisms of collagen elasticity, like a direct stretching or a side-by-side gliding of the molecules, come into play and lead to a linear stress–strain relation instead of the Misof relation.

When all the kinks are straightened, another mechanism of deformation must prevail and explain the linear dependence of stress and strain in this region of the force–elongation curve. The most probable processes are thought to be the stretching of the collagen triple helices and the cross-links between the helices, implying a side-by-side gliding of neighboring molecules, leading to structural changes at the level of the collagen fibrils.

A hierarchical structure of a collagen tendon for the model of strain-rate-dependent effects was proposed by Puxkandl *et al.* [259]. The tendon was considered as a composite material with collagen fibrils embedded in a proteoglycan-rich matrix. This matrix is mostly loaded under shear. Because the spacing between fibrils is much smaller than their length, the shear stress τ effectively applied to the matrix is much smaller than the tensile stress σ on the tendon. In reality, $\tau \approx \sigma H/L$, where L is the length of the fibrils and H is their spacing, [266]. The aspect ratio L/H is of the order of 100–1000. One may suppose that the elastic response of the matrix is mostly due to the entanglement of molecules attached to the collagen fibrils, such as proteoglycans. In addition, there is a considerable viscosity in the matrix due to the many hydrogen bonds that can form in this glassy structure.

Gupta *et al.* in 2004 carried out tensile measurements by using synchrotron X-ray diffraction [260]. A load cell was mounted on one grip while the other was moved with a motorized translation. To maintain the tendon in a native state, the sample was partially immersed in a physiological solution of phosphate-buffered saline during the test.

The most striking result was a peak splitting of the diffraction spectrum for large macroscopic tendon strains, $\geq$2–3%. The splitting implies an inhomogeneous

fibril elongation, with part of the fibrils relaxed back to their unstressed length and the remainder elongated by more than 4–5%. The peak splitting occurs shortly after the mechanical transition from approximately linear elastic to inelastic behavior in the stress–strain curve.

1.4 Remarks and Conclusions

The structure of a bone is discussed in this chapter; this discussion applies to a wide range of species, families, and orders, since, in a rough treatment, the bones of all mammals could be described in a similar manner. Figures and photographs of human bones and those of different animals are presented here without differentiation, although one should be aware of the fact that every species has its own characteristic features.

The bone components described above are essential for development and maintenance of a whole bone. For example, clinical data indicate that the nervous system influences skeletal development. Sciatic nerve injury in infants is sometimes followed by subnormal foot growth [267]. Moreover, Janet McCredie reported that the limbs of children with thalidomide malformations show changes analogous to those that can occur in the adult as a consequence of pathological alterations to peripheral nerves. The original animal tests did not show indications of this unexpected and serious side effect [268, 269].

Scurvy is a disease resulting from a deficiency of vitamin C, which is required for the synthesis of collagen in humans. Collagen is an important part of the bone, so bone formation is also affected. Most plant and animal species synthesize vitamin C. Notable exceptions in the mammalian group include most or all of the order chiroptera (bats), and one of the two major primate suborders, including human beings.

Vitamin D deficiency results in impaired bone mineralization and leads to bone-softening diseases including, rickets, a childhood disease characterized by impeded growth and deformity of the long bones [270].

Astronauts lose significant bone mass during spaceflight, in conditions of microgravity, despite rigorous musculoskeletal conditioning exercises. Femoral neck-bending strength index decreased 2.55%/month for spaceflights lasting 4–6 months.

Similarly, in a study on the influence of long-term immobilization in dogs, 32 weeks of disuse resulted in significant bone loss in both young and old dogs. After 28 weeks of remobilization, young dogs (respectively, old dogs) recovered only 70% (respectively, 40%) of the cortical bone lost during disuse.

Bears and humans have similar lower limb skeletal morphology and bears are plantigrade like humans.

In bears, during hibernation disuse, the bone mass and strength losses are small, if any. It is hypothesized that bears maintain bone cross-sectional properties and strength during annual periods of disuse because they maintain bone formation.

It would mean that bears have biological mechanisms to prevent disuse osteoporosis. This may be accomplished by targeting genes and circulating hormones that are differentially expressed in bears and humans during disuse [271].

1.5 Comments

Both the structure and function of a bone are complex characteristics that have not been understood well by researchers in the fields of medical sciences and mechanics. Since a bone could be treated as an organ, a tissue, or a hard tissue, different methods of describing behaviour of the bone and its physiology could be used, including mathematical topology, partial differential equations, elasticity, strength of materials, mechanics of porous media, diffusion and electrophoretic theories, chemistry, and optical and X-ray experimental methods. In such a description, different models of a bone could be presented including those resembling living and nonliving matter. In the present paper a number of the above methods of describing a bone, are presented.

V. I. Arnold, in his address at the Conference on Teaching of Mathematics in Palais de Découverte in Paris, on 7 March 1997, said, ''Mathematics is a part of physics. Physics as an experimental science is a part of natural science. Mathematics is a part of physics where experiments are cheap. . . . The mathematical technique of modeling consists of ignoring some experiments and providing a deductive model in such a way as if it coincided with reality. The fact that this path, which is obviously incorrect from the point of view of natural science, often leads to useful results in physics is called 'the inconceivable effectiveness of mathematics in natural sciences' (or 'the Wigner principle'). Here one can add a remark by I. M. Gel'fand: there exists yet another phenomenon which is comparable in its inconceivability with the inconceivable effectiveness of mathematics in physics noted by Wigner – this is the equally inconceivable ineffectiveness of mathematics in biology'' [272].

A mathematical structure is hidden in the world around us. A moderate opinion by Andrzej Lasota expresses belief that mathematics is the very structure of the world. ''Not a description of the structure, but structure itself. There is no doubt that a mathematician can create strange objects and he may think that he has strayed far from reality. But this is a resemblance of truth only. If his creation is good mathematics, it will sooner or later prove to be a component of reality'' [273].

A number of examples where mathematics is efficient in biology can be found in the literature. In particular, considerable progress has been made in recent years in the understanding of the molecular and microstructural properties of bone components, especially on molecular level, which is of general interest in biology, physics, and medicine. Different approaches have resulted, owing to both the difficulty and importance of the problem. As a recent example, Jakob Bohr and Kasper Olsen suggested that the close packing forms the underlying principle behind the structure of collagen. It is shown that the unique zero-twist structure

with no strain–twist coupling is practically identical to the close-packed triple helix. Further, the proposed new geometrical structure for collagen is better packed than both the 10/3 and the 7/2 structures [274].

It is characteristic in the field of medicine that, often, indirect explorations lead to proper results for the problems that are resistant to direct investigation. There is a reason to hope that by studying the bone and cartilage tissues on different levels of their organization and from different points of view, one can arrive at knowledge that can be of useful for patients [275].

1.6 Acknowledgments

I wish to thank Professors Mariusz Gajda and Jan A. Litwin from the Institute of Histology of Jagellonian University for a permission to use their unpublished microphotohraphs of a bone in the present chapter; Professor Andrzej Lissowski (Society of Polish Free University) for permitting me to insert his unpublished figures on a two-dimensional crystallization; and Professor Kenji Okuyama (Department of Macromolecular Science, Graduate School of Science, Osaka University) who let me know of his paper before publication and permitted me to present his figures on collagen structure.

I sincerely thank Professor Brian J. Ford from Cambridge University who kindly provided me with clarifications in respect of the first Leeuwenhoek paper. Professor Józef Ignaczak discussed a number of problems appearing in this chapter with me. Professor Andreas Öchsner (Technical University of Malaysia) encouraged me to complete this chapter.

I am also indebted to the State Committee for Scientific Research (KBN, Polska) for support through the project grant No 4 T07A 003 27.

References

1. Aristotle (2007) On the Generation of Animals, translated by A. Platt, Book II; eBooks@Adelaide.
2. Lowenstam, H.A. and Weiner, S. (1989) *On Biomineralization*, Oxford University Press, New York.
3. Schrödinger, E. (1944, 1945) *What is Life? The Physical Aspects of the Living Cell*, Cambridge University Press, London and Macmillan, Bentley House, New York, Toronto, Bombay, Calcutta, Madras.
4. Pasteur, L. (1922) *Oeuvres de Pasteur*, Tome Premier Dissymétrie Moléculaire, Masson et Cie, Paris.
5. Pasteur, L. (1897) *Researches on the Molecular Asymmetry of Natural Organic Products*, William F. Clay, Edinburgh and Simpkin, Marshall, Hamilton, Kent & Company, London.
6. Thomson, W. (1904) Baltimore Lectures on molecular dynamics and the wave theory of light, founded on Mr. A. S. Hathaway's stenographic report of twenty lectures delivered in Johns Hopkins University, Baltimore, in October 1884 by Lord Kelvin: followed by twelve appendices on allied subjects; C.J. Clay and Sons, Cambridge University Press, London – Glasgow; Publication Agency

of the Johns Hopkins University, Baltimore; Macmillan and Co., Bombay and Calcutta; F. A. Brockhaus, Leipzig.
7. Barron, L.D. (1997) *Q J M*, **90**(12), 793–800.
8. Cintas, P. (2007) *Angew. Chem. Int. Ed.*, **46**(22), 4016–4024.
9. Pauling, L. (1970) *General Chemistry*, Dover Publications, New York. 1988; reprint, originally published: 3rd edn, W. H. Freeman, San Francisco.
10. Maton, A., Hopkins, J.J., LaHart, S., Quon Warner, D., Wright, M., and Jill, D. (1997) *Cells: Building Blocks of Life*, Prentice Hall, New Jersey.
11. Schmitt, F.O. (1959) *Rev. Mod. Phys.*, **31**(2), 349–358.
12. Schmitt, F.O., Gross, J., and Highberger, J.H. (1953) *Proc. Natl. Acad. Sci. U.S.A.*, **39**, 459–470.
13. Gross, J., Highberger, J.H., and Schmitt, F.O. (1954) *Proc. Natl. Acad. Sci. U.S.A.*, **40**(8), 679–688.
14. Gross, J. (1956) *J. Biophys. Biochem. Cytol.*, **2**(4), 261–274.
15. Gross, J. (1961) *Sci. Am.*, **204**(5), 121–130.
16. Gustavson, K.H. (1956) *The Chemistry and Reactivity of Collagen*, Academic Press, New York.
17. Revised and expanded by Scott, T. and Eagleson, M. (eds) (1988) *Concise Encyclopedia Biochemistry*, 2nd edn, Walter de Gruyter, Berlin, New York.
18. Gregory, S.G., Barlow, K.F., McLay, K.E., Kaul, R., Swarbreck, D., Dunham, A., Scott, C.E., Howe, K.L., Woodfine, K., Spencer, C.C.A., Jones, M.C., Gillson, C., Searle, S., Zhou, Y., Kokocinski, F., McDonald, L., Evans, R., Phillips, K., Atkinson, A., Cooper, R., Jones, C., Hall, R.E., Andrews, T.D., Lloyd, C., Ainscough, R., Almeida, J.P., Ambrose, K.D., Anderson, F., Andrew, R.W., Ashwell, R.I.S., Aubin, K., Babbage, A.K., Bagguley, C.L., Bailey, J., Banerjee, R., Beasley, H., Bethel, G., Bird, C.P., Bray-Allen, S., Brown, J.Y., Brown, A.J., Bryant, S.P., Buckley, D., Burford, D.C., Burrill, W.D.H., Burton, J., Bye, J., Carder, C., Chapman, J.C., Clark, S.Y., Clarke, G., Clee, C., Clegg, S.M., Cobley, V., Collier, R.E., Corby, N., Coville, G.J., Davies, J., Deadman, R., Dhami, P., Dovey, O., Dunn, M., Earthrowl, M., Ellington, A.G., Errington, H., Faulkner, L.M., Frankish, A., Frankland, J., French, L., Garner, P., Garnett, J., Gay, L., Ghori, M.R., Gibson, R., Gilby, L.M., Gillett, W., Glithero, R.J., Grafham, D.V., Gribble, S.M., Griffiths, C., Griffiths-Jones, S., Grocock, R., Hammond, S., Harrison, E.S.I., Hart, E., Haugen, E., Heath, P.D., Holmes, S., Holt, K., Howden, P.J., Hunt, A.R., Hunt, S.E., Hunter, G., Isherwood, J., James, R., Johnson, C., Johnson, D., Joy, A., Kay, M., Kershaw, J.K., Kibukawa, M., Kimberley, A.M., King, A., Knights, A.J., Lad, H., Laird, G., Langford, C.F., Lawlor, S., Leongamornlert, D.A., Lloyd, D.M., Loveland, J., Lovell, J., Lush, M.J., Lyne, R., Martin, S., Mashreghi-Mohammadi, M., Matthews, L., Matthews, N.S., McLaren, S., Milne, S., Mistry, S., Moore, M.J., Nickerson, T., O'Dell, C.N., Oliver, K., Palmeiri, A., Palmer, S.A., Pandian, R.D, Parker, A., Patel, D., Pearce, A.V., Peck, A.I., Pelan, S., Phelps, K., Phillimore, B.J., Plumb, R., Porter, K.M., Prigmore, E., Rajan, J., Raymond, C., Rouse, G., Saenphimmachak, C., Sehra, H.K., Sheridan, E., Shownkeen, R., Sims, S., Skuce, C.D., Smith, M., Steward, C., Subramanian, S., Sycamore, N., Tracey, A., Tromans, A., Van Helmond, Z., Wall, M., Wallis, J.M., White, S., Whitehead, S.L., Wilkinson, J.E., Willey, D.L., Williams, H., Wilming, L., Wray, P.W., Wu, Z., Coulson, A., Vaudin, M., Sulston, J.E., Durbin, R., Hubbard, T., Wooster, R., Dunham, I., Carter, N.P., McVean, G., Ross, M.T., Harrow, J., Olson, M.V., Beck, S., Rogers, J. and Bentley, D.R. (2006) *Nature*, **441**(7091), 315–321.
19. Grochulski, W., Kawczyński, A., and Lissowski, A. (1978) Crystallization as rearrangement of grain boundaries and dislocations. Symposium on Computer Films for Research in Physics and Chemistry, University of Colorado, 20-22 March 1978, Boulder.
20. (a) Sadoc, J.F. and Mosseri, R. (1997) *Frustration Géometrique*, Eyroles, Paris;

(b) Sadoc, J.F. and Mosseri, R. (1999) *Geometrical Frustration*, Cambridge University Press, Cambridge.
21. Bragg, W.L. and Nye, J.F. (1947) *Proc. R. Soc. London*, **190**, 474–481, Reproduced in *The Feynman Lectures on Physics*, Vol. II, Part 2.
22. Loewenstein, W.R. (1999) *The Touchstone of Life: Molecular Information, Cell Communication, and the Foundations of Life*, Oxford University Press, New York.
23. Kendall, D.G. (1971) *Nature*, **231**(5299), 158–159.
24. Kendall, D.G. (1975) *Philos. Trans. R. Soc. London, A*, **279**(1291), 547–582.
25. Bloom, H. (2007) Who's Smarter: Chimps, Baboons or Bacteria? The Power of Group IQ. Submitted by Howard Bloom on 7 November 2007 – *www.scientificblogging.com*.
26. Fliedner, T.M., Graessle, D., Paulsen, C., and Reimers, K. (2002) *Cancer Biother. Radiopharm.*, **17** (4), 405–426.
27. Lidke, D.S., Huang, F., Post, J.N., Rieger, B., Wilsbacher, J., Thomas, J.L., Pouysségur, J., Jovin, Th.M., and Lenormand, Ph. (2010) *J. Biol. Chem.*, **285**, 3092–3102. Also *http://www.sciencedaily.com/releases/2010/01/100125112209.htm* (accessed 27 January 2010).
28. Shekhter, A.B. (1986) *Connect. Tissue Res.*, **15**(1-2) 23–31.
29. Marcello Malpighi *http://en.wikipedia.org/wiki/Marcello_Malpighi*.
30. Weiss, L. (1988) *Cell and Tissue Biology: A Textbook of Histology*, 6th edn, Urban and Schwarzenberg, Inc., Baltimore, MD.
31. Bilezikian, J.P., Raisz, L.G., and Rodan, G.A. (eds) (2002) *Principles of Bone Biology*, 2nd edn, Academic Press, San Diego, CA.
32. Franklin, R.E. (1955) *Nature*, **175**(4452), 379–381.
33. Ryzhkov, V.L. (1957) Crystallisation of viruses, in *Rost kristallov (Growth of crystals)* (eds A.V. Shubnikov and N.N. Sheftal), Izdatelstvo Akademii Nauk SSSR, Moskva, pp. 351–358, in Russian.
34. Protozoa (2010) *http://en.wikipedia.org/wiki/Protozoa*.
35. Sarindam7 (2010) Osteomyelitis, *en.wikipedia.org/wiki/Osteomyelitis*.
36. Moore L.L., Jr. Osteomyelitis (1969) Leishmania donovani in bone marrow cell. Smear. Parasite; from the Centers for Disease Control and Prevention's Public Health Image Library (PHIL), with identification number #468. *www.bioportfolio.com/search/osteomyelitis_wikipedia.html*.
37. Peters, R.A. (1930) *Trans. Farad. Soc.*, **26**, 797–807.
38. Wheatley, D.N. (2003) *J. Exp. Biol.*, **206**(Pt 12), 1955–1961.
39. Braun, A. (1831) Vergleichende Untersuchung über die Ordnung der Schuppen an den Tannenzapfen als Einleitung zur Untersuchung der Blattstellungen überhaupt. *Nova Acta Phys.-Med. Acad. Caesar. Leop.-Carol. Nat. Curiosorum*, (Verhandlung der Kaiserlichen Leopoldinsch-Carolinschen Akademie der Naturforschung) **15**, 195–402.
40. Schimper, C.F. (1831) Beschreibung des Symphytum Zeyheri und seiner zwei deutschen Verwandten der S. bulbosum Schimper und S. tuberosum Jacqu, *Mag. Pharm.* (hgb. Ph. L. Geiger) **29**, 1–92.
41. Bravais, L. and Bravais, A. (1837) Essai sur la disposition des feuilles curvisériées. *Ann. Sci. Nat. Bot.*, **7**, 42–110.
42. Bravais, L. and Bravais, A. (1837) Essai sur la disposition symétrique des inflorescences. *Ann. Sci. Nat. Bot.*, **7**, 193–221, 291–348; **8**, 11–42.
43. Schwendener, S. (1878) *Mechanische Theorie der Blattstellungen*, Engelmann, Leipzig.
44. Schwendener, S. (1883) Zur Theorie der Blattstellungen. *Sitzungsber. Königlich Preussischen Akad. Wiss. Berlin* **II. S**, 741–773.
45. Wulff, G.W. (1908) Simmetriia i ee Proiavleniia v Prirode, (Symmetry and its manifestations in the nature, in Russian), Lektsii chitannye v 1907g, Moskovskoe obshchestvo Narodnykh Universitetov, Tip. T-va I. D. Sytina, Moskva.
46. Lewis, F.T. (1931) *Anat. Rec.*, **50**, 235–265.

47. Rutishauser, R. (1998) Plastochrone ratio and leaf arc as parameters of a quantitative phyllotaxis analysis in vascular plants, in *Symmetry in Plants*, WS Series in Mathematical Biology and Medicine, vol. 4 (eds R.V. Jean and D. Barabé), (Series editors P.M. Auger and R.V. Jean), World Scientific Publishers, pp. 171–212.
48. Atela, P. and Golé, C. (2007) Phyllotaxis *http://maven.smith.edu/~phyllo/About/math.html*.
49. Thompson D'Arcy, W. (1917, 1942) *On Growth and Form*, Cambridge University Press.
50. Rivier, N. and Lissowski, A. (1982) *J. Phys. A: Math. Gen.*, **15**(3), L143–L148.
51. Hofmeister, W.F.B. (1868) Allgemeine Morphologie der Gewächse, *Handbuch der Physiologischen Botanik*, vol. 1, Part 2, Wilhelm Engelmann, Leipzig, pp. 405–664.
52. Wojnar, R. (2009) Strains in tissue development: a vortex description, in *More Progresses in Analysis, Proceedings of the 5th International ISAAC Congress, Catania, Italy, 25–30 July 2005* (eds H.G.W. Begehr and F. Nicolosi), World Scientific, New Jersey, London, Singapore, Beijing, Shanghai, Hong Kong, Taipei, Chennai, pp. 1271–1281.
53. Newell, A.C., Shipman, P.D., and Sun, Z. (2008) *Plant Signal Behav.*, **3**(8), 586–589.
54. Gebhardt, W. (1911) Knochenbildung und Colloidchemie. *Arch. Entwickl. Mech.*, **32**, 727–734.
55. Counce, S.J. (1994) *Dev. Genes. Evol.*, **204**(2), 79–92.
56. Giraud-Guille, M.M. (1988) *Calcif. Tissue Int.*, **42**, 167–180.
57. Erickson, R.O. (1998) Phyllotactic symmetry in plant growth, in *Symmetry in Plants* (eds R.V. Jean and D., Barabé), World Scientific, Singapore, pp. xvii–xxvi.
58. Dumais, J. and Kwiatkowska, D. (2002) *Plant J.*, **31**(2), 229–241.
59. Gibson, M.C., Patel, A.B., Nagpal, R., and Perrimon, N. (2006) *Nature*, **442**, 1038–1041.
60. Farhadifar, R., Röper, J.-Ch., Aigouy, B., Eaton, S., and Jülicher, F. (2007) *Curr. Biol.*, **17**(24), 2095–2104.
61. Ross, M.H., Romrell, L.J., and Kaye, G.I. (1995) *Histology: A Text and Atlas*, 3rd edn, Williams & Wilkins, Baltimore.
62. Ross, M.H. and Pawlina, W. (2006) *Histology: A Text and Atlas, with Correlated Cell and Molecular Biology*, Lippincott Williams & Wilkins, Hagerstown, MD.
63. Gray, H. (1918) *Anatomy of the Human Body*, Lea & Febiger, Philadelphia. Also (2010) *http://www.bartleby.com/107/*.
64. Gray, H. (2008) *Gray's Anatomy: The Anatomical Basis of Clinical Practice*, 40th edn, Elsevier, Churchill-Livingstone.
65. Downey, P.A. and Siegel, M.I. (2006) *Phys. Ther.*, **86**(1), 77–91.
66. Bochenek, A. (1924) *Anatomia człowieka*, tom 2, wyd.IV, Nakładem Polskiej Akademii Umiejętności, Kraków.
67. National Center for Biotechnology Information (2004) *http://www.ncbi.nlm.nih.gov/About/primer/genetics_cell.html*.
68. Connective Tissue (2010) *http://training.seer.cancer.gov/module_anatomy/unit2_2_body_tissues2_connective.html*.
69. Marino, Th.A., Lamperti, A.A., and Sodicoff, M. (2000) Connective Tissue Web Book, Temple University School of Medicine, *http://astro.temple.edu/~sodicm/labs/CtWeb/sld004.htm*.
70. Strum, J.M., Gartner, L.P., and Hiatt, J.L. (2007) *Cell Biology and Histology*, Lippincott Williams & Wilkins, Hagerstwon, MD.
71. McLean, F.C. (1955) *Sci. Am.*, **192**(2), 84.
72. Bone Development and Growth *http://training.seer.cancer.gov/module_anatomy/unit3_3_bone_growth*.
73. School of Anatomy and Human Biology The University of Western Australia Blue Histology – Skeletal Tissues – Bone (2009) *http://www.lab.anhb.uwa.edu.au/mb140/CorePages/Bone/Bone.htm*.
74. National Cancer Institute, SEER Training Modules: Classification of Bones

(2000) : *http://training.seer.cancer.gov/anatomy/skeletal/classification.html*.

75. Fruitsmaak, S. (2008) Gallery Medical Images. *http://commons.wikimedia.org/wiki/User:Stevenfruitsmaak/Gallery*.

76. General Osteology (2005) *http://commons.wikimedia.org/wiki/File:Illu_long_bone.jpg*.

77. Bernard Dery (2005) Skeleton Human Body. Squeleton, in *The Visual Dictionary*, vol. 3. *http://www.infovisual.info/03/011_en.html*.

78. Hydroxylapatite (2010) *http://en.wikipedia.org/wiki/Hydroxylapatite*.

79. Le Geros, R.Z. (1991) Calcium phosphates in oral biology and medicine, in *Monographs in Oral Science*, vol. 15 (ed. H.M. Myers), Karger Publishing, Basilea, Freiburg, Paris, London, New York, New Delhi, Bangkok, Singapore, Tokyo, Sydney, pp. 110–118.

80. Ślósarczyk, A., Paszkiewicz, Z., and Paluszkiewicz, Cz. (2005) *J. Mol. Struct.*, **744–747**, 657–661.

81. Beevers, C.A. and McIntyre, D.B. (1946) *Mineral. Mag.*, **27**, 254–257 + 3 plates. Also *www.minersoc.org/pages/Archive-MM/Volume_27/27-194-254.pdf*.

82. Wopenka, B. and Pasteris, J.D. (2005) *Mater. Sci. Eng. C*, **25**(2), 131–143.

83. Elliott, J.C., Wilson, R.M., and Dowker, S.E.P. (2002) Apatite structures. Proceedings of the 50th Annual Denver X-ray Conference, Steamboat Springs, Colorado, 30th July – 3rd August 2001, Advances in X-ray Analysis, vol. 45, 2002. International Centre for Diffraction Data, Newtown Square, Pennsylvania. Invited presentation for R.A. Young Rietveld Analysis Session (ed. Huang, T.C.), pp. 172–181.

84. Ellis, D.I. and Goodacre, R. (2006) *Analyst*, **131**(8) 875–885. Also *www.rsc.org/analyst*.

85. Wilson, R.M., Dowker, S.E.P., and Elliott, J.C. (2006) *Biomaterials*, **27**(27), 4682–4692.

86. Dowker, S.E.P., Elliott, J.C., Davis, G.R., Wilson, R.M., and Cloetens, P. (2006) *Eur. J. Oral Sci.*, **114** (Suppl. 1), 353–359.

87. Cooper, R. and Blystone, R. (1999) SLiBS Synergistic Learning in Biology and Statistics. *http://www.trinity.edu/rblyston/bone/intro2.htm*.

88. Piekarski, K. and Munro, M. (1977) *Nature*, **269**(5623), 80–82.

89. Cooper, R.R., Milgram, J.W., and Robinson, R.A. (1966) Morphology of the osteon. An electron microscopic study. *J. Bone Joint Surg. Am.*, **48**(7), 1239–1271.

90. Leeuwenhoek, A. (1674) Microscopical observations about blood, milk, bones, the brain, spitle, cuticula. Letter published in *Philos. Trans. R. Soc. London, Ser.* **9**, 121.

91. Leeuwenhoek, A. (1693) Several observations on the texture of bone of animals compared with that of wood: on the bark of trees: on the little scales found on the cuticula, etc. *Philos. Trans. R. Soc. London*, **17**, 838–843.

92. Leeuwenhoek, A. (1800) The select works of antony van Leeuwenhoek, containing his microscopical discoveries in many of the works of nature, translated from the Dutch and Latin editions published by the author, by Samuel Hoole, Volume the first –part the first. G. Sidney, London MDCCC.

93. Havers, C. (1691) *Osteologia Nova, or Some New Observations of the Bones, and the Parts Belonging to Them, with the Manner of their Accretion and Nutrition*, Samuel Smith, London.

94. Dobson, J. (1952) *J. Bone Joint Surg.*, **34-B**(4), 702–707.

95. Martin, R.B. and Burr, D.B. (1989) *Structure Function, and Adaptation of Compact Bone*, Raven Press, New York.

96. Ford, B.J. (1992, access on line 2009) From dilettante to diligent experimenter, a reappraisal of Leeuwenhoek as microscopist and investigator, *http://www.brianjford.com/a-avl01.htm*.

97. Frost, H.M. (1963) *Bone Remodelling Dynamics*, Charles C. Thomas, Springfield, Il.

98. Frost, H.M. (1964) *Mathematical Elements of Lamellar Bone Remodelling*, Charles C. Thomas, Springfield, Il.

99. Frost, H.M. (1973) *Bone Remodelling and its Relation to Metabolic Bone Diseases*, C. Thomas, Springfield, IL.

100. Frost, H.M. (2001) *Anat. Rec. A*, **262**(4), 398–419.

101. Seeman, E. (2006) *Osteoporos. Int.*, **17**(10), 1443–1448.

102. Osteon (2010) *http://en.wikipedia.org/wiki/Osteon*.

103. BME/ME 456 Biomechanics. *http://www.engin.umich.edu/class/bme456/bonestructure/bonestructure.htm*.

104. Gebhardt, W. (1901, 1905) Über funktionell wichtige Anordnungsweisen der feineren und gröberen Bauelemente des Wirbelthierknochens.II. Spezieller Teil. *Arch. Entwickl. Mech. Roux's Arch. Dev. Biol.)*, **20**, 187–322.

105. Gebhardt, W. (1901) Über funktionell wichtige Anordnungsweisen der gröberen und feineren Bauelemente des Wirbelthierknochens. I. Allgemeiner Teil. *Arch. Entwickl. Mech. Roux's Arch. Dev. Biol.*, **11**, 383–498; **12**, 1–52, 167–223.

106. Ascenzi, A. and Bonucci, E. (1961) *Acta Anat. (Basel)*, **44**(3), 236–262.

107. Ascenzi, A. and Bonucci, E. (1968) *Anat. Rec.*, **161**(3), 377–391.

108. Ascenzi, A. and Bonucci, E. (1967) *Anat. Rec.*, **158**(4), 375–386.

109. Ascenzi, A. and Benvenuti, A. (1986) *J. Biomech.*, **19**(6), 455–463.

110. Ascenzi, A. and Bonucci, E. (1976) *Clin Orthop.*, **121**, 275–294.

111. Ascenzi, M.-G. and Lomovtsev, A. (2006) *J. Struct. Biol.*, **153**(1), 14–30.

112. Ascenzi, M.-G., Gill, J., and Lomovtsev, A. (2008) *J. Biomech.*, **41**(16), 3426–3435.

113. Figurska, M. (2007) *Russ. J. Biomech.*, **11**(3), 26–35.

114. Frasca, P., Hari Rao, C.V., Harper, R.A., and Katz, J.L. (1976) *J. Den. Res.*, **55**(3), 372–375.

115. Weiner, S., Arad, T., and Traub, W. (1991) *FEBS Lett.*, **285**(1), 49–54.

116. Enlow, D.H. (2005) *Am. J. Anat.*, **110**(3), 269–305.

117. Gros, N. (1846) *C. R. Acad. Sci.*, **23**(24), 1106–1108.

118. Ottolenghi, D. (1901) *Atti R. Accad. Sci. Torino*, **36**(15), 611–618.

119. Kuntz, A. and Richins, C.A. (1945) *J. Comp. Neurol.*, **83**, 213–221.

120. Röhlich, K. (1961) *Z. Mikroskopischanat. Forsch.*, **49**, 425–464.

121. Efferent Nerve Fiber (2009) *http://en.wikipedia.org/wiki/Efferent_nerve_fiber*.

122. Vento, P. and Soinila, S. (1999) *J. Histochem. Cytochem.*, **47**(11), 1405–1415.

123. Carter, M.S., Cremins, J.D., and Krause, J.E. (1990) *J. Neurosci.*, **10**(7), 2203–2214.

124. Goto, T. (2002) *Microsc. Res. Tech.*, **58**(2), 59–60.

125. Goto, T. and Tanake, T. (2002) *Microsc. Res. Tech.*, **58**(2), 91–97.

126. Substance P. (2006) *http://en.wikipedia.org/wiki/Substance_P*.

127. Dudás, B. and Merchenthaler, I. (2002) *J. Clin. Endocrinol. Metab.*, **87**(6), 2946–2953.

128. Gajda, M., Litwin, J.A., Cichocki, T., Timmermans, J.-P., and Adriaensen, D. (2005) *J. Anat.*, **207**(2), 135–144.

129. Enchanted Learning. *http://www.enchantedlearning.com/subjects/*.

130. Cytoskeleton (2010) *en.wikipedia.org/wiki/Cytoskeleton*.

131. Frixione, E. (2000) *Cell Motil. Cytoskeleton.*, **46**(2), 73–94.

132. Smith, D.A. and Geeves, M.A. (1995) *Biophys. J.*, **69**(8), 524–537.

133. Streater, R.F. (1997) *Rep. Math. Phys.*, **40**(3), 557–564.

134. Astumian, R.D. and Hanggi, P. (2002) *Phys. Today*, **55**(11), 33–39.

135. Wojnar, R. (2002) *Rep. Math. Phys.*, **49**(2), 415–426.

136. Evert, R.F. and Eichhorn, S.E. (2006) *Esau's Plant Anatomy, Meristems, Cells, and Tissues of the Plant Body: Their Structure, Function, and Development*, 3rd edn, John Wiley & Sons, Inc.

137. Cell_Membrane (2010) *en.wikipedia.org/wiki/Cell_membrane*.

138. Bederson, B. and Silbermann, B. (2000) Cellupedia library, *www.thinkquest.org/C004535/cell_membranes.html*.

139. Poniewierski, A. and Stecki, J. (1982) *Phys. Rev. A*, **25**(4), 2368–2370.

140. Degiorgio, V. and Corti, M. (eds) (1985) *Physics of Amphiphiles: Micelles,Vesicles*

and Microemulsions, Italian Physical Society, North-Holland Physics Publishing, Amsterdam.
141. Stecki, J. (2008) *J. Phys. Chem. B*, **112**(14), 4246–4252.
142. Enzyme (2009) *http://en.wikipedia.org/wiki/Enzyme*.
143. Juliano, R.L. and Ling, V. (1976) *Biochim. Biophys. Acta*, **455**(1), 152–162.
144. Payen, A. and Persoz, J.-F. (1833) Mémoire sur la diastase, les principaux produits de ses réactions et leurs applications aux arts industriels. *Ann. Chim. Phys., 2 e Sér.*, **53**, 73–92.
145. Henri, V. (1902) *C. R. Acad. Sci. Paris*, **135**, 916–919.
146. Henri, V. (1903) *Lois Générales de L'action des Diastases*, Hermann, Paris.
147. Michaelis, L. and Menten, M.L. (1913) *Biochem. Z.*, **49**, 333–369.
148. Membrane Transport Protein (2009) *http://en.wikipedia.org/wiki/Membrane_transport_protein*.
149. Becker, W.M., Kleinsmith, L.J., and Hardin, J. (2006) *The World of the Cell*, 6th edn, Pearson and Benjamin Cummings, San Francisco, CA.
150. Van Winkle, L.J. (1999) *Biomembrane Transport*, Academic Press, New York.
151. Voituriez, R., Moreau, M., and Oshanin, G. (2005) *Europhys. Lett.*, **69**(2), 177–183.
152. Voituriez, R., Moreau, M., and Oshanin, G. (2005) *J. Chem. Phys.*, **122**(8), 084103/13.
153. Runge, S.W., Hill, B.J.F., and Moran, W.M. (2006) *CBE Life Sci. Edu.*, **5**(4), 348–352.
154. Stryer, L. (1995) *Biochemistry*, 4th edn, W. H. Freeman and Company, New York.
155. Brozek, J., Bryl, E., Ploszynska, A., Balcerska, A., and Witkowski, J. (2009) *J. Pediatr. Hematol. Oncol.*, **31**(7), 493–499.
156. Morita, Y., Sobel, M.L., and Poole, K. (2006) *J. Bacteriol.*, **188**(5), 1847–1855.
157. D'ippolito, G., Schiller, P.C., Ricordi, C., Roos, B.A., and Howard, G.A. (1999) *J. Bone Miner. Res.*, **14**(7), 1115–1122. Also *http://en.wikipedia.org/wiki/Osteoblast#cite_note-Dippolito1999-0*.
158. Bone Cell (2009) *http://en.wikipedia.org/wiki/Bone_cell*.
159. Osteoblast (2009) *http://en.wikipedia.org/wiki/Osteoblast*.
160. Klein-Nulend, J., van der Plas, A., Semeins, C.M., Ajubi, N.E., Frangos, J.A., Nijweide, P.J., and Burger, E.H. (1995) *FASEB J.*, **9**(5), 441–445.
161. Bonewald, L.F. (2005) *J. Musculoskelet. Neuronal Interact.*, **5**(4), 321–324.
162. Caceci, Th. (2008) BoneVM8054 Veterinary Histology Exercise 8. *http://education.vetmed.vt.edu/curriculum/vm8054/labs/Lab8/lab8.htm*.
163. Tanaka, K., Yamaguchi, Y., and Hakeda, Y. (1995) *J. Bone Miner. Metab.*, **13**, 61–70.
164. Rubinacci, A., Covini, M., Bisogni, C., Villa, I., Galli, M., Palumbo, C., Ferretti, M., Muglia, M.A., and Marotti, G. (2002) *Am. J. Physiol. Endocrinol. Metab.*, **282**(4), E851–E864.
165. Bonewald, L. (2006) *J. Musculoskelet. Neuronal Interact.*, **6**(4), 331–333.
166. Osteoclast (2008) *en.wikipedia.org/wiki/Osteoclast*.
167. Väänänen, H.K., Zhao, H., Mulari, M., and Halleen, J.M. (2000) *J. Cell Sci.*, **113**(Pt 3), 377–381.
168. RANKL (2007) *http://en.wikipedia.org/wiki/RANKL*.
169. RANK (2010) *http://en.wikipedia.org/wiki/RANK*.
170. Simonet, W.S., Lacey, D.L., Dunstan, C.R., Kelley, M., Chang, M.-S., Lüthy, R., Nguyen, H.Q., Wooden, S., Bennett, L., Boone, T., Shimamoto, G., DeRose, M., Elliott, R., Colombero, A., Tan, H.L., Trail, G., Sullivan, J., Davy, E., Bucay, N., Renshaw-Gegg, L., Hughes, T.M., Hill, D., Pattison, W., Campbell, P., Sander, S., Van, G., Tarpley, J., Derby, P., Lee, R., and Boyle, W.J. (1997) *Cell*, **89**(2), 309–319.
171. Tsuda, E., Goto, M., Mochizuki, S., Yano, K., Kobayashi, F., Morinaga, T., and Higashio, K. (1997) *Biochem. Biophys. Res. Commun.*, **234**, 137–142.
172. Yasuda, H., Shima, N., Nakagawa, N., Yamaguchi, K., Kinosaki, M., Mochizuki, S., Tomoyasu, A., Yano, K., Goto, M., Murakami, A., Tsuda, E., Morinaga, T., Higashio, K., Udagawa,

N., Takahashi, N., and Suda, T. (1998) *Proc. Natl. Acad. Sci. U.S.A.*, **95**, 3597–3602.
173. Yasuda, H., Shima, N., Nakagawa, N., Mochizuki, S.I., Yano, K., Fujise, N., Sato, Y., Goto, M., Yamaguchi, K., Kuriyama, M., Kanno, T., Murakami, A., Tsuda, E., Morinaga, T., and Higashio, K. (1998) *Endocrinology*, **139**(3), 1329–1337.
174. Kryokiewicz, E. and Lorenc, I.R.S. (2006) *TERAPIA*, **3**(177), 58–63.
175. Malyankar, U.M., Scatena, M., Suchland, K.L., Yun, Th.J., Clark, E.A., and Giachelli, C.M. (2000) *J. Biol. Chem.*, **275**(28), 20959–20962.
176. Rogers, A. and Eastell, R. (2005) *J. Clin. Endocrinol. Metab.*, **90**(11), 6323–6331.
177. Boyce, B.F. and Xing, L. (2007) *Arthritis Res. Ther.*, **9** (Suppl 1), 1–7.
178. Bucay, N., Sarosi, I., Dunstan, C.R., Morony, S., Tarpley, J., Capparelli, C., Scully, Sh., Tan, H.L., Xu, W., Lacey, D.L., Boyle, W.J., and Scott Simonet, W. (1998) *Genes Dev.*, **12**, 1260–1268.
179. Ducy, P., Schinke, Th., and Karsenty, G. (2000) *Science*, **289**(5484), 1501–1504.
180. Boyle, W.J., Simonet, W.S., and Lacey, D.L. (2003) *Nature*, **423**(6937), 337–342.
181. Schoppet, M., Preissner, K.T., and HofbauerI, L.C. (2002) *Arterioscler. Thromb. Vasc. Biol.*, **22**(4), 549–553.
182. Hofbauer, L.C. and Schoppet, M. (2004) *J. Am. Med. Assoc.*, **292**, 490–495.
183. Bekker, P.J., Holloway, D.L., Rasmussen, A.S., Murphy, R., Martin, S.W., Leese, Ph.T., Holmes, G.B., Dunstan, C.R., and DePaoli, A.M. (2004) A single-dose placebo-controlled study of AMG 162, a fully human monoclonal antibody to RANKL. *J. Bone Miner. Res.*, **19**(7), 1059–1066.
184. Black, R.A. (2002) Tumor necrosis factor-alpha converting enzyme. *Int. J. Biochem. Cell Biol.*, **34**(1), 1–5.
185. Black, R.A., Rauch, C.T., Kozlosky, C.J., Peschon, J.J., Slack, J.L., Wolfson, M.F., Castner, B.J., Stocking, K.L., Reddy, P., Srinivasan, S., Nelson, N., Boiani, N., Schooley, K.A., Gerhart, M., Davis, R., Fitzner, J.N., Johnson, R.S., Paxton, R.J., March, C.J., and Cerretti, D.P. (1997) A metalloproteinase disintegrin that releases tumour-necrosis factor-alpha from cells. *Nature*, **385**(6618), 729–733.
186. Dziedzic-Goc3awska, A., Tyszkiewicz, J., and Uhrynowska-Tyszkiewicz, I. (2000) *Nowa Klin.*, **7**(7), 704–712.
187. Pan, B., Farrugia, A.N., To, L.B., Findlay, D.M., Green, J., Lynch, K., and Zannettino, A.C. (2004) *J. Bone Miner. Res.*, **19**(1), 147–154.
188. Wedemeyer, Ch., Knoch, Fv., Pingsmann, A., Hilken, G., Sprecher, Ch., Saxler, G., Henschke, F., Löer, F., and Knoch, Mv. (2005) *Biomaterials*, **26**(17), 3719–3725.
189. Stawińska, N., Ziętek, M., and Kochanowska, I. (2005) *Dent. Med. Prob.*, **42**(4), 627–635.
190. Khosla, S. (2001) Minireview: the OPG/RANKL/RANK system. *Endocrinology*, **142**(12), 5050–5055.
191. Kearns, A.E., Khosla, S., and Kostenuik, P.J. (2008) *Endocrinol. Rev.*, **29**(2), 155–192.
192. McClung, M. (2007) *Arthritis Res. Ther.*, **9** (Suppl 1), 1–3.
193. Yeung, Rae S.M. (2004) The Osteoprotegerin/Osteoprotegerin ligand family: role in inflammation and bone loss. *J. Rheumatol.*, **31**(5), 844–846.
194. Kong, Y.Y., Yoshida, H., Sarosi, I., Tan, H.L., Timms, E., Capparelli, C., Morony, S., Oliveira-dos-Santos, A.J., Van, G., Itie, A., Khoo, W., Wakeham, A., Dunstan, C.R., Lacey, D.L., Mak, T.W., Boyle, W.J., and Penninger, J.M. (1999) *Nature*, **397**(6717), 315–323.
195. Silvestrini, G., Ballanti, P., Patacchioli, F., Leopizzi, M., Gualtieri, N., Monnazzi, P., Tremante, E., Sardella, D., and Bonucci, E. (2005) Detection of osteoprote gerin (OPG) and its ligand (RANKL) mRNA and protein infemur and tibia of the rat. *J. Mol. Hist.*, **36**(1-2), 59–67.
196. Kim, D.W., Lee, H.J., Karmin, J.A., Lee, S.E., Chang, S.S., Tolchin, B., Lin, S., Cho, S.K., Kwon, A., Ahn, J.M., and Lee, F.Y.-I. (2006) *Ann. N.Y. Acad. Sci.*, **1068**(1), 568–572.

197. Bhagavan, N.V. (2002) *Medical Biochemistry*, 4th edn, Academic Press, Harcourt.

198. Amino Acid (2007) *http://en.wikipedia.org/wiki/Amino_acid*.

199. Proteinogenic Amino Acid (2009) *http://en.wikipedia.org/wiki/Proteinogenic_amino_acid*.

200. Astbury, W.Th. (1938) *Trans. Faraday Soc.*, **34**, 378–388.

201. Braconnot, H.M. (1820) Sur la conversion des matières animales en nouvelles substances par le moyen de l'acide sulfurique. *Ann. Chim. Phys. Ser 2*, **13**, 113–125.

202. Hershey, A.D. and Chase, M. (1952) *J. Gen. Physiol.*, **36**, 39–56.

203. Herzog, R.O. and Jancke, W. (1920) *Ber. Dtsch. Chem. Ges.*, **53**, 2162–2164.

204. Pauling, L. and Corey, R.B. (1951) *Proc. Natl. Acad. Sci. U.S.A.*, **37**(5), 272–281.

205. Ramachandran, G.N. and Ambady, G.K. (1954) *Curr. Sci.*, **23**, 349.

206. Cochran, W., Crick, F.H.C., and Vand, V. (1952) *Acta Crystallogr.*, **5**, 581–586.

207. Ramachandran, G.N. (1967) Structure of collagen at the molecular level, in *Treatise on Collagen*, vol. 1, (ed. G.N. Ramachandran), Chapter 3, Academic Press, New York, pp. 103–183.

208. Rich, A. and Crick, F.H.C. (1955) *Nature*, **176**(4489), 915–916.

209. Rich, A. and Crick, F.H.C. (1961) *J. Mol. Biol.*, **3**, 483–506.

210. Boedtker, H. and Doty, P. (1956) *J. Am. Chem. Soc.*, **78**, 4267–4280.

211. Yonath, A. and Traub, W. (1969) *J. Mol. Biol.*, **43**, 461–477.

212. Okujama, K., Bächinger, H.P., Mizuno, K., Boudko, S., Engel, J., Berisio, R., and Vitagliano, L. (2006) *Proc. Natl. Acad. Sci.*, **103**, 9001–9005 (Comments on *Microfibrillar structure of type I collagen in situ* by Orgel *et al.* PNAS, submitted for publication).

213. Okuyama, K. (2008) *Connect. Tissue Res.*, **49**(5), 299–310.

214. Orgel, J.P.R.O., Irving, Th.C., Miller, A., and Wess, T.J. (2006) *Proc. Natl. Acad. Sci.*, **103**(24), 9001–9005.

215. Okuyama, K., Takayanagi, M., Ashida, T., and Kakudo, M. (1977) *Polym. J.*, **9**(3), 341–343.

216. Okuyama, K., Nagarajan, V., Kamitori, Sh., and Noguchi, K. (1998) *Chem. Lett.*, **27**(5), 385–386.

217. Royce, P.M. and Steinmann, B.U. (eds) (2002) *Connective Tissue and its Heritable Disorders: Molecular, Genetic, and Medical Aspects*, 2nd edn, Wiley-Liss, New York.

218. Bansal, M. (1977) *Pramana*, **9**(4), 339–347.

219. Piez, K.A. (1976) Primary structure, in *Biochemistry of Collagen*, Chapter 1 (eds G.N. Ramachandran and A.H. Reddi), Plenum Press, New York, pp. 1–44.

220. Millane, R.P. (1991) *Acta Crystallogr.*, **A47**, 449–451.

221. Rainey, J.K. and Goh, M.C. (2002) *Protein Sci.*, **11**(11), 2748–2754.

222. Vincent, J. (1990) *Structural Biomaterials*, Princeton University Press, Princeton, NJ.

223. Kucharz, E.J. (1992) *The Collagens: Biochemistry and Pathophysiology*, Springer-Verlag, Berlin.

224. Sikorski, Z.E. (2001) *Chemical and Functional Properties of Food Proteins*, CRC Press.

225. Collagen (2010) *http://en.wikipedia.org/wiki/Collagen*.

226. Privalov, P.L. (1982) *Adv. Protein Chem.*, **35**, 1–104.

227. Privalov, P.L. (1989) *Annu. Rev. Biophys. Biophys. Chem.*, **18**, 47–69.

228. Makhatadze, G.I. and Privalov, P.L. (1996) *Protein Sci.*, **5**(3), 507–510.

229. Brodsky, B., Eikenberry, E.F., Belbruno, K.C., and Sterling, K. (1982) *Biopolymers*, **21**(5), 935–951.

230. Brodsky, B. and Ramshaw, J.A.M. (1997) *Matrix Biol.*, **15**(8-9), 545–554.

231. Coxeter, H.S.M. (1948) *Regular Polytopes*, Macmillan, New York; (Dover, 1973).

232. Coxeter, H.S.M. (1961) *Introduction to Geometry*, 1st edn, John Wiley & Sons, Inc., New York.

233. Bernal, J.D. (1964) *Proc. R. Soc. London A*, **280**(1382), 299–322.

234. Zheng, Ch., Hoffman, R., and Nelson, D.R. (1990) *J. Am. Chem. Soc.*, **112**, 3784–3791.

235. Buckmister Fuller, R. (1975) *Synergetics*, MacMillan, New York, also: Gray, R.W.

(1997) *http://www.rwgrayprojects.com/synergetics/synergetics.html*.
236. Lord, E.A. and Ranganathan, S. (2001) *Eur. Phys. J. D*, **15**(3), 335–343.
237. Lord, E.A. (2002) *Struct. Chem.*, **13**(3/4), 305–314.
238. Sadoc, J.F. and Rivier, N. (1999) *Eur. Phys. J. B*, **12**(2), 309–319.
239. Sadoc, J.F. and Rivier, N. (2000) *Mater. Sci. Eng. A*, **294–296**, 397–400.
240. Sadoc, J.F. and Charvolin, J. (2009) *J. Phys. A: Math. Theor.*, **42**, 465209 (17 pp).
241. Buehler, M.J. and Wong, S.Y. (2007) *Biophys. J.*, **93**(1), 37–43.
242. Kuhn, W. (1934) *Kolloid-Z.*, **68**(1), 2–15.
243. Flory, P.J. (1953) *Principles of Polymer Chemistry*, Cornell University Press, Ithaca, NY.
244. Treloar, L.R.G. (2005) *The Physics of Rubber Elasticity*, 3rd edn, Oxford University Press.
245. Kratky, O. and Porod, G. (1949) *Rec. Trav. Chim. Pays-Bas*, **68**, 1106–1123.
246. Polymer Physics (2010) *en.wikipedia.org/wiki/Polymer_physics*.
247. Worm-like_chain (2010) *en.wikipedia.org/wiki/Worm-like_chain*.
248. Bustamante, C., Marko, J.F., Siggia, E.D., and Smith, S. (1994) *Science*, **265**(5178), 1599–1600.
249. Bustamante, C., Bryant, Z., and Smith, S.B. (2003) *Nature*, **421**(6921), 423–427.
250. Fratzl, P. (2003) *Curr. Opin. Colloid Interface Sci.*, **8**(1), 32–39.
251. Fraser, R.D., MacRae, T.P., and Miller, A. (1987) *J. Mol. Biol.*, **193**(1), 115–125.
252. Wess, T.J., Hammersley, A.P., Wess, L., and Miller, A. (1998) *J. Mol. Biol.*, **275**(2), 255–267.
253. Sionkowska, A., Wisniewski, M., Skopinska, J., Kennedy, C.J., and Wess, T.J. (2004) *Biomaterials*, **25**(5), 795–801.
254. Wess, T.J. (2008) Collagen fibrillar structure and hierarchies, in *Collagen, Structure and Mechanics*, (ed. P. Fratzl), Springer, pp. 49–80.
255. Cameron, G.J., Cairns, D.E., and Wess, T.J. (2007) *J. Mol. Biol.*, **372**(4), 1097–1107.
256. Cowan, P.M., North, A.C.T., and Randall, J.T. (1955) *Symp. Soc. Exp. Biol.*, **9**, 115–126.
257. Cowan, P.M. and McGavin, S. (1955) *Nature*, **176**(4480), 501–503.
258. Misof, K., Rapp, G., and Fratzl, P. (1997) *Biophys. J.*, **72**(3), 1376–1381.
259. Puxkandl, R., Zizak, I., Paris, O., Keckes, J., Tesch, W., Bernstorff, S., Purslow, P., and Fratzl, P. (2002) *Philos. Trans. R. Soc. London B Biol. Sci.*, **357**(1418), 191–197.
260. Gupta, H.S., Messmer, P., Roschger, P., Bernstorff, S., Klaushofer, K., and Fratzl, P. (2004) *Phys. Rev. Lett.*, **93**(15), 158101(4).
261. Gupta, H.S., Seto, J., Wagermaier, W., Zaslansky, P., Boesecke, P., and Fratzl, P. (2006) *Proc. Natl. Acad. Sci*, **103**(47), 17741–17746. Also *www.pnas.org_cgi_doi_10.1073_pnas.0604237103*
262. Diamant, J., Keller, A., Baer, E., Litt, M., and Arridge, R.G.C. (1972) *Proc. R. Soc. London B*, **180**, 293–315.
263. Silver, F.H., Kato, Y.P., Ohno, M., and Wasserman, A.J. (1992) *J. Long-Term Eff. Med. Implants*, **2**(2-3), 165–195.
264. Mosler, E., Folkhard, W., Knörzer, E., Nemetschek-Gonsler, H., Nemetschek, Th., and Koch, M.H.J. (1985) *J. Mol. Biol.*, **182** (4), 589–596.
265. Hodge, A.J. and Petruska, J.A. (1963) in *Aspects of Protein Structure* (ed. G.N. Ramachandran), Academic Press, New York, pp. 289–300.
266. Hull, D. (1981) *An Introduction to Composite Materials*, Cambridge University Press.
267. Edoff, K., Hellman, J., Persliden, J. and Hildebrand, C. (1997) *Anat. Embryol.*, **195**(6), 531–538.
268. McCredie, J. (1973) *Lancet*, **2**(7837), 1058–1061.
269. McCredie, J. (2009) *J. Med. Imaging Radiat. Oncol.*, **53**(5), 433–441.
270. Adams, J.S. and Hewison, M. (2010) *J. Clin. Endocrinol. Metab.*, **95**(2), 471–478.

271. Donahue, S.W., McGee, M.E., Harvey, K.B., Vaughan, M.R. and Robbins, Ch.T. (2006) *J. Biomech.*, **39**(8), 1480–1488.
272. Arnold, V.I. (1998) *Russ. Math. Surv.*, **53**(1), 229–236; also *http://pauli.uni-muenster.de/~munsteg/arnold.html.*
273. Myjak, J. (2008) *Opuscula Math.*, **28**(4), 343–351.
274. Jakob, B. and Kasper, O. (2010) The close-packed triple helix as a possible new structural motif for collagen, *arXiv:1004.1781v1 [physics.bio-ph]* 11 Apr 2010.
275. Sommerfeldt, D.W. and Rubin, C.T. (2001) *Eur. Spine J.*, **10**(S2), S86–S95.

Further Reading

Bostanci, N., Emingil, C., Afacan, B., Han, B., Ilgenli, T., Atilla, G., Hughes, F.J., and Belibasakis, G.N. (2008) *J. Dent. Res.*, **87**(3), 273–277.
Di LulloDagger, G.A., Sweeney, Sh.M., Körkkö, J., Ala-Kokko, L., and San Antonio, J.D. (2002) *J. Biol. Chem.*, **277**(6), 4223–4231.
McMurry, J. (2008) *Organic Chemistry*, 7th edn., Brooks/Cole-Cengage, Belmont, CA.
Sikorski, Z.E. (2001) *Chemical and Functional Properties of Food Proteins*, Boca Raton: CRC Press.